

JAN 29 1987

HAWAII INSTITUTE OF
LIBRARY

Geochemical study of the Hawi Formation
AC .H3 no. S86 15502



Spengler, Steven R.
SOEST Library

070
Spe
Geo
ms

GEOCHEMICAL STUDY OF THE HAWI FORMATION OF KOHALA VOLCANO, HAWAII:
THE HAWAIIITE TO TRACHYTE TRANSITION

A THESIS SUBMITTED TO THE GRADUATE DIVISION OF THE
UNIVERSITY OF HAWAII IN PARTIAL FULFILLMENT
OF THE REQUIREMENTS FOR THE DEGREE OF

MASTER OF SCIENCE

IN GEOLOGY AND GEOPHYSICS

DECEMBER 1986

By

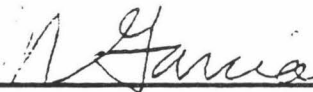
Steven Robert Spengler

Thesis Committee:


Michael O. Garcia, Chairman
John M. Sinton
John J. Manonney

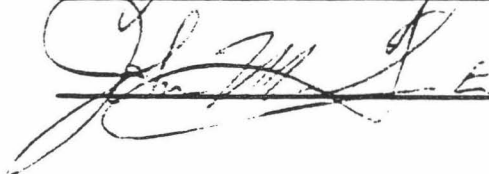
We certify that we have read this thesis and that in our opinion it is satisfactory in scope and quality as a thesis for the degree of Master of Science in Geology and Geophysics.

THESIS COMMITTEE



Chairman





ACKNOWLEDGEMENTS

Several people deserve recognition for making the past two and a half years here in Hawaii a very special time. Thanks go to Dr. Mike Garcia who allowed me the opportunity to come to Hawaii, to Dr. Shiv Sharma who allowed me the financial means to stay, and to Dr. John Sinton and Dr. John Mahonney who patiently listened to my idle ranting and raving about this thesis. Fellow graduate students Donna Buxton and Julie Hood made me smile which allowed me to laugh at it all. Housemates Mark and Suzie Underwood nourished me with cooking and love. Trips to Germany and the warmth of Angela's touch allowed me to maintain sanity. Financial and analytical support from the United States Geological Survey, in particular the director of the mapping project, Dr. Ed Wolfe, helped facilitate the completion of this thesis. The use of the neutron activation facilities at MIT and the help of Dr. Fred Frey are also greatly appreciated. Microprobe analysis of Hawaii apatites for REE content by Dr. Jim Nichols and his introduction to the utility of molar ratio plots were very helpful. Support for the analyses and living costs in Boston were defrayed by Penrose grant #3499-85 and a Harold Stearns Fellowship.

ABSTRACT

Alkalic volcanism of the Hawi Formation began on Kohala at or near the end of volcanic activity of the underlying Pololu Formation, roughly .25-.30 Ma ago. Within the Hawi Formation, hawaiite is the predominant rock type followed in abundance by mugearite, benmorites and transitional lavas. The rocks are typically aphyric containing small modal amounts of olivine, magnetite, apatite and plagioclase microphenocryst set in a matrix of fine grained feldspar laths. Eruptive temperatures ranged from about 1100°C for hawaiites to 1000°C for benmorites based on apatite and plagioclase compositions found in the lavas. The chemical variation observed within the Hawi can be best explained by fractional crystallization of the observed phase assemblage in conjunction with variable amounts of high pressure clinopyroxene fractionation. Because plagioclase is a major fractionating phase, despite its being less dense than the magma from which it fractionated, suggests that crystallizing phases were removed by plating to the conduit walls. The anomalously high concentrations of phosphorous and rare earth elements observed in Hawi lavas as compared to other Hawaiian alkalic suites are the result of apatite assimilation, presumably during ascent of these lavas to the surface. Isotopic and chemical differences between Pololu, Transitional and Hawi lavas necessitate the existence of at least three distinct source regions to produce the eruptive products found on Kohala.

TABLE OF CONTENTS

ACKNOWLEDGEMENTS.....	iii
ABSTRACT.....	iv
LIST OF TABLES.....	viii
LIST OF ILLUSTRATIONS.....	iv
INTRODUCTION.....	1
GEOMORPHOLOGY.....	2
Structural and erosional features.....	3
Relative volume percentage of rock type in Hawi.....	7
CHRONOLOGY.....	10
Range of Pololu age dates.....	11
Range of Hawi age dates.....	14
KOHALA-TYPE ALKALIC CAPS.....	16
Eruptive frequency during the Hawi.....	17
NOMENCLATURE.....	18
PREVIOUS GEOCHEMICAL STUDIES.....	21
SAMPLE COLLECTION AND FORMATION ASSIGNMENT.....	30
Criteria for identifying Hawi lavas.....	30
Definition of transitional lavas.....	32
PETROGRAPHY.....	33
Pololu lavas.....	36
Hawi lavas.....	37
Modal abundances of mineral phases.....	39

MINERAL COMPOSITIONS.....	40
Fe/Mg ratio of olivines in Hawi lavas.....	40
Opagues and plagioclase.....	43
Pyroxenes and apatite.....	50
ANALYTICAL METHODS.....	57
Precision of analysis.....	57
PETROGENESIS.....	58
Published $^{87}\text{Sr}/^{86}\text{Sr}$ and $^{143}\text{Nd}/^{144}\text{Nd}$ values for Kohala lavas.....	58
Homogeneity of eruptive products from a single eruptive center...	67
Alteration of Hawi lavas.....	76
Variation diagrams.....	79
Molar ratio plots.....	82
LEAST SQUARES MODELLING.....	85
Choice of fractionating assemblage.....	86
Relative proportion of fractionating phases.....	94
Compositional crossing of low pressure thermal divide.....	97
TRACE ELEMENTS.....	97
Log-log plots.....	108
Calculated mineral partition coefficient values.....	115
Anomalous enrichment observed in Hawi.....	121
EXPERIMENTAL EVIDENCE ON CRYSTAL FRACTIONATION IN HAWAIITE.....	127
Plagioclase densities as a function of whole rock density.....	129
Nature of flow in conduit during ascent.....	134
PHYSICAL CONDITIONS OF ERUPTION.....	135
Temperature of eruption.....	135

Dike dimensions on Kohala in relation to yield strength.....	138
WHY ARE SUCH HIGH PHOSPHOROUS CONTENTS OBSERVED IN HAWI LAVAS.....	138
Differentiation trends for other Hawaiian alkalic suites.....	139
P ₂ O ₅ vs. Nd for various alkalic suites.....	139
Disequilibrium Process.....	142
Difference in incompatible element contents: Hawi and Mauna Kea.	147
Apatite assimilation.....	152
RELATIONSHIP TO THE POLOLU.....	155
CONCLUSIONS.....	164
REFERENCES.....	167

LIST OF TABLES

Table 1. Modal analysis of Hawi lavas.....	34
Table 2. Olivine compositions in Hawi lavas.....	41
Table 3. Opaque compositions in Hawi lavas.....	46
Table 4. Plagioclase compositions in Hawi lavas.....	48
Table 5. Pyroxene compositions in Hawi lavas.....	51
Table 6. Apatite compositions in Hawi lavas.....	53
Table 7. Major element compositions in Hawi lavas.....	59
Table 8. Trace element concentrations in Hawi lavas.....	63
Table 9. Least-squares calculations for Hawi lavas (4 phases).....	90
Table 10. Least-squares calculations for Hawi lavas (5 phases).....	92
Table 11. Least-squares calculations for average hawaiiite to average mugearite.....	116
Table 12. Mineral partition coefficients in Hawi lavas.....	119
Table 13. Enrichment of Rb in Hawi lavas.....	124
Table 14. Least-squares calculations for Pololu to Transitional and Transitional to Hawi compositions.....	156

LIST OF ILLUSTRATIONS

Figure 1. Geologic and sample locality map of Kohala volcano.....	5
Figure 2. Rock type distribution within the Hawi.....	8
Figure 3. K-Ar age dates for Kohala volcano.....	12
Figure 4. Alkali-silica diagram for Kohala lavas.....	19
Figure 5. Coombs and Wilkinson classification scheme.....	22
Figure 6. Measured Sr partition coefficient values.....	25
Figure 7. $^{143}\text{Nd}/^{144}\text{Nd}$ vs. $^{87}\text{Sr}/^{86}\text{Sr}$ values for Kohala lavas.....	28
Figure 8. Fe/Mg ratio of olivines found in Kohala lavas.....	44
Figure 9. $^{87}\text{Sr}/^{86}\text{Sr}$ vs. K_2O	68
Figure 10. $^{143}\text{Nd}/^{144}\text{Nd}$ vs. K_2O	70
Figure 11. Differentiation Index vs. Number of samples collected of a particular range of differentiation index.....	72
Figure 12. Multiply sampled flow from Puu Kawaiwai.....	74
Figure 13. Rb vs. Zr and K_2O vs. Zr.....	77
Figure 14. Major element variation diagrams.....	80
Figure 15. Molar ratio plots for Hawi lavas.....	83
Figure 16. Sc vs. K_2O	87
Figure 17. Amount of fractionating mineral phases as a function of F..	95
Figure 18. Normative nepheline/hypersthene composition of Hawi lavas..	98
Figure 19. Chondrite normalized rare earth element patterns.....	101
Figure 20. Relative decrease in rare earth element content.....	103
Figure 21. Partition coefficients for apatite and plagioclase.....	105

Figure 22. REE/K ₂ O vs. P ₂ O ₅ /K ₂ O content.....	109
Figure 23. Log-log plots for trace elements.....	111
Figure 24. Enrichment of incompatible contents in Hawi.....	122
Figure 25. Plagioclase density variation as a function of temperature and anorthite content.....	130
Figure 26. Whole rock densities of Hawi lavas.....	132
Figure 27. P ₂ O ₅ vs. SiO ₂ for Hawi lavas.....	136
Figure 28. P ₂ O ₅ vs. SiO ₂ for other natural melt series.....	140
Figure 29. P ₂ O ₅ /Nd ratios for various Hawaiian volcanoes.....	143
Figure 30. P ₂ O ₅ /Nd ratio for Kohala lavas.....	145
Figure 31. Possible rare earth element pattern resulting from disequilibrium melting of apatite bearing source.....	148
Figure 32. Enrichment of various incompatible elements in Hawi hawaiites over Mauna Kea hawaiites.....	150
Figure 33. Difference in incompatible element contents of Hawi hawaiite and Mauna Kea hawaiite plus 2.9 grams apatite.....	153
Figure 34. Hf/Zr for Kohala lavas.....	159
Figure 35. ⁸⁷ Sr/ ⁸⁶ Sr and ¹⁴³ Nd/ ¹⁴⁴ Nd vs. stratigraphic position.....	162

INTRODUCTION

Kohala Mountain is the northernmost and oldest of the five volcanoes comprising the island of Hawaii. Initial reconnaissance mapping by Stearns and Macdonald (1946) led to the subdivision of Kohala lavas into two stratigraphic units; the Pololu and Hawi Formations. The older Pololu Formation constitutes roughly 99 volume percent of the subaerial volume of the volcano and is composed predominately of shield building tholeiitic lavas. The upper 100 meters of the Pololu Formation exposed in Waipio Valley shows a progressive up-section increase in alkalinity and incompatible element content. The overlying Hawi Formation is composed of alkalic lavas ranging in composition from hawaiite through trachyte and is locally separated from the underlying Pololu Formation by a discontinuous soil horizon.

A detailed study of the geochemical variation within the alkalic Hawi Formation was undertaken using major, transition and rare earth element data in conjunction with mineral data for rocks spanning the compositional range from hawaiite to trachyte. Major element and transition metal abundances are sensitive to crystal fractionation and are used to evaluate various minerals roles in controlling the composition of Hawi lavas. Trace element variation in Hawi lavas is used to further evaluate the role of crystal fractionation, and to examine the role of partial melting, source homogeneity and alteration processes in the petrogenesis of Hawi lavas. Previous studies on Kohala have treated the alkalic Hawi lavas in a cursory manner, while placing

the emphasis on chemical variation within the shield building stage (ie. Feigenson et al., 1983). In addition, studies on other Hawaiian volcanoes have tended to study the overall variation observed throughout the history of the volcano rather than concentrating on the late-stage alkalic lavas. This study is one of the first to concentrate solely on the alkalic stage of a Hawaiian volcano combining detailed field mapping with a relatively comprehensive set of geochemical data.

The rocks analyzed in this study were collected while mapping the geology of Kohala Mountain as part of the United States Geological Survey's Big Island Mapping Project. Representative rocks from each flow unit in the area mapped were collected and the relative stratigraphy of many of the samples was determined. This relative stratigraphy in conjunction with the 17 published K-Ar dates for the Hawi (McDougall and Swanson, 1972; Malinowski, 1977; Lanphere and Frey, 1986) is used to model the temporal geochemical variation in the rocks erupted during the alkalic capping stage. Based on these major and trace element abundances as well as the isotopic characteristics reported in Hofmann et al. (1986) and Lanphere and Frey (1986), it will be shown that fractional crystallization was the first order process giving rise to the observed chemical variability found within the Hawi, and that these lavas are chemically and isotopically distinct from the underlying Pololu and transitional lavas (to be described).

GEOMORPHOLOGY

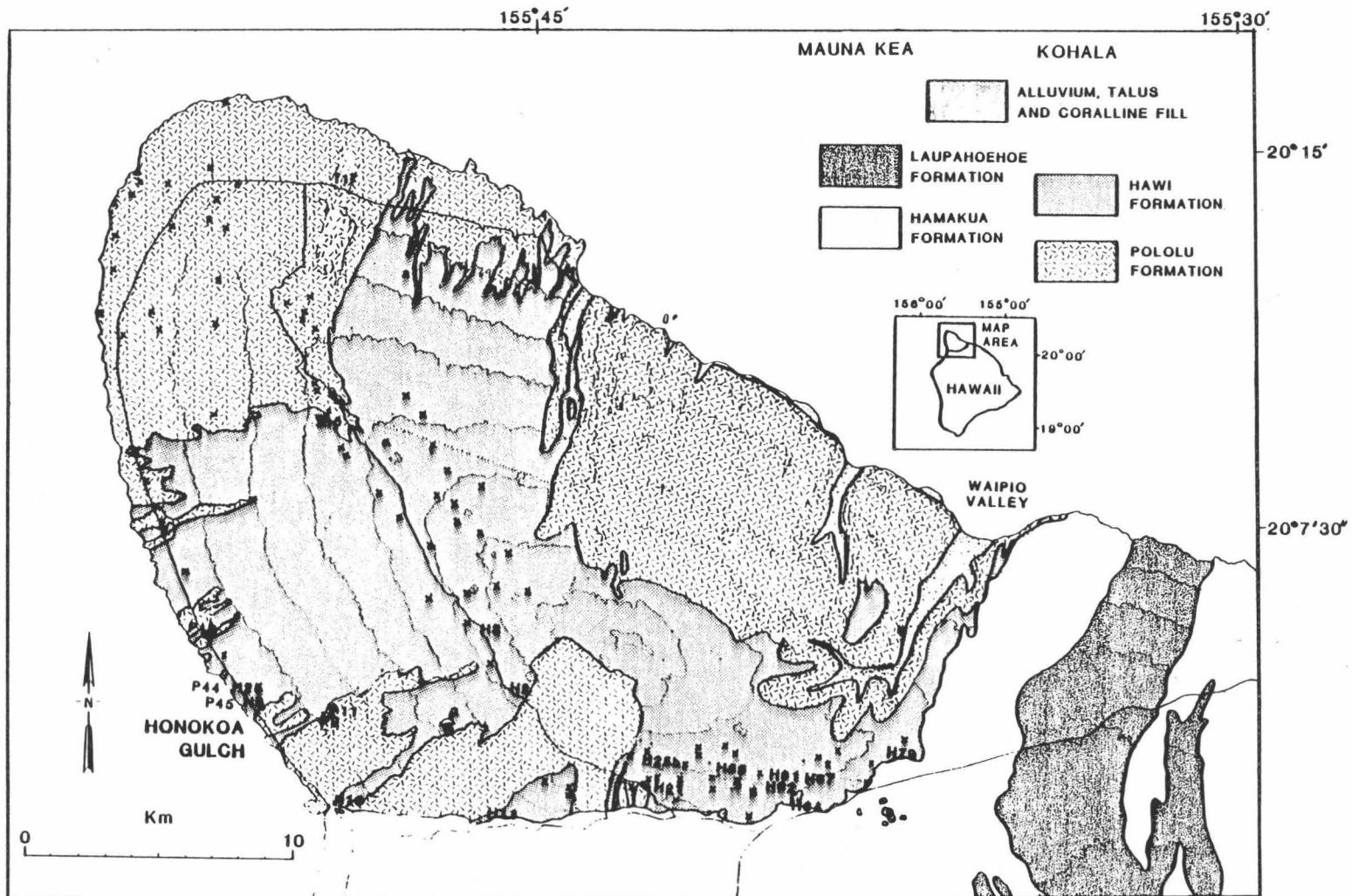
Kohala Mountain is situated at the northern end of the island of Hawaii. It is an elongate, oval shield (864 Km²) formed by two nearly

parallel rift zones that trend N35W and S65E (Figure 1). The majority of eruptive activity was concentrated along the northwest rift. A subsidiary rift trending S50W has had little influence on the morphology of the shield (Stearns and Macdonald, 1946). Either caldera collapse or late stage faulting at the summit of the volcano during the end of Pololu activity produced a graben roughly 10 Km long and 0.6 Km wide that trends N50W. The graben consists of en echelon faults, whose curved character has been used to infer the previous existence of an oval shaped caldera (Stearns and Macdonald, 1946). Evidence has been found for extreme subsidence, on the order of 1250 meters, owing to normal faulting of the submarine portion of the western flank of Hawaii (Campbell and Erlandson, 1981).

In cross section, the Kohala shield is quite asymmetrical. The western, leeward side has undergone little erosion and generally reflects the original topography. Most existing erosional features have been attributed to stream erosion. Stream beds commonly follow flow contacts. Spectacular examples of concentrated stream erosion are found in Honokoa and Mamaewa gulches where walls as high as 120 meters with corresponding channels as narrow as 5 meters across have been cut. The upper portion of Honokoa gulch consists of a sequence of waterfalls and plunge pools created where the stream cut through the younger more resistant Hawi lavas and then deeply incised the underlying, less resistant Pololu lavas. The deep, narrow portions of the gulch were apparently cut by intermittent streams and flash floods funneled into the gulch by branching tributaries upslope.

Figure 1. Map of Kohala Volcano showing sample localities. Labelled samples were analyzed for major and trace elements while localities marked with crosses were only analyzed for major elements.

5



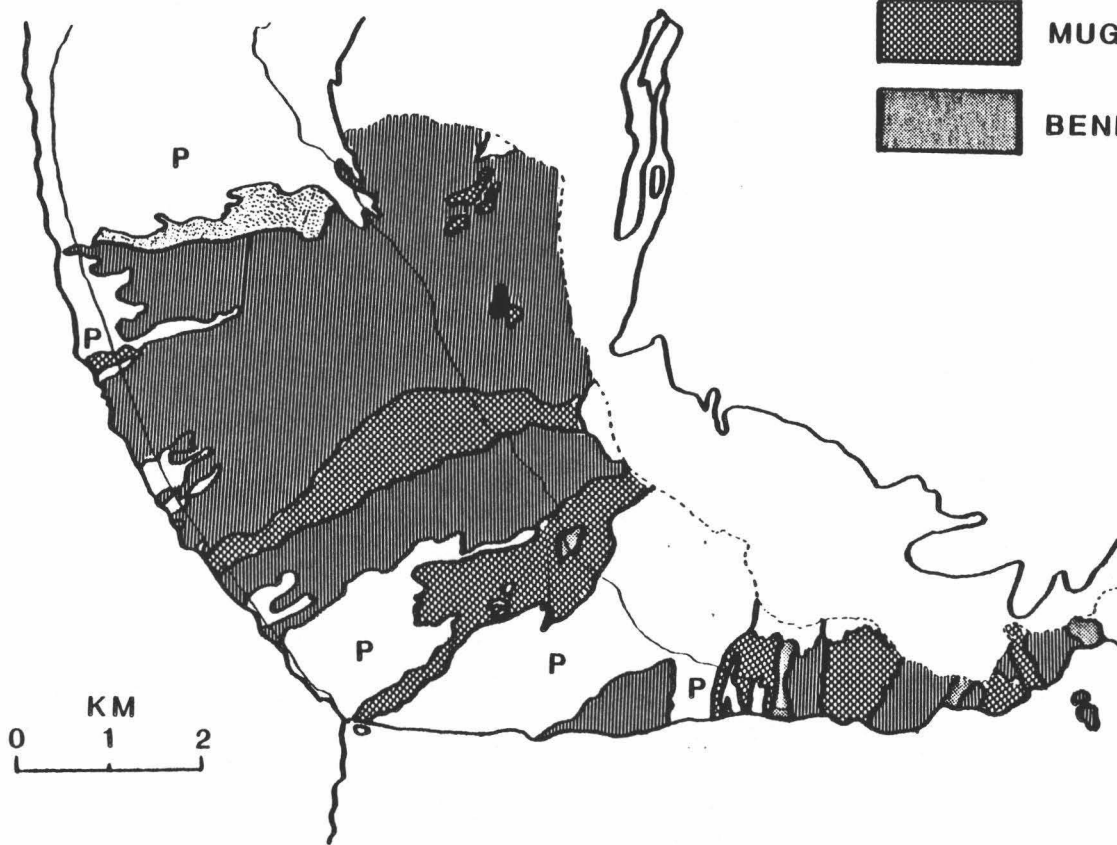
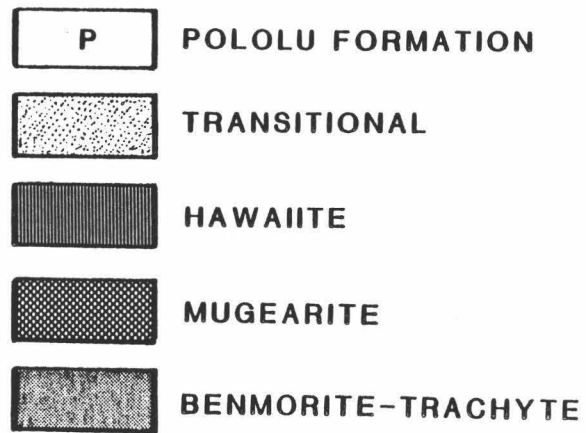
In contrast, the eastern, windward side of the volcano is deeply incised by canyons 305 to 763 meters deep and has sea cliffs up to 427 meters high. Stearns and Macdonald (1946) suggested that the extreme erosion of Kohala's northwest side was not primarily due to the much higher rainfall typical on the windward side. Rather, the absence of the more resistant Hawi lavas on this side of the volcano led to the uninterrupted erosion of the Pololu lavas on this side of Kohala (Stearns and Macdonald, 1946). The absence of Hawi lavas on the eastern side of Kohala is due to the presence of higher fault scarps bounding the eastern side of the summit graben than to the west.

The Hawi Formation forms a cap up to 153 meters thick which thins abruptly away from the summit region, forming massive, relatively thick (2-5 meters) flows ranging in composition from hawaiite to trachyte (Stearns and Macdonald, 1946). As can be seen on Figure 1, Hawi lavas are widespread on the northern, western and southern slopes of Kohala Mountain but are confined on the northeastern side to a few flows that cascaded into the heads of deep valleys cut into Pololu lavas (Figure 1). McDougall and Swanson (1972) determined two identical K-Ar ages of 0.15 Ma on a massive flow of Hawi "mugearite" (probably actually a hawaiite based on K content) that poured into an ancestral Pololu Valley more than 500 meters deep (Stearns and Macdonald, 1946). Comparatively little erosion of the valley has taken place since eruption of this flow (Stearns and Macdonald, 1946). This suggests that Pololu Valley had reached essentially its present size prior to emplacement of this flow 0.15 Ma ago.

Figure 2 is a map of the distribution of surficial rock types found within the Hawi Formation. In the study area, the hawaiite flows cover approximately 71% of the map area, mugearites 24.8%, benmorites and trachytes 1.65% and transitional lavas 2.55%. If one assumes an average thickness of 3 meters for transitional and hawaiite flows, 5 meters for mugearite flows and 7 meters for benmorite flows then relative volume abundances of 60% hawaiite, 35% mugearite, 3% transitional and 2% benmorite are obtained. Because an attempt was made to collect a sample from each mappable flow unit, the relative proportion of rock types analyzed is representative of the relative percentage of rock types present within the Hawi. The distribution of 96 chemically analyzed Hawi samples gives relative proportions of 47% hawaiite, 39% mugearite, 10% benmorite, 1% trachyte, and 3% transitional lavas. The disparity between this estimate and the one based on surficial cover presumably reflects the more fluid character of the hawaiite flows, which tended to flow greater distances from the eruptive center due to their lower viscosities. Both of these new values are in marked contrast to the initial estimates given in Macdonald (1970), who reported a distribution of 1% hawaiite, 58.5% mugearite, .5% trachyte and 40% alkalic basalt on Kohala.

Volcanism during the Hawi was mildly explosive in nature, producing large, steep-sided cinder cones (which predominately follow the trend of the pre-existing rift zones formed during Pololu activity) and voluminous lava flows (up to $160 \times 10^6 \text{ m}^3$). In comparison, the largest volume phase erupted from Pu'u O'o since 1983 has been $40 \times 10^6 \text{ m}^3$. The paucity of obvious multiple flow units from individual eruptive centers

Figure 2. Map of rock type distribution found within the Hawi for areas mapped during the 1984 and 1985 field seasons. In this study area, hawaiite flows cover approximately 71% of the surface area, mugearites 24.8%, benmorites and trachytes 1.65% and transitional lavas 2.55%.



6

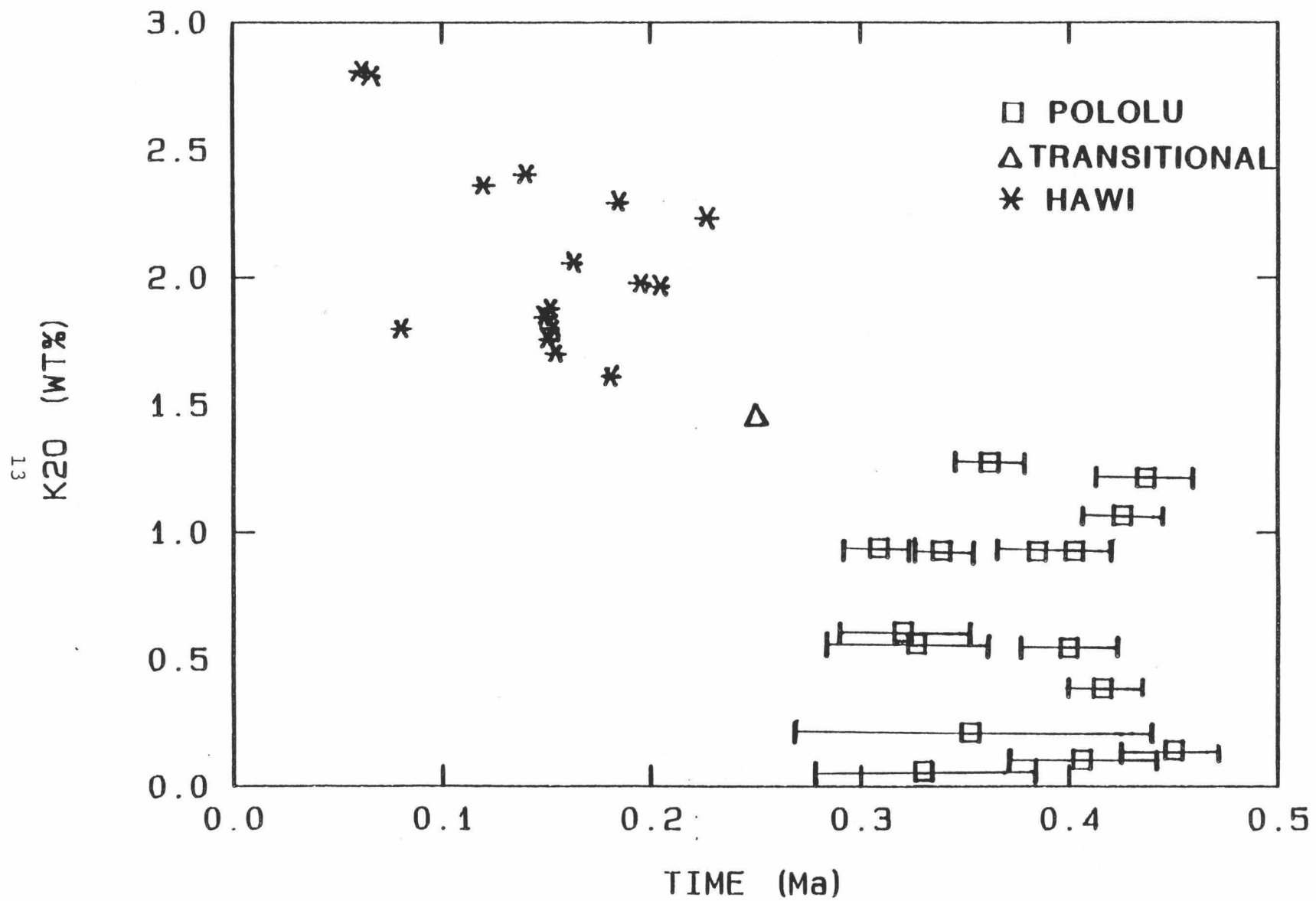
suggests that many of the eruptions during the Hawi were continuous, short duration events. In hand sample the aphyric Hawi lavas are quite distinct from the typically more porphyritic Pololu lavas. In the field, the massive lava flows of the Hawi Formation are distinguishable by their rough, hummocky surface which is in marked contrast to the typically thin (average 1 meter thick) pahoehoe flows of the Pololu Formation which form gentle slopes and rolling hill topography.

CHRONOLOGY

The absolute age of the subaerially exposed portion of Kohala Mountain is constrained by paleomagnetic and K-Ar studies. Doell and Cox (1965) found that all rocks exposed in the deeply dissected portions of Kohala Mountain had a normal direction of remanent magnetization indicating a maximum age of 700,000 years. Dating of the lower exposed section of the Pololu Formation using the K-Ar dating technique is hindered by the lavas youthful age, low K-content and susceptibility to weathering. Dalrymple (1971) attempted to date rocks collected from the lowest part of Waipio Valley and obtained widely varying ages (0.46-1.28 Ma, weighted mean= 0.68 ± 0.15 Ma) which did not correlate with their relative stratigraphic position. Potassium loss in these rocks is indicated by their low K_2O contents (.06-.15 wt%). Rocks collected by Feigenson et al. (1983) from similar stratigraphic levels in Waipio Valley containing low K_2O contents similar to those analyzed by

Dalrymple, are characterized by anomalously high $\text{TiO}_2/\text{K}_2\text{O}$ ratios (14-18) compared to $\text{TiO}_2/\text{K}_2\text{O}$ ratios observed in unaltered tholeiites on Kilauea and Mauna Loa (4.95-7.80) at similar TiO_2 concentration. Furthermore, Sibray (1977) found that in Pololu tholeiites most of the K_2O is concentrated in the residual potash-silica rich glass (up to 8.0 wt% K_2O) which is very susceptible to leaching during weathering processes. Thus, some of Dalrymple's samples had probably undergone some potassium loss during weathering causing the anomalously old K-Ar ages (>0.60 Ma for 4 out of 5 samples). McDougall (1972) determined K-Ar dates on 6 Pololu samples collected from the section exposed in Pololu Valley and from the uppermost olivine phyric flows exposed in Waipio Valley which have more typical Hawaiian tholeiitic-type potassium contents (0.17-0.55 wt% K_2O) and obtained dates ranging from 0.33-0.45 Ma. Three, more evolved samples collected south of Mahukona along the Kawaihae to Hawi road gave ages ranging from 0.34-0.40 Ma (McDougall and Swanson, 1972). Six additional samples collected from Kohala's leeward side by Dalrymple (1986, personal communication) give ages ranging from 0.32-0.44 Ma. An additional age obtained by Lanphere and Frey (1986) for an uppermost, alkalic Pololu flow exposed along the Kawaihae-Hawi road yielded a date of 0.32 Ma. Because there is no geologic evidence for any significant time break within the sections exposed in Waipio and Pololu Valleys, the oldest exposed rocks on Kohala are probably only slightly older than those dated by McDougall at the base of Pololu Valley. The narrow range of ages for dated rocks suggests that a significant portion of the sub-aerially exposed shield building lavas on Kohala (600 m) were erupted from 0.45 to 0.32 Ma (Figure 3). The presence of weathering horizons

Figure 3. Compilation of measured K-Ar age dates for Kohala lavas. Dates found in McDougall and Swanson (1972), Malinowski (1977), Lanphere and Frey (1986) and Dalrymple (pers. comm.).



between flow units towards the top of the Pololu section suggests that eruptive activity either waned toward the end of shield building activity or that the eruptions were of a more explosive nature during the later stages of activity, which would have presumably produced thicker deposits of more easily eroded ash and vesicular cinder.

Reported potassium-argon age dates for seventeen Hawi lavas range from 0.06-0.245 Ma (Figure 3). The oldest reported age (0.245 Ma, HW-20) is for a sample collected by McDougall (1972) which has a lower K_2O content (1.46 wt%) than any other definitive Hawi sample collected during this study. A sample (H_g85-23, $K_2O=1.44$ wt%) was collected from the same flow unit the past field season and was also initially mapped as Hawi based on its massive and aphyric character. However, its low P_2O_5 content (0.83 wt%) and lack of modal apatite suggest that this flow is similar to flows which are here termed "transitional". The fact that it bridges the time gap between Pololu and Hawi samples further attests to its transitional character.

For Hawi lavas, there is no obvious gradation in rock type with eruptive age (Figure 3). This interpretation is supported by the field relationships. In localities where relative stratigraphic position could be determined, no consistent trend was observed. For instance, within the Kawaihae Quadrangle, the oldest evolved hawaiite (almost mugearite) flow from Puu Pili was followed by a hawaiite flow from Puu Lapalapa, possibly followed by intrusion of a benmorite dome (Puu Makela) which was partially overrun by a mugearite flow from Puu Loa which is probably of similar age as a hawaiite flow from Puu Aiea. Based on this limited information, one can infer that the eruption of

the various rock types observed within the Hawi was chronologically random.

Porter (1979) collected a sample from the oldest exposed stratigraphic flow of the Hamakua Group on the western side of Mauna Kea and obtained an age of $.38 \pm .06$ Ma. Dating of additional flows from the Hamakua and Laupahoehoe Formations give ages ranging from 0.38-0.15 Ma and 0.12-0.04 Ma respectively (Porter 1979; Dalrymple, 1986 pers com). Comparison of these ages with those obtained for Kohala (Figure 3) suggests that the shield building lavas of Mauna Kea (Hamakua Group) were contemporaneous with eruption of the Pololu and Hawi Formations and that the alkalic capping stage (Laupahoehoe Group) began towards the end of Hawi activity and continued up until the mid-Holocene (4000 years ago). Fiske and Jackson (1972), on the basis of their analysis of rift zone trends, proposed that volcanism on Hualalai preceeded Mauna Kea. If this interpretation is correct, then extensive subaerial, shield building volcanism occurred contemporaneously on these three volcanoes. Additionally, it is important to bear in mind that although Hawi rocks represent less than 1% of the volume of subaerially exposed lavas on Kohala, they seem to have erupted over a roughly equivalent interval of time (0.15 Ma) as the subaerial portion of the shield.

"KOHALA-TYPE" ALKALIC CAPS

Macdonald (1962) used Kohala as the type locality for one of the two types of alkalic caps found on Hawaiian volcanoes. Kohala-type activity was characterized by the existence of an erosional unconformity between overlying evolved alkalic rocks (mugearite-trachyte) and underlying basalts in contrast to the "Haleakala type" where a succession of tholeiitic basalts passes upward without any widespread erosional break into a series of interbedded basalts, ankaramites and hawaiites. On Kohala the duration represented by local unconformities is difficult to estimate based on field evidence alone. The K-Ar ages suggest that the time interval between the eruption of evolved tholeiitic basalts in the upper Pololu and the alkalic rocks of the Hawi was less than 0.07 Ma (McDougall and Swanson 1972; Dalrymple, 1986 pers. comm). The oldest Hawi lavas are most likely buried within the infilling of the collapsed caldera at the summit (Stearns and Macdonald, 1946), and thus the oldest Hawi lavas have yet to be dated. Additional dating of "transitional" character lavas (ie. T_g⁸⁵⁻¹⁶, T_g⁸⁵⁻¹⁷) would also most likely close the existing gap between measured age dates. For example, the type-locality for Hawi activity described by Stearns and Macdonald (1946) turns out to be chemically and petrographically a "transitional" lava. Based on the degree of weathering of this flow, Stearns and Macdonald (1946) hypothesized that this was one of the oldest exposed Hawi flows. Mapping during this study has shown that this flow actually originated from a line of vents located southwest of

Puuokumau reservoir and is overlain by upper Pololu plagioclase-phyric lavas. The common occurrence of soil horizons between upper Pololu and Hawi flows simply reflects a decrease (rather than cessation) in eruptive activity since large parts of Kohala probably remained uncovered for relatively long periods of time before being buried by the more episodic eruptions which typified Hawi activity.

There are approximately 65 mappable eruptive centers of Hawi activity (this is a minimum estimate since some centers within the caldera complex were probably partially or totally buried by later activity). The continuity in ages for analyzed Hawi rocks (Figure 3) suggests that volcanic activity was relatively constant and that an eruption occurred on average a minimum of once every 3000 years during Hawi activity.

The other prime example of a "Kohala-Type" alkalic cap cited by Macdonald was West Maui. A detailed field and geochemical study of a part of West Maui was undertaken by Diller (1982) who found a thick hawaiite flow more than 100 meters below the shield building/alkalic stage contact in the east wall of Ukumehana Canyon. In addition, Wisham (1975) studied the Honolua area on west Maui and concluded that "It is possible that there was no real cessation in eruptive activity (between the Wailuku and Honolua Formations), but rather that the frequency of eruptions slowed with the change in rock types." Thus the transition from tholeiitic shield building to alkalic capping stages in Hawaii is uniformly characterized by a slowing rather than absolute cessation in eruptive activity. The subdivision of Hawaiian alkalic volcanism into two distinct types based on the chemical composition of eruptive

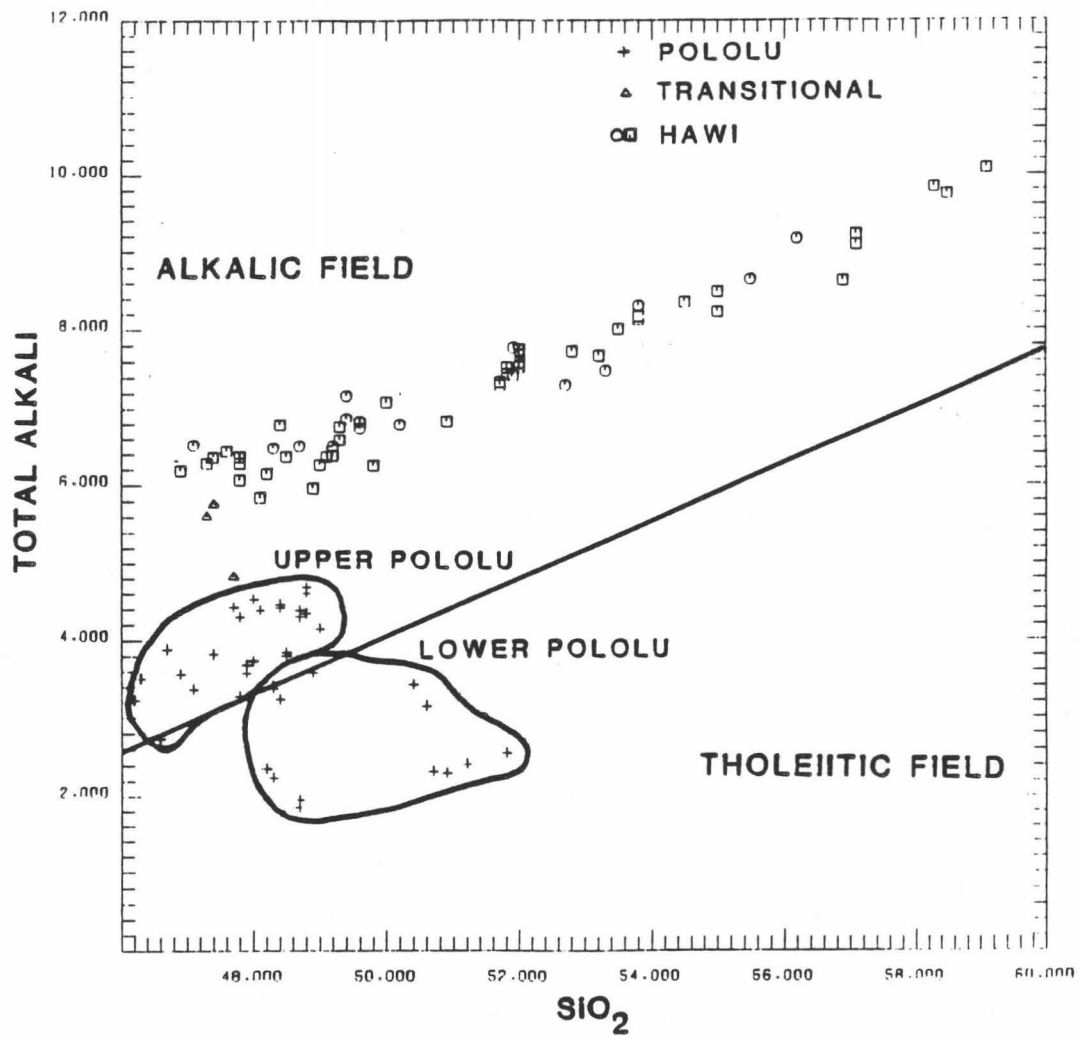
products and the duration of eruptive hiatus is less distinct than originally outlined by Macdonald (1970).

NOMENCLATURE

Macdonald and Katsura (1964) noted that the Hawaiian tholeiitic and alkalic suites show two distinct evolutionary trends: the tholeiites leading to iron enrichment, while the alkalic suite shows an enrichment in silica and alkalis and a lesser extent of iron enrichment. They produced a line which is based primarily on olivine fractionation from an inferred parental magma to discriminate between tholeiitic and alkalic lavas. The Macdonald-Katsura line (Macdonald and Katsura 1964) can be used to roughly discriminate between tholeiitic and alkalic lavas found in Hawaii (Figure 4). All Hawaiian lavas plot within the alkalic field as well as many of the more evolved rocks found in the upper Pololu, as has been observed on other Hawaiian volcanoes (i.e. Haleakala, Waianae; Macdonald and Katsura, 1964; Chen and Frey 1985).

The lavas erupted during the alkalic capping stage have always presented a problem in classification. In classifications in which plagioclase composition is the principle index, they fall into the andesite class. However, other workers have termed these rocks andesine or oligoclase basalts. Because Hawaiian "andesites" are quite distinct from the typical calc-alkaline andesites of continental margins and island arc environments, Macdonald (1966) proposed that the "andesite"

Figure 4. Alkali-silica diagram (in weight percent) for Kohala lavas. The dashed line is the Macdonald-Katsura line commonly used to distinguish between Hawaiian tholeiitic and alkalic rocks. Upper Pololu lavas are those lavas containing greater amounts of modal plagioclase than modal olivine (the type locality being the upper 100 meters of the Waipio Valley section).

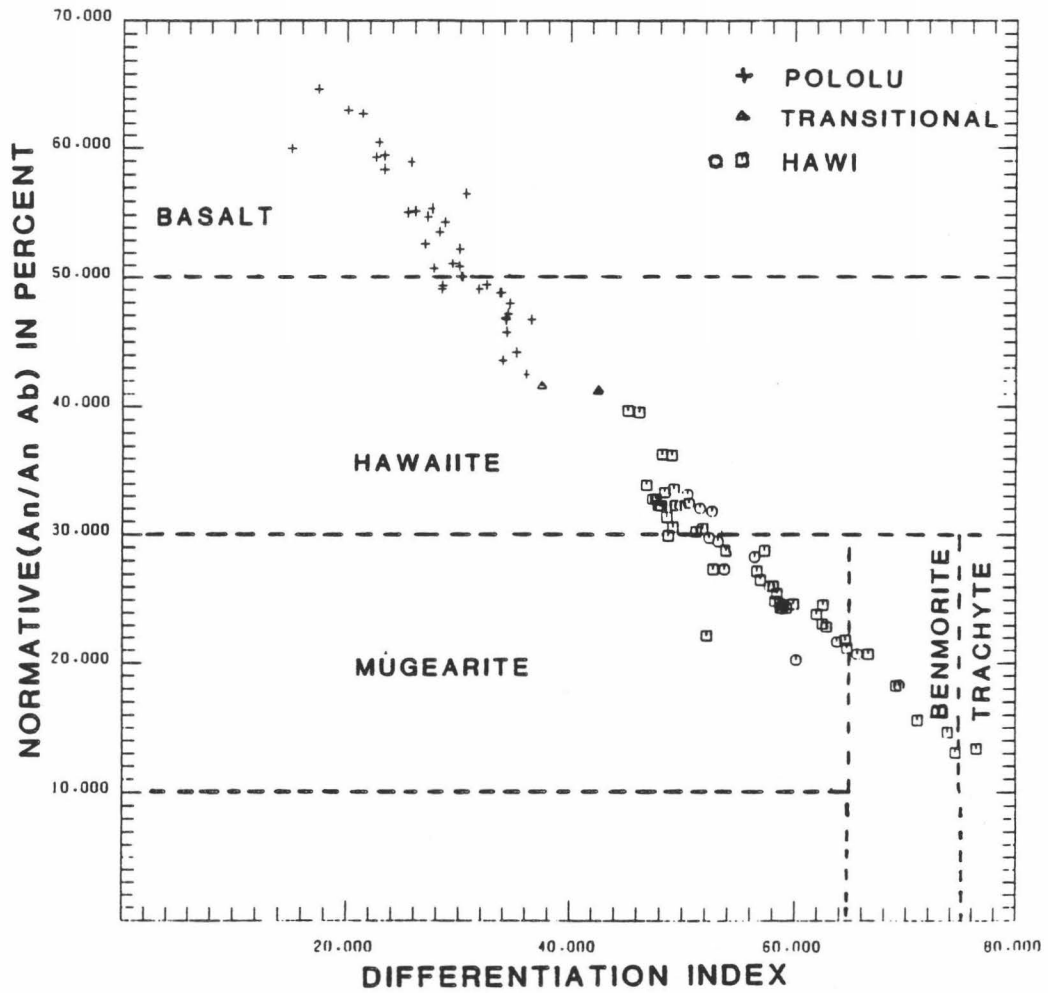


term be dropped for oceanic alkalic suite andesites, and that "hawaiite" be used in place of andesine andesites and "mugearite" be used in place of oligoclase andesite. Due to the difficulty in estimating modal compositions in these relatively aphyric rocks, the classification scheme of Coombs and Wilkinson (1969), which is based on the chemical parameters of DI index and normative plagioclase, was used. Figure 5 shows the boundary lines for the various rock types and the range of compositions observed on Kohala. Using this classification scheme, lavas in the Pololu formation range in composition from basalt for lavas found in the lower part of the section to hawaiite for lavas found near the top of the section. Transitional lavas also plot in the hawaiite field while Hawi lavas range in composition from hawaiite to trachyte.

PREVIOUS GEOCHEMICAL STUDIES

The reconnaissance mapping of Kohala Mountain by Stearns and Macdonald (1946) was the first modern geologic study of the area. They subdivided Kohala into two stratigraphic units; the older, predominately tholeiitic Pololu Formation and the younger, alkalic Hawi Formation. Macdonald and Katsura (1964) suggested that the two evolutionary trends observed in Hawaiian lavas resulted from different oxygen fugacities in the magma chambers during eruption of tholeiitic and alkalic lavas. Macdonald (1949, 1968) believed that these evolved alkalic lavas represented the most siliceous of the differentiation products of the

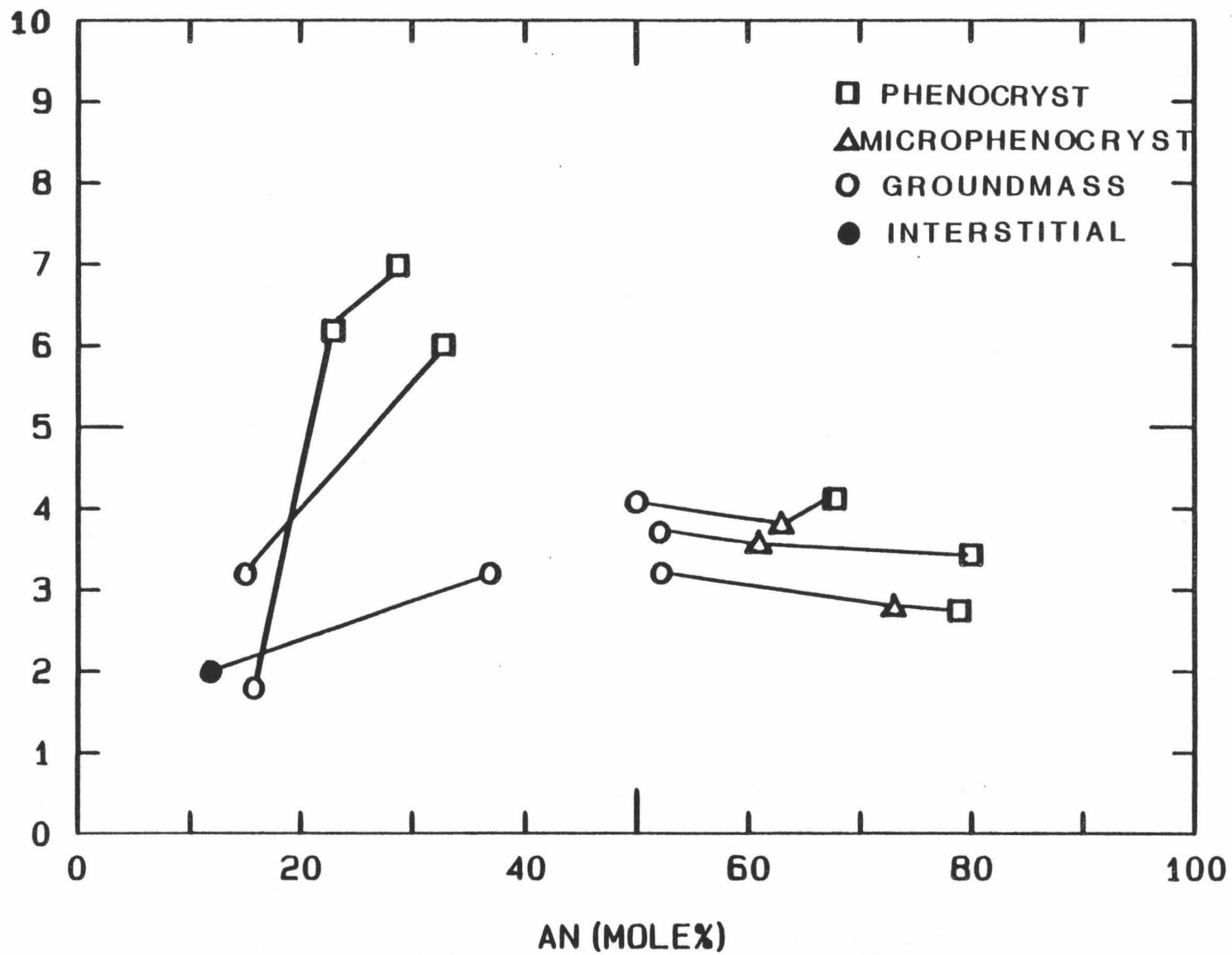
Figure 5. Classification scheme for basalt, hawaiite, mugearite, benmorite and trachyte (from Coombs and Wilkinson, 1969). The Differentiation Index is the sum of the normative Quartz, Orthoclase, Albite, Nepheline, Potassium Metasilicate and Leucite content of the rock.



volcanoes of Hawaii and were derived from the associated tholeiitic basalts by extensive fractional crystallization. Petrologic and chemical analysis of Kohala rocks can be found in Stearns and Macdonald (1946), Macdonald (1949), Macdonald and Katsura (1964) and Macdonald (1968). The field mapping and petrologic studies of the Kawaihae and Hawi Quadrangles by Malinowski (1977) and Giza (1979) contain additional chemical analyses as well as some microprobe data of mineral phases found in Hawi lavas. Sibray (1977) carried out an extensive microprobe study of the mineral phases found in Pololu and Hawi rocks and determined the phenocryst-matrix distribution coefficient for SrO in apatite and plagioclase as a function of rock type (Figure 6). He concluded that the high strontium contents observed in the intermediate members of the alkalic suite (hawaiites and mugearites) was due to the fractional crystallization of pyroxene and olivine outweighing the effects of the depletion of strontium produced by the fractional crystallization of plagioclase with high anorthite content (low Sr partition coefficient). Later fractional crystallization of apatite and more sodic plagioclase (with a higher Sr partition coefficient) depleted Sr in the later residual liquids (benmorites and trachytes). He further suggested that amphibole fractionation may have been important in the petrogenesis of the benmorites and trachytes. Furst (1982) undertook a study of the major element and isotopic variation ($\text{Sr}^{87}/\text{Sr}^{86}$) observed within the Hawi Formation and provided 40 new major element analyses of Hawi rocks. He found that rocks in the Hawi show a limited range in $^{87}\text{Sr}/^{86}\text{Sr}$ ratio from 0.7031 to 0.7036 in comparison to a single value of 0.7036 obtained for a Pololu tholeiite. Based on the observed major

Figure 6. Measured partition coefficient values for Sr in plagioclase for Hawi lavas as a function of plagioclase composition. Data taken from Sibray (1977).

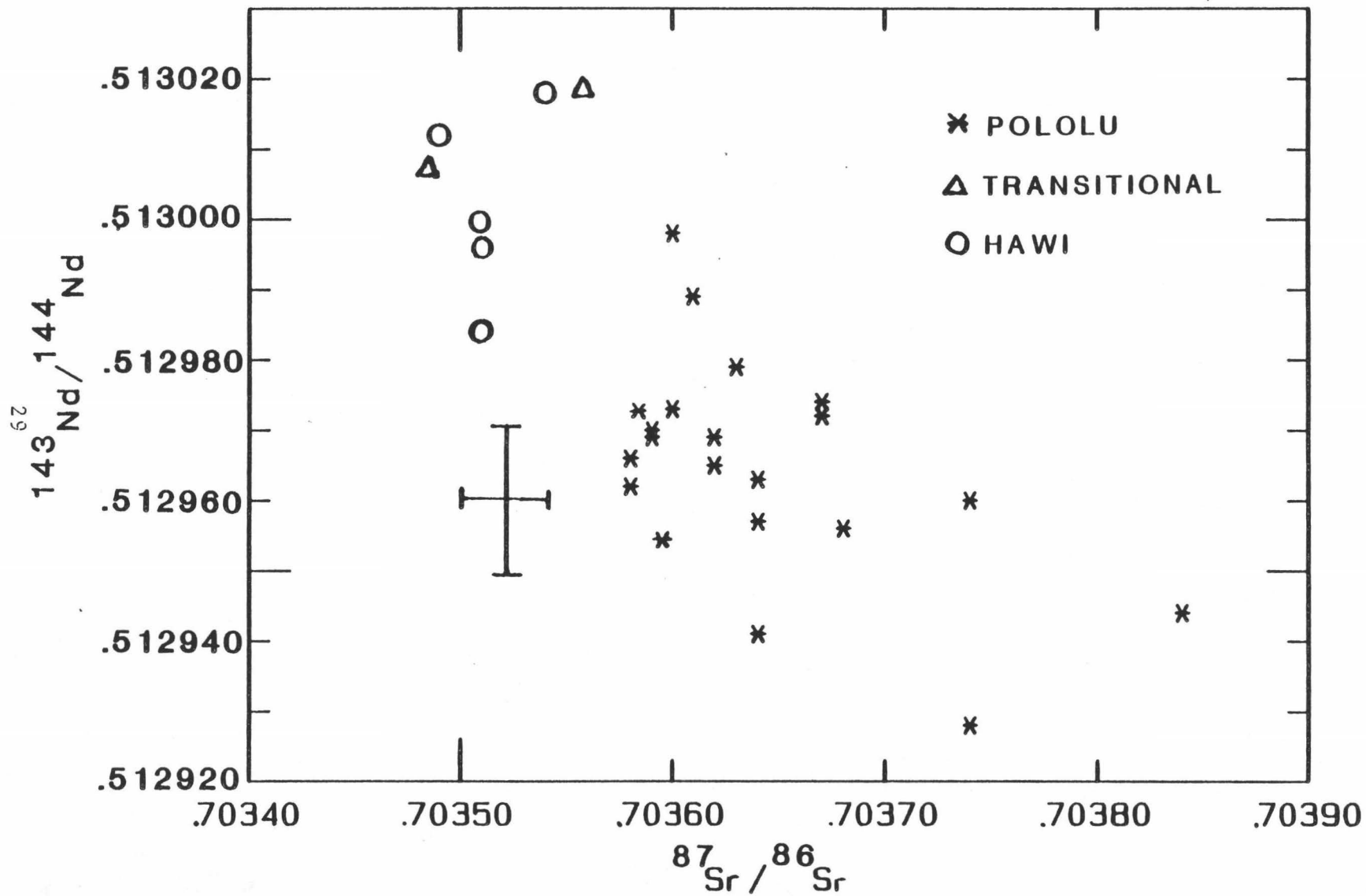
Kd Sr



element variations and the narrow range of Sr isotopic values obtained, he concluded that fractional crystallization of clinopyroxene, along with plagioclase, olivine, opaques and kaersutite controlled the evolution of the alkalic series. However, he also noted that clinopyroxene is not a liquidus mineral phase at the low pressures where fractionation was proposed to have taken place.

Feigenson et al. (1983) collected a stratigraphically controlled series of Pololu rocks from Waipio Valley and Mamaewa Gulch as well as alkalic rocks of the Hawi Formation originating from unspecified cones along the crest of Kohala. They concluded that the transition from the tholeiitic to alkalic stage is marked by a gradual and monotonic decrease in the degree of melting from a single, isotopically homogenous source. Feigenson and Spera (1981) proposed a model of viscous dissipation for generation of melt under Hawaii where a reduction in the shear stress that produces deformation causes both a decrease in the amount of mantle partial melting and an increase in the eruption interval. However, further isotopic work by Lanphere and Frey (1986) showed that Pololu and Hawi lavas are isotopically distinct and noted that the trend of $\text{MgO-P}_2\text{O}_5$ defined by Pololu samples does not extrapolate to the high $\text{MgO-P}_2\text{O}_5$ end of the Hawi field. This difference in isotopic content as well as other discontinuous chemical trends (i.e. $\text{P}_2\text{O}_5/\text{Nd}$) suggest that the inversion approach outlined by Hofmann and Feigenson (1983) can not be used to model the evolution of Pololu and Hawi lavas simultaneously. Hofmann et al. (1986) re-analyzed the rocks used in their previous study for $^{87}\text{Sr}/^{86}\text{Sr}$ and $^{143}\text{Nd}/^{144}\text{Nd}$ and found that there is in fact a gap in Sr isotope values between the Hawi and

Figure 7. $^{143}\text{Nd}/^{144}\text{Nd}$ vs. $^{87}\text{Sr}/^{86}\text{Sr}$ plot for Kohala lavas. Data from Hofmann et al. (1986).



the Pololu but that the Nd isotopic values overlap. The scatter observed on the resulting Nd-versus-Sr diagram (Figure 7) is much larger than can be ascribed to analytical error suggesting that more than two isotopically distinct sources contributed to volcanism on Kohala (Hofmann et al, 1986).

SAMPLE COLLECTION AND FORMATION ASSIGNMENT

One of the objectives of the field mapping study of Kohala was to collect a sample from each mappable surficial flow unit. Because the vast majority of eruptive centers during Hawi activity were concentrated along the previously existing rift zone trends, most of the Hawi samples collected on Kohala were taken from near the crest of Kohala. The localities of sampled flows are shown on Figure 1. The following criteria were used in order of relative importance to identify Hawi flows in the field: 1) location of a flow at the top of an exposed section (no lava of Pololu chemical characteristics has been observed overlaying a Hawi flow); 2) the thicker, non-vesicular character of Hawi flows tend to form pronounced ridges emanating away from the steep sided cinder cones produced during Hawi activity; 3) the dark, aphyric appearance of Hawi rocks; 4) the presence of an underlying soil horizon. Hawi lavas are characterized by the presence of apatite (a reflection of the anomalously high P_2O_5 contents of these lavas) and the absence of

pyroxene in the less evolved members of the Hawi suite (groundmass pyroxene is observed in evolved mugearites and benmorites).

Previous geochemical studies of Kohala have often misidentified upper Pololu lavas as belonging to the Hawi. Of the seven Hawi rocks that Feigenson et al. (1983) analyzed for REE and trace elements, three of them (KH11, KH14, KH16) are geochemically, as well as lithologically (in the case of KH11) more akin to alkalic Pololu rocks. A re-examination of the outcrops of these samples showed that they are not from the Hawi cones indicated by Feigenson et al (1983), but rather were overlain by the flows from these cones. However, there is no weathering horizon separating them from overlying Hawi lavas. Petrographically, they are similar to uppermost Pololu lavas (plagioclase phyrlic) and are unlike typical aphyric Hawi lavas. A rock collected during this study (P 84-9), which is separated from an overlying Hawi flow by a weathering horizon two feet thick, has major and trace element contents similar to these three rocks.

This sampling problem points out the occasional difficulty in distinguishing Pololu from Hawi rocks when randomly sampling surficial flow units (as in the case of Feigenson et. al., 1983). While Pololu rocks tend to be porphyritic, there do exist aphyric flows in the upper Pololu which lithologically are hard to distinguish in hand sample from Hawi rocks. Additionally, the presence of an underlying weathering horizon is not conclusive proof that a flow is Hawi since soil horizons also occur between flows in the upper part of the Pololu section. However, by using the four field criteria listed above, Hawi lavas can be recognized from Pololu lavas in the field in most instances. In the

rare cases where field criteria and petrographic criteria (i.e. absence or presence of apatite microphenocrysts) give conflicting interpretations, the discontinuous trends in chemical and isotopic characteristics between rocks obviously associated with Pololu and Hawi activity can be used to assign a rock of uncertain position ex post facto to the correct formation.

In this study, aphyric flows of uncertain origin which could not be chemically related in a simple manner to Hawi or Pololu lavas were termed "transitional". Transitional lavas are stratigraphically located at or near the top of the Pololu section, have intermediate chemical characteristics between Pololu and Hawi lavas, lack modal apatite and have an isotopic signature lying either within the Hawi field or between the previous gap which exists in measured $^{87}\text{Sr}/^{86}\text{Sr}$ ratios for Hawi and Pololu lavas. An example is sample T_g85-16 from Puu Kehena which was originally mapped as Hawi based on the aphyric character and youthful appearance of the flow. Chemically this flow is more evolved than upper Pololu flows and can not be successfully related to these lavas by simple fractional crystallization. A combination of variable degrees of partial melting in conjunction with fractional crystallization can better explain the observed chemical differences but the parameters for modelling this difference are largely unconstrained. Additionally this flow contains no modal apatite while having an isotopic content that lies within the Hawi field.

PETROGRAPHY

Thin sections of all samples analyzed for major elements (about 120 samples) were prepared for petrographic scrutiny. Special attention was paid to those rocks which were also analyzed for transition and rare-earth element contents. Olivine, opaque and apatite mineral compositions in samples representing the compositional range found on Kohala were analyzed using the Cameca microprobe at the University of Hawaii. In addition, modal point counts were taken of rocks spanning the compositional range in the Hawi (Table 1).

In describing these rocks, the terms phenocryst, microphenocryst, groundmass grain and interstitial material are used. Phenocrysts are usually at least 10 times the size of groundmass grains and in the rocks on Kohala, probably crystallized under intratelluric conditions. Grains that are somewhat larger (usually 2-9 times) than the average size of the groundmass grains are termed microphenocrysts. Groundmass grains are the smallest distinguishable crystals and are interpreted as forming late in the crystallization sequence, presumably upon cooling after extrusion. Phenocrysts are typically larger than 1 mm while groundmass grains are typically smaller than 0.1 mm with microphenocryst generally falling between these two size limits. The term interstitial is given to material typically of feldspar composition that fills the interstices between microphenocrysts and phenocrysts.

The Pololu samples from the dry westward side of Kohala, where the mapping activity during this study was concentrated, are predominately

Table 1. Modal analysis of Hawi lavas based on 1000 point counts per sample. Values are for both phenocryst and microphenocryst found in the rocks.

MODAL COMPOSITIONS (VOL%) OF HAWI LAVAS
 BASED ON 1,000 CTS/SAMPLE

SAMPLE	K ₂ O ROCK (WT%)	PLAGIOCLASE	OLIVINE	OPAQUE	APATITE	CLINOPYROXENE	AMPHIBOLE	GROUNDMASS
H _g -84-11	1.59	0	6	29	2	0	0	963
H _g -84-3	1.76	19	7	19	2	0	0	953
H _p -84-64	1.79	38	37	23	2	0	0	900
H _p -84-67	1.82	50	21	9	1	0	0	919
H _p -84-25b	2.02	5	6	22	2	1	0	964
H _p -84-15	2.08	2	6	15	3	1	0	973
H _g -84-2	2.12	20	29	21	5	0	0	925
H _p -84-54	2.30	70	34	17	3	0	0	876
H _g -84-10	2.35	22	13	11	1	0	0	953
H _p -84-21	2.56	37	8	5	2	1	0	947
H _g -84-1	2.74	107	36	19	2	4	1	831
H _g -84-5	2.82	80	6	20	2	8	2	882
H _p -84-61	3.41	35	10	12	2	3	10	928
H _p -84-14	3.43	45	0	21	2	4	1	927
H _p -84-22	3.45	23	1	11	2	1	1	961

porphyritic, moderately alkalic basalts. Because the majority of flows mapped on this side are surficial flows (rocks collected from Honokoa Gulch being an exception), sampled Pololu rocks are biased towards rocks erupted during the later stage of Pololu activity. In previous geochemical studies of Kohala (Feigenson et al. 1983; Lanphere and Frey 1986), the deeply dissected section from Waipio Valley, which represents the complete sub-aerially exposed portion of Kohala, was sampled. The shield building tholeiitic basalts from the bottom 200 meter portion of Waipio Valley are microcrystalline, containing less than 15% olivine phenocrysts ($\text{Fo}_{81.7-68.6}$) in a groundmass of acicular plagioclase (An_{79-46}) and small microphenocryst and groundmass grains of pyroxene ($\text{Wo}_{41.1-28.1}\text{En}_{46.6-46.2}\text{Fs}_{12.7-25.3}$). Ti-rich magnetite and ilmenite are present in the groundmass as small, subhedral grains whereas chromite is present as small inclusions in the olivine microphenocrysts (Feigenson et al., 1983).

Near the 200 meter level in the Waipio Valley section, plagioclase phenocrysts (5-15%) appear in conjunction with a decrease in olivine content to less than 5% (Feigenson et al. 1983, Stearns and MacDonald 1946). This petrographic change correlates with a discontinuous chemical jump from true tholeiitic rocks to more evolved alkalic basaltic compositions (higher TiO_2 , Al_2O_3 , Na_2O and P_2O_5 contents and lower MgO contents). Up-section (toward the Pololu-Hawi contact), the amount of modal plagioclase tends to increase. These transitional alkalic olivine basalts contain plagioclase (An_{80-52}), olivine (Fo_{82-73}) and augite ($\text{Wo}_{45.0-41.6}\text{En}_{43.9-41.5}\text{Fs}_{13.5-16.3}$) phenocrysts, but feldspar phenocrysts are by far the most abundant, comprising up to nearly 15% of

the mode and 90% of the phenocryst assemblage. Augite phenocrysts are very rare throughout the Pololu and are found in abundance only in the alkalic lavas erupted very late in the shield-building stage.

The most distinctive single feature of the alkalic lavas of the Hawi Formation is that they are consistently aphyric. Hawaiites found on Kohala are typically dark grey in color and sometimes glisten in hand sample due to the parallel to sub-parallel alignment of microcrystalline feldspar laths. They have a fine grained, intergranular texture with trachytic flow texture. The groundmass is much darker in color than the more evolved alkalic rocks on Kohala. Plagioclase (An_{48-32}) is the dominant mineral and occurs as subhedral to euhedral, zoned phenocrysts interspersed in the groundmass. The groundmass plagioclase grains are normally zoned and overlap in composition with the phenocrysts (An_{42-32}). Euhedral to subhedral magnetites and olivines (Fo_{82-68}), whose rims are slightly altered to iddingsite, are the next most abundant phases, and are primarily restricted to the groundmass. In some samples, very thin, colorless to pale green needles of clinopyroxene are present. Rare hexagonal, brownish phenocrysts of apatite (200 micrometers maximum) are also found dispersed within the groundmass commonly in contact with euhedral magnetites.

Mugearites are typically massive and very fine grained. They are lighter in color than hawaiites due to their increased plagioclase content. Most flows are aphyric (<10 modal percent microphenocrysts and phenocrysts), but some contain rare, relatively large phenocrysts of plagioclase. The rocks are almost always intergranular and composed predominantly of groundmass plagioclase laths. Trachytic flow textures

are also common in these lavas, presumably reflecting their high viscosity upon extrusion. Plagioclase phenocrysts and microphenocrysts (An_{51-32}) are mostly euhedral to subhedral and commonly exhibit albite and Carlsbad twinning. Olivine (Fo_{78-62}) is predominantly restricted to the groundmass, although some samples contain olivine microphenocrysts. Partial to complete alteration of olivine to iddingsite is quite common. Colorless to light green clinopyroxene ($Wo_{41.6}En_{42.6}Fs_{15.9}$) is confined to the groundmass. Magnetite is the predominant opaque phase and is typically euhedral. Small amounts (0.1-0.3 modal percent) of apatite occur in two forms; tiny needles, colorless to light brown in color, and as occasional large, euhedral, pinkish-brown pleochroic crystals that are commonly found associated with magnetite grains. Interstitial alkali feldspar is also present.

Benmorites are typically more porphyritic and lighter in color than the hawaiites and mugearites and are distinguished by the appearance of amphibole (kaersutite). Phenocrysts of kaersutite are often rounded with reaction rims of opacite which in places completely replaces the preexisting phenocryst. The groundmass is composed largely of untwinned, subhedral to anhedral grains of oligoclase (An_{30-22}). Andesine (An_{42-23}) again predominates as the phenocryst phase with subordinate amounts of kaersutite, aegirine-augite ($Wo_{43.1-46.1}En_{44.8-30.6}Fs_{12.1-23.3}$), olivine (Fo_{48-46}) and magnetite set in a very fine-grained groundmass composed almost entirely of feldspar. Apatite predominantly occurs as microphenocrysts in association with magnetite although it occasionally is included in amphibole. Olivine grains are subhedral and are almost entirely altered to iddingsite.

Biotite is also seen as an accessory phase in some samples. Kaersutite ranges from subhedral to anhedral in shape and sometimes replaces olivine. It is commonly surrounded by a fine-grained reaction rim of opacite which in places completely replaces it. Anorthoclase ($\text{Ab}_{70.9}\text{An}_{11.0}\text{Or}_{18.0}$) is also present as tiny groundmass grains.

The modal abundance of apatite in Hawi lavas is quite constant throughout the suite (Table 1). Small amounts of modal clinopyroxene and amphibole occur in evolved rocks containing approximately 2.60 weight percent K_2O and greater (near the mugearite-benmorite boundary). The lack of variation in the modal abundance of apatite suggests that apatite accumulation is not responsible for the anomalously high P_2O_5 contents observed in Kohala hawaiites (2.2 wt% vs. 1.0 wt% in benmorites). The absence of modal clinopyroxene in Kohala hawaiites and mugearites suggests that clinopyroxene was not a liquidus phase at low pressures and that shallow level fractionation of clinopyroxene did not occur. This is consistent with one atmosphere experimental work on a hawaiite from the Isle of Skye (Thompson, 1974) which indicates that clinopyroxene does not crystallize until the melt is 40-60°C below the liquidus.

Dunite nodules are the most common xenolith type found in Hawi lavas and are most commonly associated with hawaiites and mugearites. The olivine crystals are un-altered, anhedral and commonly exhibit kink-banding. The olivines are of uniform composition with high Fo contents (Fo_{89}) and opaque grains included within the olivine are chromite. Very rare dunite and gabbroic xenoliths also occur in a few flows of transitional alkalic rocks of the upper Pololu.

MINERAL COMPOSITIONS

Phenocryst and groundmass grains of olivine and magnetite were analyzed using the Cameca microprobe at the University of Hawaii. The microprobe was operated at an accelerating potential of 15 Kv and a sample current of 0.03 microamps. Standard correction was made for background and drift by periodically analyzing mineral standards of known composition. The counting time per analysis was 10 seconds and each grain was analyzed in at least 8 different points. These analyses in conjunction with previous microprobe analyses of mineral phases observed in Kohala lavas (Sibray, 1977; Malinowski, 1977; Nichols, 1985, personal communication), form a large body of mineral compositional data for crystal fractionation modelling. Mineral data for the major phases present in Kohala lavas are given in Tables 2-6 along with host rock K_2O content. Compositional data for accessory phases such as kaersutite and biotite can be found in Sibray (1977).

The olivines found in the alkalic suite show a decrease in Fo content as differentiation proceeds and range in composition from Fo_{74} in the hawaiites to Fo_{46} in the benmorites (Table 2). The amount of Mn in the olivines increases drastically from about 0.60 wt % in hawaiites up to 2.4 wt % in benmorites. Roeder and Emslie (1970) showed that olivines in equilibrium with the basaltic melts from which they were crystallized have a nearly constant ratio of $(FeO/MgO)_{rock} / (FeO/MgO)_{olv}$ of 0.30 independent of temperature. The olivines found in hawaiites (FeO/MgO whole rock ratio of 2.5-3.0) are for the most part too

Table 2. Olivine compositions found in Kohala lavas. Analysis from Sibray (1977) and this study.

OLIVINE

ROCK TYPE	DUNITE		THOLEIITE		TRANSITIONAL			HAWAIIITE		MUGEARITE			BENMORITE	
SAMPLE #	----	P _g -84-9		II-47-74	II-19-74	II _g -85-16	II-4-74	II _p -84-64	II-22-74	II _g -84-2	II-28-74	II-11-74		
ANALYST	S.S.	S.S.	Sib	Sib	S.S.	Sib	S.S.	Sib	S.S.	Sib	Sib	Sib		
K ₂ O ROCK (WT%)	---	0.32	0.43	1.36	1.47	1.63	1.79	1.90	2.12	2.58	2.88			
GRAIN ANALYZED	ph	ph rim	ph core	mph	mph rim	mph core	g	g	g	mph rim	mph core	g	g	
SiO ₂	39.69	38.05	38.59	38.90	37.70	37.12	37.70	37.30	36.50	37.40	35.56	35.76	34.60	35.10
TiO ₂				0.07	0.08			0.14		0.20			0.04	0.06
FeO	10.94	20.90	18.81	20.40	24.10	25.37	22.23	25.30	26.93	23.30	32.44	31.61	41.10	42.40
MnO				0.26	0.37			0.60		1.06			2.41	2.25
MgO	48.54	40.42	42.46	39.80	36.90	37.79	40.09	35.10	35.45	36.40	30.85	31.38	20.90	20.20
CaO				0.60	0.57			0.53		0.59			0.32	0.48
NiO				0.18	0.14			0.02		--			--	--
TOTAL	99.17	99.32	99.86	100.21	99.9	100.28	100.02	99.00	98.88	99.00	98.85	98.75	99.40	100.50
mole %														
Fo	88.9	77.7	80.2	77.6	73.2	72.9	76.3	71.2	70.3	73.6	63.2	64.1	47.5	45.9
Fa	10.1	22.3	19.8	22.4	26.8	27.1	23.7	28.8	29.7	26.4	36.8	35.9	52.5	54.1

magnesian to be in equilibrium with the liquid in which they are found (Figure 8). Most of the olivines probed were small, groundmass grains which showed no obvious disequilibrium textures. It is possible that early fractionation of oxides (suggested by the rapid decrease in TiO_2 abundance in hawaiites (Figure 14)) lowered the FeO/MgO ratio of the residual liquid. Subsequent olivine crystallization from this residual liquid yielded more forsteritic olivine than predicted by the whole rock FeO/MgO ratio and a D of 0.30. Olivines found within the more evolved mugearites (Fe/Mg Whole Rock 3-4) seemingly had enough time to re-equilibrate with the Fe-Ti depleted residual liquid. Olivines found in the benmorites are very iron-rich and plot off the experimental equilibrium trend. The rocks used in the experimental study of Roeder and Emslie(1970) were basaltic in composition. Extrapolation of this trend to more evolved compositions may not be valid, especially for rocks which have undergone large amounts of iron loss due to magnetite fractionation.

The predominant opaque phase in Hawi lavas is titaniferous magnetite. Magnetites found in the hawaiites have generally higher titanium and magnesium contents and lower manganese contents than those in the more differentiated Hawi lavas (Table 3).

Plagioclase phenocrysts and groundmass grains are observed to increase in albite and orthoclase content in going from hawaiite to benmorite (Table 4). Sibray (1977) used long counting times (80 to 200 seconds) and up to 20 point analyses per plagioclase grain to accurately measure the SrO content of Kohala plagioclases by microprobe. Figure 6 shows the measured variation of the distribution coefficient of Sr as a

Figure 8. Fe/Mg ratios of olivines found in Kohala lavas as a function of whole rock Fe/Mg. Of note are olivines found in the hawaiites (Fe/Mg 2.5-3.0) which are too forsteritic to be in equilibrium with whole rock composition. This could be due to the rapid depletion of iron content by magnetite crystallization which gives rise to a residual liquid with a low FeO/MgO ratio from which a more forsteritic composition olivine can crystallize..

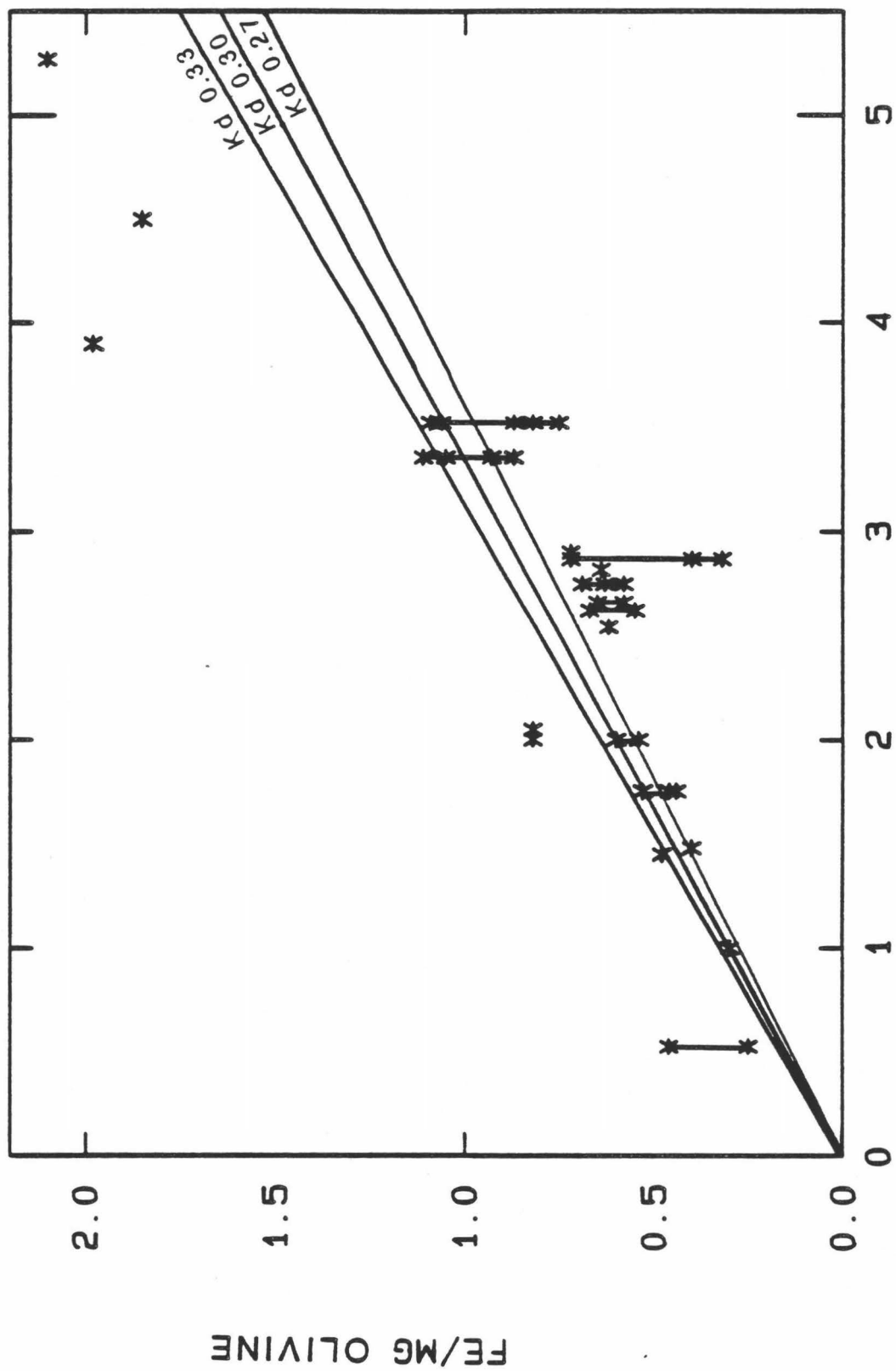


Table 3. Opaque compositions found in Kohala lavas. Analysis
from this study.

OPAQUE

ROCK TYPE	DUNITE	THOLEIITE	TRANSITIONAL				HAWAIIITE		MUGEARITE		BENMOREITE	TRACHYTE
SAMPLE #	----	P _g -84-9	II _g -85-17	II _g -85-16	II _g -84-11	II _p -84-67	II _g -84-2	II _g -84-10	II _p -84-89	II _p -84-61		
K ₂ O ROCK (WT%)	--	0.32	1.34	1.47	1.59	1.82	2.12	2.35	2.55	3.41		
GRAIN ANALYZED	ph	ph	ph	g core rim	ph	ph	ph	mph	mph	mph		
MnO	--	--	0.53	0.65	0.63	0.64	0.85	1.24	1.13	1.24	1.70	1.41
MgO	10.97	9.92	2.52	1.76	3.27	2.81	3.29	2.79	2.49	2.42	1.95	1.29
Al ₂ O ₃	14.21	14.89	2.19	1.18	3.63	2.61	2.08	1.60	0.87	1.80	0.94	1.56
FeO	27.87	31.05	68.1	70.9	68.9	68.85	67.86	73.23	70.45	71.19	72.96	71.39
TiO ₂	2.37	2.82	23.9	24.5	23.7	24.46	24.68	19.78	23.84	20.22	21.50	22.42
Cr ₂ O ₃	42.64	41.84	0.90	0.11	---	---	---	---	---	---	---	---
TOTAL	98.01	100.52	98.1	99.1	100.0	99.37	98.76	98.64	98.78	96.87	99.05	98.07

Table 4. Plagioclase compositions found in Kohala lavas.
Analysis from Sibray (1977) and Malinowski (1977).

PLAGIOCLASE

ROCK TYPE	THOLEIITE		TRANSITIONAL		HAWAIIITE		MUGEARITE		BENMORITE	
SAMPLE #	H-32-74	H-23-74	H37-74	H-19-74	H-4-74	C-12-1	H-45-74	H-22-74	H-28-74	H-11-74
ANALYST	Sib	Sib	Sib	Sib	Sib	Mal	Sib	Sib	Sib	Sib
K ₂ O ROCK (WT%)	0.32	0.62	1.28	1.36	1.63	1.56	1.76	1.90	2.58	2.88
GRAIN ANALYZED	g	ph	ph	ph	ph	mph	g	g	ph	mph
SiO ₂	52.20	48.80	47.70	50.90	59.50	57.83	56.30	59.30	58.98	60.40
Al ₂ O ₃	30.30	32.50	33.30	31.60	25.20	26.77	27.40	24.90	26.00	25.10
FeO	0.97	0.65	0.81	0.73	0.38	0.86	1.01	1.02	0.42	0.38
CaO	13.90	16.10	16.40	14.10	7.15	7.76	8.96	7.70	6.98	5.98
Na ₂ O	3.54	2.24	2.20	3.48	6.64	5.85	5.88	6.51	6.69	6.99
K ₂ O	0.12	0.13	0.12	0.24	0.48	1.04	0.42	0.57	0.58	0.80
SrO	0.08	0.12	0.21	0.23	0.77	--	0.71	0.56	0.67	0.95
TOTAL	101.11	100.50	100.17	100.70	100.12	100.44	100.70	100.60	100.44	100.60
MOLE %										
Ab	31.4	19.9	19.4	30.6	60.8	54.0	53.0	58.4	61.3	64.6
An	67.9	79.3	79.8	68.1	36.3	40.0	44.5	38.2	35.3	30.6
Or	0.7	0.8	0.8	1.3	2.9	6.0	2.4	3.4	3.4	4.9

function of An content of the plagioclase. Distribution coefficients as large as 7 have been measured for plagioclases found in Hawi lavas. Because of these large values, plagioclase should exert a strong control on the observed Sr content in Hawi lavas.

Pyroxenes are either absent or too small for analysis by microprobe in hawaiites and most mugearites. Sibray (1977) analyzed a groundmass augite in a mugearite and a microphenocryst in a benmorite. The pyroxene in the benmorite has a higher Fs content and larger amounts of Na_2O and MnO as would be expected from crystallization from a more evolved magma (Table 5). Their compositions are similar to values reported for augites in evolved alkalic lavas on Maui (Fodor et al, 1975).

An interesting aspect of the apatite analyses is their compositional similarity in rocks of widely different compositions (Table 6). Many of the apatites found in the highly evolved rocks are found as inclusions in magnetite and amphibole and thus their composition could possibly reflect the chemistry of the magma at an earlier stage of differentiation. This is further suggested by the similar Sr contents of apatites found as inclusions in the benmorites and the groundmass apatites found in the more Sr-rich hawaiites and mugearites. The measured distribution coefficient of Sr between apatite and matrix ranges from 2.3 to 2.5. The increase in fluorine content of apatite in going from core to rim suggests that they are normally zoned (Nichols, pers. comm.).

Table 5. Pyroxene compositions found in Kohala lavas. Analysis from Sibray (1977).

PYROXENE

ROCK TYPE	THOLEIITE		TRANSITIONAL		MUGEARITE	BENMORITE
SAMPLE #	H-32-74	H-23-74	H-37-74	H-19-74	H-22-74	H-11-74
ANALYST	Sib	Sib	Sib	Sib	Sib	Sib
K ₂ O ROCK (WT%)	0.32	0.62	1.28	1.36	1.90	2.88
GRAIN ANALYZED	ph	ph	ph	ph	g	mph
SiO ₂	51.60	51.40	49.00	50.30	53.10	53.60
TiO ₂	0.96	0.96	2.51	1.80	1.36	0.38
Al ₂ O ₃	2.32	3.04	4.54	4.78	2.22	0.46
Cr ₂ O ₃	0.16	0.17	0.04	0.34	--	--
FeO	12.70	7.80	9.66	8.11	7.59	13.20
MnO	0.28	0.18	0.21	0.16	0.33	0.63
MgO	16.10	15.90	13.00	14.00	14.30	9.34
CaO	15.50	19.70	21.20	21.10	20.00	20.40
Na ₂ O	0.27	0.36	0.48	0.45	0.83	1.17
TOTAL	99.90	99.50	100.60	101.00	99.70	99.20
En	46.9	46.2	38.8	41.5	43.3	30.6
Fs	20.6	12.7	16.3	13.5	13.0	23.3
Wo	32.5	41.1	44.9	45.0	43.7	46.1

Table 6. Apatite compositions found in Kohala lavas. Analysis from Sibray (1977) and Nicholls (personal communication).

ROCK TYPE	APATITE													
	HAWAIIITE					NUGEARITE					BENBORITE			
SAMPLE #	II-4-74	II 84-3			II-45-74	II-22-74	II 84-25b					II-28-74	II 84-62	
ANALYST	Sib	core	rim	gmass	Sib	Sib	core	rim	core	rim	gmass	Sib	core	rim
K ₂ O ROCK (WT%)	1.63	1.76			1.76	1.90	2.02					2.58	3.07	
GRAIN ANALYZED	mph	mph			mph	ph	ph					mph	ph	
SiO ₂	-	0.18	0.19	0.14	-	-	0.14	0.22	0.14	0.31	0.17	-	0.08	0.12
Al ₂ O ₃	0.87	>0.04	>0.04	>0.04	0.83	0.82	>0.04	>0.04	>0.04	>0.04	>0.04	0.87	>0.04	>0.04
FeO	-	1.28	0.93	0.77	-	-	0.76	1.37	0.61	0.82	0.95	-	0.53	0.52
MnO	-	0.07	0.07	0.08	-	-	0.09	0.09	0.09	0.08	0.10	-	0.13	0.11
NiO	-	0.49	0.37	0.49	-	-	0.54	0.49	0.42	0.43	0.48	-	0.43	0.42
SrO	0.40	-	-	-	0.42	0.40	-	-	-	-	-	0.39	-	-
CaO	52.70	53.68	53.79	53.88	53.60	53.80	53.13	52.82	53.54	53.30	53.36	53.50	53.27	53.63
P ₂ O ₅	40.5	40.63	40.58	40.92	40.60	41.20	40.24	40.11	40.72	40.61	40.58	41.10	40.80	40.61
F	4.64	3.42	3.73	3.75	4.45	3.59	2.44	3.33	3.52	3.55	3.45	4.20	2.00	2.63
Cl	0.48	-	-	-	0.28	0.44	-	-	-	-	-	0.30	-	-
TOTAL	99.60	99.68	99.60	99.89	98.30	98.30	97.34	98.43	99.04	99.21	99.09	98.60	97.24	98.04
PPM														
La		DL	>263	>290			>560	DL	>350	>325	>475		>790	>245
Ce		>589	>210	>120			>240	>755	>860	>480	>530		1990	>585
Pr		>30	DL	>70			DL	115	>275	DL	>110		>141	>65
Nd		DL	>650	>520			905	805	>500	845	>635		920	>870

> = Below Detection Limit

DL = Gives negative counts/second

APATITE

ROCK TYPE	BENMOREITE			TRACHYTE		
	SAMPLE #	core	Prim	gmass	core	Prim
ANALYST		Nic		Nic		
K ₂ O ROCK (WT%)		3.07		3.41		
GRAIN ANALYZED		mph		mph		
SiO ₂	0.17	0.14	0.26	0.17	0.26	0.21
Al ₂ O ₃	0.19	>0.04	0.08	>0.04	0.35	>0.05
FeO	0.73	0.56	1.02	0.97	1.75	2.10
MnO	0.10	0.07	0.10	0.13	0.14	0.12
NiO	0.48	0.44	0.45	0.38	0.23	0.24
SrO	-	-	-	-	-	-
CaO	53.77	54.00	53.46	53.18	52.55	52.88
P ₂ O ₅	40.75	40.99	40.42	40.02	39.60	39.73
F	2.82	3.48	3.12	3.68	3.81	3.78
Cl	-	-	-	-	-	-
TOTAL	99.01	99.61	98.91	98.53	98.69	99.11
PPM						
La	>385	>570	>440	>490	>385	>475
Ce	>1100	>610	>770	>1025	1529	>285
Pr	>30	>30	>70	>173	>50	>150
Nd	955	750	>640	865	>532	860

ANALYTICAL METHODS

Major element analysis of the rocks was performed by USGS technicians using X-ray fluorescence spectroscopy at the USGS's Branch of Analytical Chemistry at Lakewood, Colorado. The H_2O and CO_2 contents of the rocks were also determined by the USGS using a CHN analyzer. Great effort was taken to collect only the freshest, least altered rocks available from a given flow unit for analysis. Thin sections of each analyzed sample were prepared. Samples were chosen for further analyses by INAA and XRF based on freshness as determined by petrographic analysis of the slides (degree of alteration of mineral phases) and low measured water contents. Based on replicate analyses of USGS standard rocks BCR-1 and BHVO-1, the precision for the major elements is stated to be better than 1% for SiO_2 , Al_2O_3 , FeO, CaO, K_2O and TiO_2 , 2% for MgO and 5% for Na_2O and P_2O_5 (Wright, personal communication). Na_2O abundances were also determined by INAA whose precision is better than 2% (Chen and Frey, 1985). The average deviation of Na_2O values obtained by XRF and INAA for the same crushed powder is 2%. Transition metal abundances were determined by INAA at MIT (Sc, Cr, Co) and by XRF at the University of Massachusetts (V, Cr, Ni, Zn). Ba, Zr, Rb, Nb and Sr abundances were determined by myself using X-ray fluorescence at the University of Massachusetts. The abundances of rare-earth elements, Hf, Ta and Th were determined by myself using INAA at MIT. Chen and Frey (1985) reported that the average standard deviations for five replicate INAA analyses of an alkalic lava from Haleakala ranged from 1 to 3% for

Sc, Co, Na, La, Sm, 4 to 6% for Nd, Eu, Tb, Cr, and 7 to 12% for Hf, Ta, Th, Lu and Yb. The reported analytical precision of XRF analysis at the University of Massachusetts is 0.6-1.0% for Rb, Sr, Y, Zr and Zn, 2.0-3.5% for V and Nb, 5% for Ga and about 25.0-30.0% for Ni and Cr for replicate analysis of standard BCR-1. Major element data for analyzed Kohala lavas are presented in Table 7; trace element data for these same lavas are given in Table 8.

PETROGENESIS

The small range in $^{143}\text{Nd}/^{144}\text{Nd}$ values observed in the Hawi (0.512982-0.513018) precludes the derivation of these rocks from an isotopically uniform source (Figure 7). In reality, the assumption that a suite of samples erupted over long time intervals is cogenetic has often been shown to be in error once the isotopic abundances have been accurately measured (eg. Hawkesworth et. al. 1979, Lanphere and Frey 1986). If one observes that the isotopic variability is either random or of negligible magnitude, relevant petrogenetic processes affecting a suite of rocks can still be deduced from geochemical modelling. The plot of $^{87}\text{Sr}/^{86}\text{Sr}$ vs. $^{143}\text{Nd}/^{144}\text{Nd}$ (Figure 7) shows that the isotopic variation is not well correlated for Hawi samples as would be expected if the isotopic variation was systematic within the source region(s) (ie. two-end member mixing model). While the $^{87}\text{Sr}/^{86}\text{Sr}$ values for Hawi

Table 7. Whole rock major element analysis of rocks further analyzed for trace elements. Analysis were made by XRF at the USGS's Branch of Analytical Chemistry at Lakewood.

609

	POLOLU FORMATION				TRANSITIONAL		HAHI FORMATION					
	P _P 84-11	P _P 84-9	P _P 85-44	P _P 85-45	T _R 85-17	T _R 85-16	H _P 84-11	H _P 84-3	H _P 84-64	H _P 84-67	H _P 84-25b	H _P 84-2
SiO ₂	48.70	51.80	47.80	45.80	47.70	47.30	47.60	49.30	49.30	49.80	51.70	52.80
TiO ₂	1.88	2.28	3.36	2.98	3.83	3.52	3.02	2.63	2.57	2.67	2.18	2.03
Al ₂ O ₃	10.40	14.00	14.00	14.50	14.90	16.70	15.90	16.60	16.60	17.10	16.90	17.20
Fe ₂ O ₃	13.10	12.10	13.50	14.00	14.10	13.10	13.20	12.00	12.10	11.60	10.70	10.40
MnO	0.17	0.17	0.18	0.18	0.22	0.19	0.23	0.23	0.24	0.22	0.24	0.24
MgO	15.90	6.91	7.06	7.80	5.10	4.99	4.59	3.94	3.45	4.00	3.29	3.10
CaO	8.66	11.00	10.70	10.50	7.99	7.66	7.56	7.04	6.14	7.12	5.93	5.59
Na ₂ O	1.61	2.24	2.77	2.66	3.59	4.11	4.85	5.00	5.01	4.43	5.32	5.60
K ₂ O	0.25	0.32	0.80	0.76	1.34	1.47	1.59	1.76	1.79	1.82	2.02	2.12
P ₂ O ₅	0.17	0.22	0.50	0.39	0.77	0.93	2.28	1.96	1.97	1.63	1.57	1.47
SUM	100.84	101.04	100.67	99.57	99.54	99.97	100.82	100.46	98.96	100.39	99.85	100.55
H ₂ O	0.04	0.01	0.20	1.49	1.01	0.01	0.01	0.09	0.40	0.01	0.35	0.01
Or	1.50	1.90	3.80	3.60	7.90	8.70	9.40	10.40	10.60	10.80	11.90	12.50
Ab	13.60	19.00	22.30	20.30	29.50	32.30	37.00	40.30	40.60	37.50	45.00	47.40
An	20.40	27.20	27.50	28.90	21.00	22.60	16.90	17.70	17.60	21.40	16.30	15.50
Ne	0.00	0.0	0.00	0.00	0.00	1.50	2.20	1.10	0.00	0.00	0.00	0.00
Pl	34.00	46.20	49.70	45.60	50.60	55.00	54.00	58.00	58.20	58.90	61.30	62.90
Di	17.20	21.30	21.80	18.90	11.20	7.60	4.70	3.70	0.00	2.70	2.40	2.20
Hy	7.20	19.80	5.80	6.90	9.40	0.00	0.00	0.00	7.40	5.80	1.60	0.30
Ol	14.40	0.0	9.70	13.40	6.50	13.80	15.00	13.60	8.80	9.40	11.20	11.80
Nt	2.30	2.10	2.30	2.50	3.80	3.50	3.50	3.20	3.20	3.10	2.90	2.80
Il	3.60	4.30	5.80	4.50	7.30	6.70	5.70	5.00	4.90	5.10	4.10	3.90
Ap	0.50	0.50	0.90	0.80	1.80	2.20	5.30	4.50	4.60	3.80	3.60	3.40

Table 7 continued

HAWI FORMATION

	II 85-25 E	II 84-10 E	II 84-21 P	II 84-79 P	II 84-62 P	II 84-61 P
SiO ₂	53.80	54.50	53.80	55.00	57.10	58.50
TiO ₂	1.69	1.74	1.92	1.46	1.46	1.17
Al ₂ O ₃	17.40	17.40	17.20	17.60	17.80	17.50
Fe ₂ O ₃	9.26	9.45	9.15	9.56	7.69	6.65
MnO	0.25	0.25	0.19	0.24	0.17	0.18
MgO	2.80	2.62	2.44	2.27	1.54	1.49
CaO	4.81	4.77	5.14	4.40	3.46	2.87
Na ₂ O	6.03	6.00	5.60	5.47	6.02	6.34
K ₂ O	2.27	2.35	2.56	2.75	3.07	3.41
P ₂ O ₅	1.23	1.22	1.30	1.03	0.89	0.72
SUM	99.54	100.30	99.87	99.78	99.20	98.83
H ₂ O	0.40	0.01	0.57	0.23	0.76	1.06
Or	13.40	13.90	15.10	16.30	18.10	20.20
Ab	49.60	50.80	47.40	46.30	50.90	53.60
An	13.70	13.60	14.20	15.10	11.40	9.20
Ne	0.80	0.00	0.00	0.00	0.00	0.00
Pl	63.30	64.40	61.60	61.40	62.30	62.90
Di	1.80	1.70	2.30	0.00	0.00	0.30
Hly	0.00	0.30	2.70	9.00	10.50	7.60
Ol	11.00	10.60	7.60	4.60	0.30	1.80
Nt	2.50	2.50	2.40	2.50	2.10	1.80
Tl	3.20	3.30	3.60	2.80	2.80	2.20
Ap	2.80	2.80	3.00	2.40	2.10	1.70

Table 8. Trace element concentrations of Kohala lavas analyzed in this study. La, Ce, Nd, Sm, Eu, Tb, Yb, Lu, Ta, Th, Hf, Co and Sc concentrations were determined by instrumental neutron activation at MIT and Zr, Nb, Y, Rb, Ba, Sr, Cr, Ni, V and Ga concentrations were determined by XRF at the University of Massachussets.

	POLOLU FORMATION				TRANSITIONAL			HAWI FORMATION				
	P 84-11 P	P 84-9 P	P 85-44 P	P 85-45 P	T 85-17 P	T 85-16 P	H 84-11 P	H 84-3 P	H 84-64 P	H 84-67 P	H 84-25b P	H 84-2 P
Rb	3.6	19.3	3.9	8.4	25.3	31.4	28.0	35.9	31.4	31.9	42.1	47.0
Sr	222.7	281.9	511.9	492.2	685.4	1193.9	1854.4	1720.5	1650.0	1538.5	1775.2	1747.0
Ba	68.5	65.4	278.8	219.4	395.3	526.6	611.6	663.3	731.7	726.9	817.4	816.4
Sc	27.0	33.5	28.7	29.2	20.2	12.9	9.1	7.6	7.5	8.3	6.3	5.8
Cr	965.0	344.0	285.2	135.6	16.3	1.6	1.4	1.5	3.8	1.2	nd	nd
Co	74.1	41.7	71.6	71.3	53.1	55.5	15.7	13.6	13.3	16.3	9.7	8.2
Ni	690.3	102.0	138.4	149.6	35.0	10.1	14.3	8.7	5.0	17.2	19.7	11.3
V	221.1	275.1	283.5	277.8	215.7	147.8	53.2	37.9	36.8	56.3	27.0	17.6
Zr	106.7	138.5	273.3	208.6	365.3	347.9	337.4	373.8	417.8	435.4	446.5	458.8
Nb	8.6	9.2	28.6	21.2	40.7	48.4	52.0	55.3	59.4	63.5	64.1	64.5
Hf	2.6	3.4	6.5	5.1	8.2	7.6	7.7	8.2	9.1	9.1	9.6	10.1
Ta	0.45	0.49	2.98	1.69	2.82	3.94	2.93	3.19	3.41	3.52	3.60	3.84
Th	0.4	0.8	2.6	1.0	3.4	3.0	3.2	4.2	4.2	4.1	4.6	4.5
La	7.33	8.25	25.14	20.33	36.0	42.8	55.6	57.1	61.9	89.4	62.8	63.5
Ce	18.7	24.2	64.5	50.45	90.5	100.5	149.5	143.2	149.6	140.3	150.7	155.1
Nd	13.4	16.5	38.5	31.4	50.9	53.7	88.3	82.9	85.8	87.5	78.4	80.3
Sm	3.85	4.92	9.26	7.81	11.92	12.19	20.15	18.35	19.74	18.82	17.89	17.57
Eu	1.39	1.78	2.90	2.54	3.68	3.70	6.22	5.64	5.89	5.77	5.50	5.47
Tb	0.67	0.81	1.20	1.12	1.62	1.46	2.35	2.13	2.29	2.33	2.19	2.11
Yb	1.67	2.08	2.56	2.16	3.02	2.74	3.66	3.36	3.41	4.63	3.77	3.59
Lu	0.23	0.30	0.37	0.31	0.44	0.36	0.50	0.49	0.56	0.64	0.52	0.49
Y	20.5	26.4	34.4	28.9	40.8	37.3	55.6	51.7	56.9	77.4	53.5	51.7

Table 8 continued

HAWI FORMATION

	H 85-25 P	H 84-10 P	H 84-21 P	H 84-79 P	H 84-62 P	H 84-61 P
Rb	42.6	53.2	53.5	59.3	67.8	81.6
Sr	1650.2	1615.2	1115.0	945.2	781.7	647.7
Ba	790.9	823.2	710.6	816.4	621.6	579.7
Sc	4.8	4.8	5.6	5.0	4.0	3.5
Cr	2.6	nd	2.1	4.3	5.4	2.3
Co	-	6.8	9.8	8.6	1.7	4.7
Ni	4.4	15.5	11.7	-	12.0	11.5
V	9.4	12.5	34.1	-	12.3	14.9
Zr	532.8	531.5	586.4	801.3	694.1	743.7
Nb	77.7	74.4	75.1	81.4	88.6	93.0
Hf	11.1	11.0	12.2	16.3	14.2	15.7
Ta	5.7	4.1	4.2	4.7	5.0	5.5
Th	5.0	4.8	6.3	6.9	7.5	8.4
La	72.4	65.1	67.3	72.4	85.7	63.5
Ce	176.9	163.5	144.9	174.7	137.9	146.9
Nd	91.7	79.3	71.6	80.5	84.5	64.8
Sm	18.6	16.6	15.3	16.4	16.1	12.6
Eu	5.4	5.0	4.2	4.8	3.8	2.8
Tb	2.07	1.94	1.83	1.84	2.45	1.46
Yb	4.06	3.6	3.1	3.9	3.3	3.8
Lu	0.53	0.50	0.46	0.57	0.46	0.57
Y	51.4	49.0	41.5	47.4	43.4	43.5

lavas are identical within analytical uncertainty (Figure 9), the observed variation in $^{143}\text{Nd}/^{144}\text{Nd}$ shows no systematic correlation with degree of differentiation (Figure 10). The absence of a strong correlation between these parameters for Hawi lavas suggests that source differences are non-systematic. Because of the lack of an obvious correlation between chemical and isotopic characteristics, the observed chemical variability was modelled using simple crystal fractionation calculations. This is in keeping with applying Occam's Razor to the solution of a relatively unconstrained problem such as the present one. Other processes, such as variations in partial melting or an open magma chamber system, are likely to be second order in importance in controlling the observed variation and can only be evaluated after correction is made for both shallow and deep level fractionation.

The relative abundances of rock types can be used as one test of the validity of crystal fractionation as the process controlling differentiation. If a suite of samples is derived from a chemically homogeneous source region by roughly equivalent degrees of partial melting, and the ascending melts are sampled randomly by the volcano, one should observe a negative correlation between the volume of erupted material and the degree of differentiation. Figure 11 shows that for Hawi lavas there is a strong negative correlation between the differentiation index and the number of mappable flow units of a given differentiation index.

The flow from Puu Kawaiwai was sampled at four different localities and thus provides a good test for the homogeneity in composition of eruptive products from a single cinder cone (Figure 12). The four

Figure 9. $^{87}\text{Sr}/^{86}\text{Sr}$ isotopic content of Kohala lavas as a function of K_2O content. Data from Lanphere and Frey (1986) and Hofmann et al. (1986).

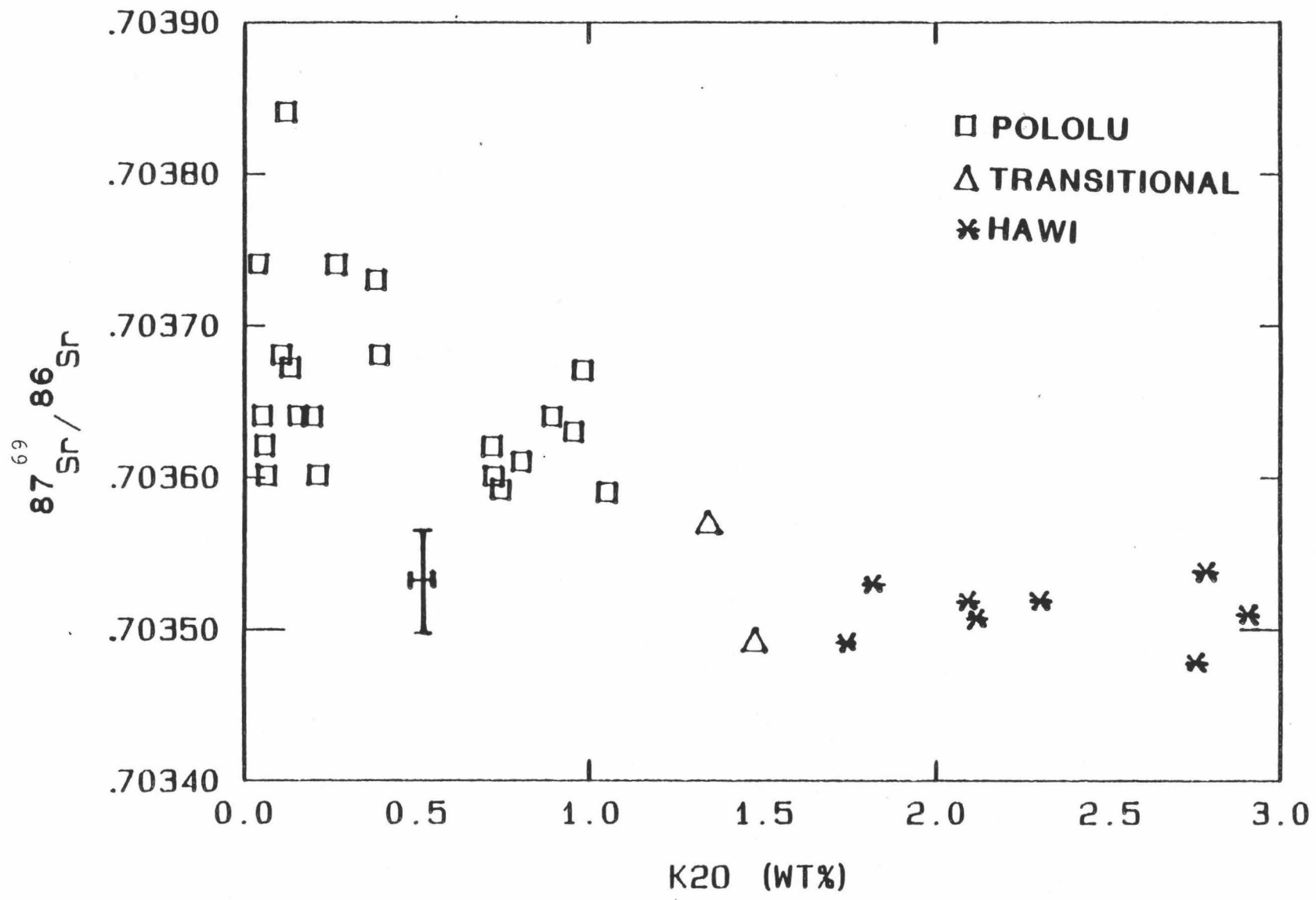


Figure 10. $^{143}\text{Nd}/^{144}\text{Nd}$ isotopic content of Kohala lavas as a function of K_2O content. Data taken from Hofmann et al. (1986).

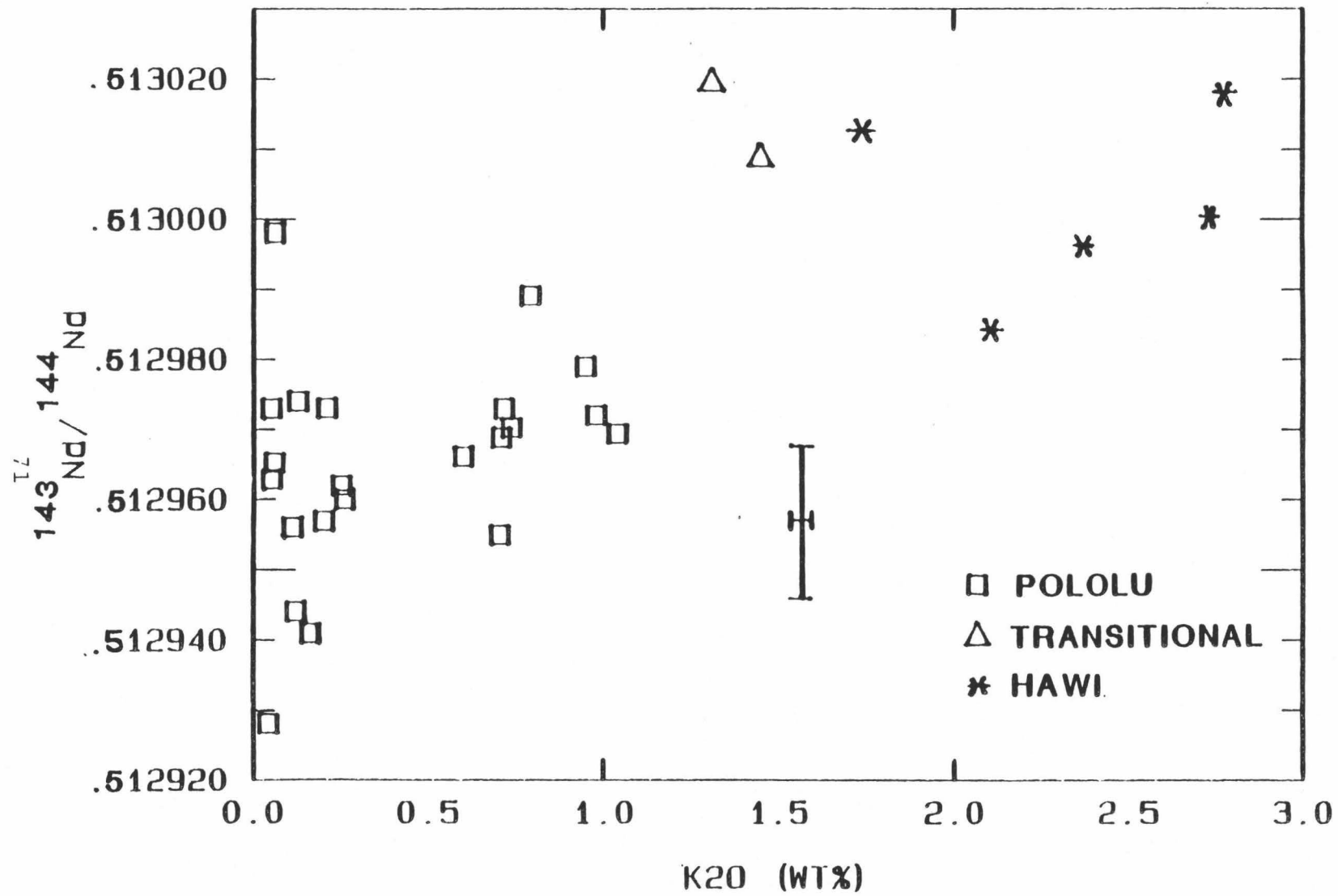


Figure 11. Histogram showing the number of mapped Hawi flow units sampled for various ranges of differentiation.

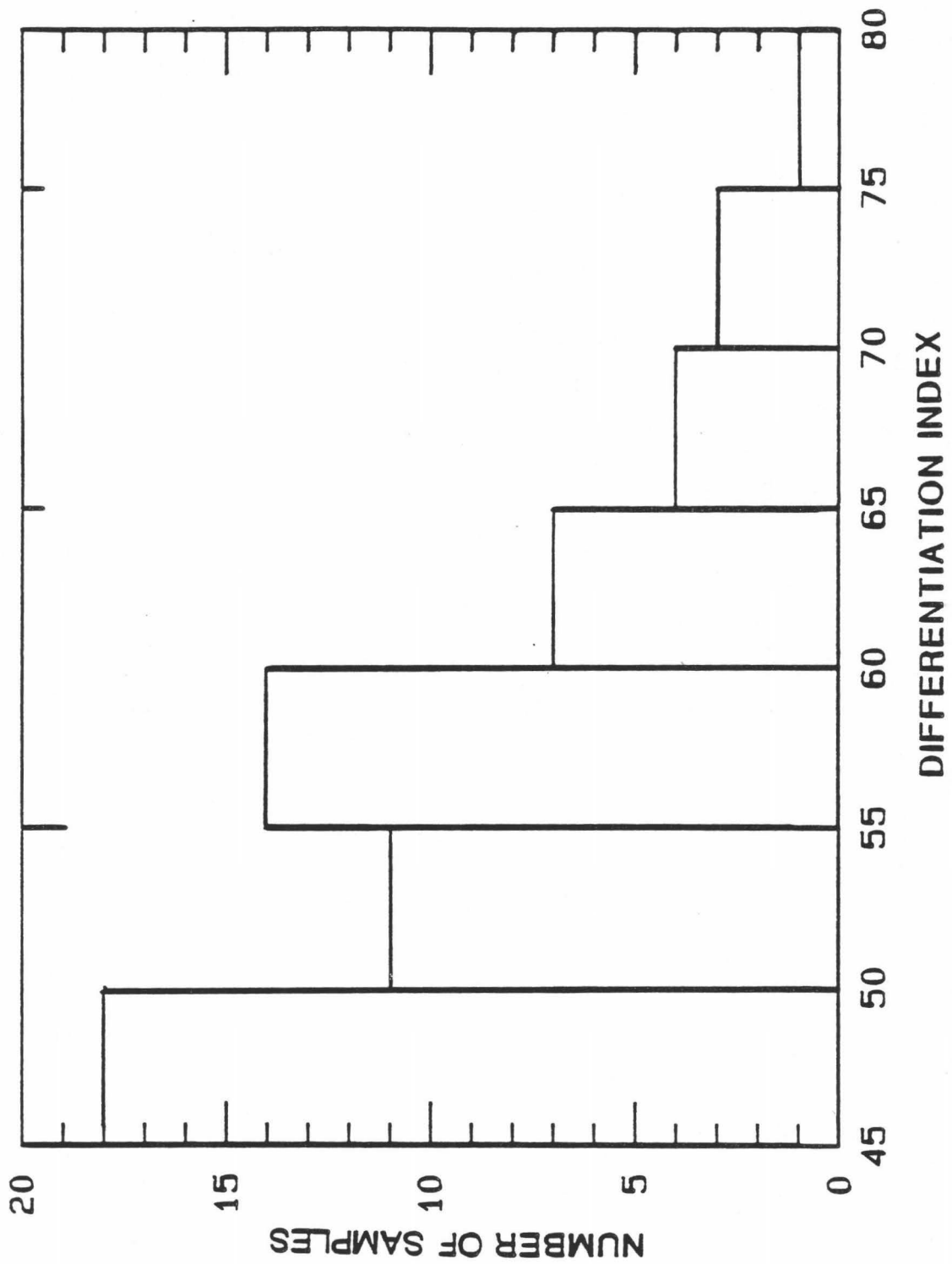
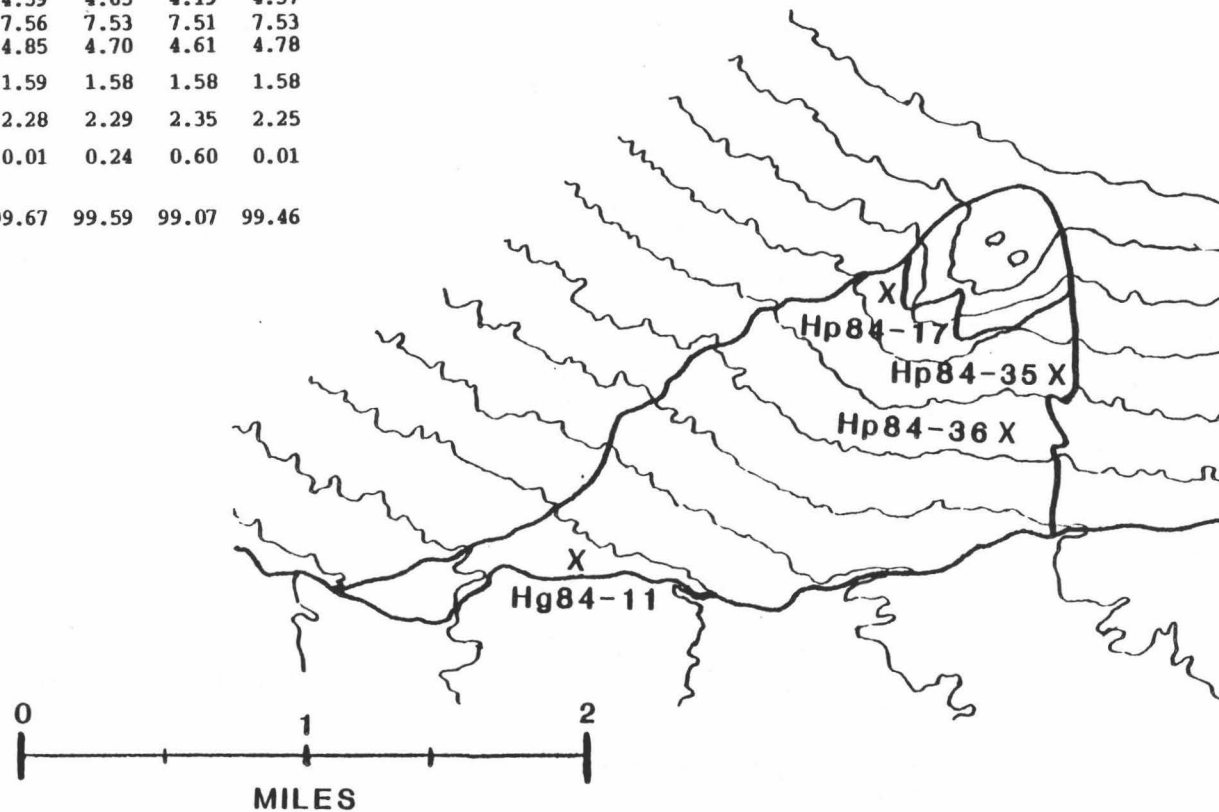


Figure 12. Multiply sampled flow from Puu Kawaiwai. The homogeneity in composition of samples collected from variable distances from vent suggest that the eruptive products of this volcano were homogeneous.

KAWAIWAI ANALYSIS

	H11	P17	P35	P36
SiO ₂	47.60	47.30	46.90	47.40
TiO ₂	3.02	3.04	3.06	3.07
Al ₂ O ₃	15.90	15.90	16.00	16.00
FeO _{tot}	11.88	11.95	11.89	11.88
MnO	0.23	0.23	0.23	0.23
MgO	4.59	4.65	4.19	4.57
CaO	7.56	7.53	7.51	7.53
Na ₂ O	4.85	4.70	4.61	4.78
K ₂ O	1.59	1.58	1.58	1.58
P ₂ O ₅	2.28	2.29	2.35	2.25
H ₂ O	0.01	0.24	0.60	0.01
TOTAL	99.67	99.59	99.07	99.46

7.5

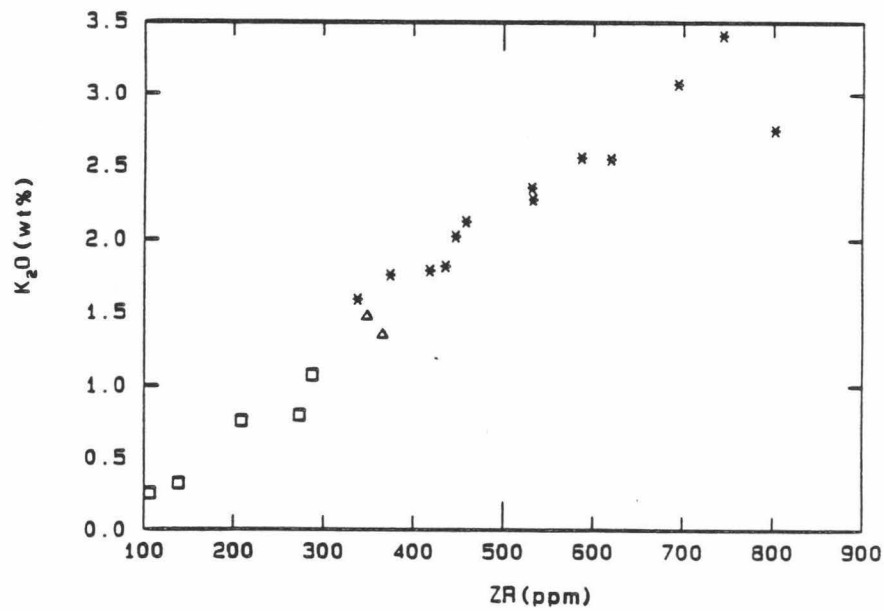
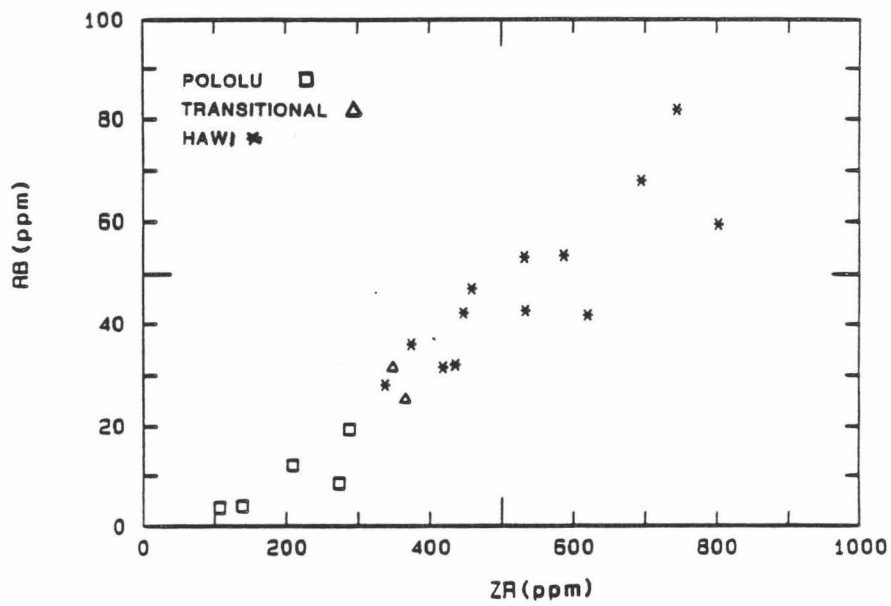


analysis of Puu Kawaiwai are essentially identical within analytical uncertainty, except for sample P35 which has lower SiO_2 , MgO and Na_2O contents and a lower total than the other three analyses. This sample also has a higher water content and might have undergone some alteration. Thus at least in this hawaiite flow, little variation in composition occurred during the course of eruption. In addition, the constancy of the P_2O_5 contents of these lavas suggests that their anomalously high phosphorous contents are not due to apatite accumulation. This is also suggested by the low, constant amounts of modal apatite observed throughout the Hawi (Table 1).

The amount of alteration in the rocks analyzed is probably minimal due to the majority of the samples having been collected from the dry leeward side of Kohala. The generally low H_2O contents (0.01-1.06 wt% H_2O , most are $<.41$ wt% H_2O) of samples analyzed for trace and REE elements further confirms this conclusion (Table 7). The evolved rocks tend to have higher H_2O contents which is, in part, due to the presence of hydrous mineral phases (kaersutite and biotite) in these lavas. Plots of Zr vs. K_2O and Zr vs. Rb (Figure 13) show very good correlation, indicating minimal loss of K or Rb from alteration.

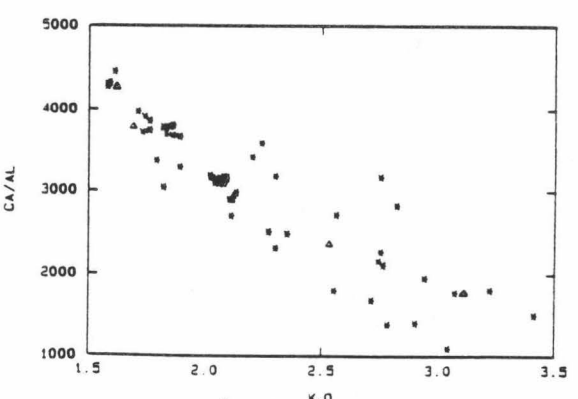
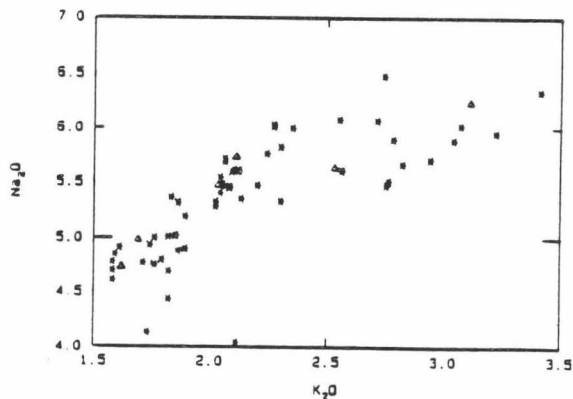
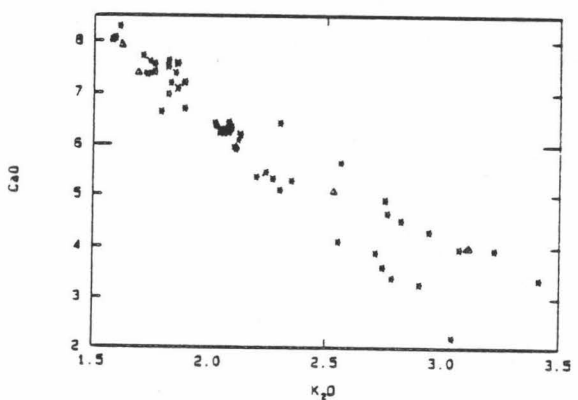
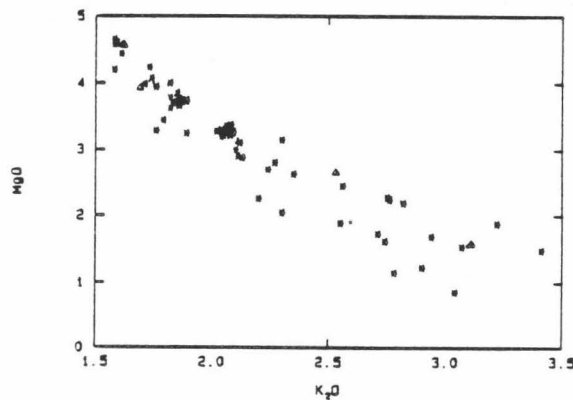
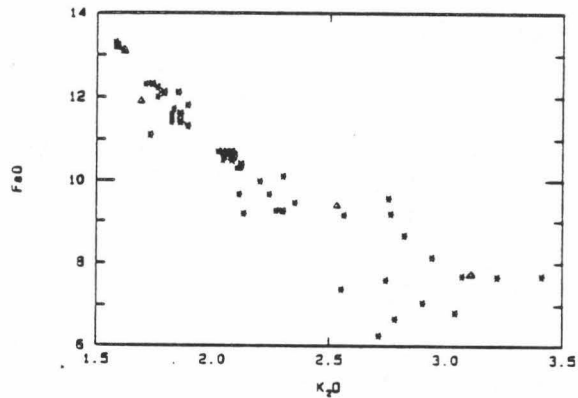
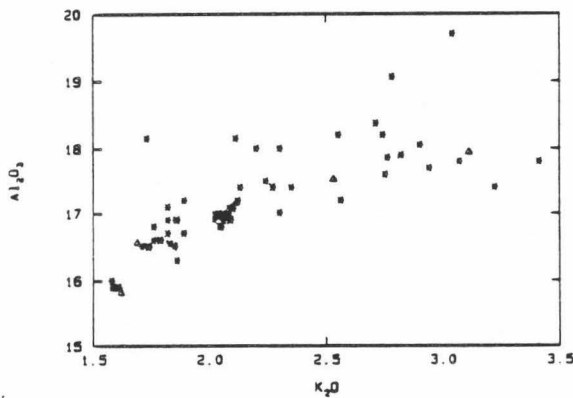
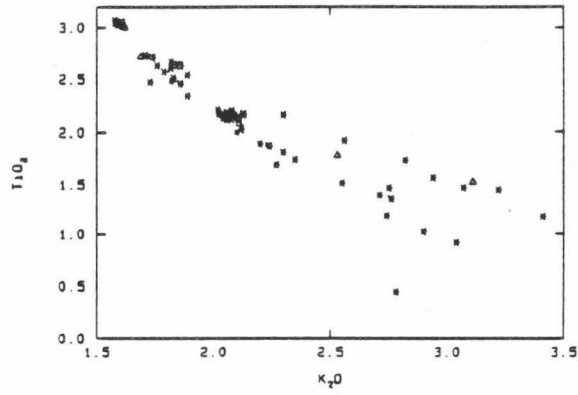
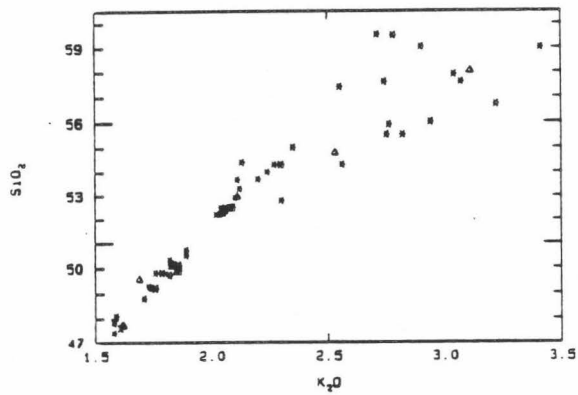
The least evolved rocks found in the Hawi can not be produced directly by partial melting of any reasonable mantle assemblage. The low content of MgO and CaO as well as of highly compatible elements such as Co, Cr, Ni and Sc indicates that extensive fractionation had taken place in these lavas prior to their eruption at the surface. The lavas observed within the Hawi Formation generally show smooth compositional variation with respect to the major elements, ranging in composition

Figure 13. Elements susceptible to alteration (Rb and K) plotted versus the concentration of a low mobility, highly incompatible element (Zr). Large deviations from linearity for a given suite of rocks suggests that alteration of these mobile elements occurred.



from hawaiite to trachyte. Figure 14 shows the observed major element variation in Kohala lavas, using K_2O as a measure of the degree of differentiation (K_2O being the most incompatible major element analyzed). Consideration of these variation diagrams allows certain qualitative constraints to be placed on possible fractionating phases. P_2O_5 , CaO, FeO, TiO_2 and MgO abundances decrease strongly, Na_2O and SiO_2 abundances strongly increase, and Al_2O_3 abundance slightly increase (up to about 3% K_2O) as differentiation proceeds. The continual decrease in FeO and TiO_2 content indicate the fractionation of an iron-titanium rich phase, presumably titaniferous magnetite, which is a common microphenocryst in Hawi lavas. The decrease in P_2O_5 content throughout the series indicates that apatite fractionation also occurred (Figure 27). The decrease in MgO content indicates that olivine or clinopyroxene fractionation was important while the drop in CaO observed could be due to clinopyroxene, apatite or plagioclase fractionation. A plot of CaO/Al_2O_3 vs. K_2O shows a slightly negative trend with increasing differentiation which is what would be anticipated for clinopyroxene or apatite fractionation, but opposite to that normally expected for plagioclase fractionation. However, because the hawaiites have low calcium contents (6.0-7.5 wt %) and high aluminum contents (16-17 wt %), the fractionation of appreciable amounts of plagioclase ($Al_2O_3 = 27$ wt %, $CaO = 9$ wt %) would give rise to only a slightly positive Ca/Al trend. Therefore, the fractionation of plagioclase in conjunction with fractionation of another Ca-bearing phase such as apatite (CaO 52 wt%) and/or clinopyroxene (CaO 15 wt%) would give rise to the observed negative slope.

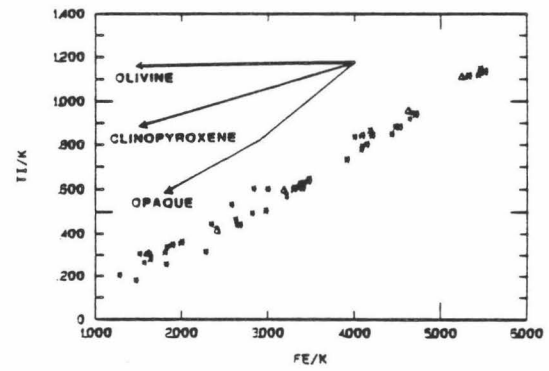
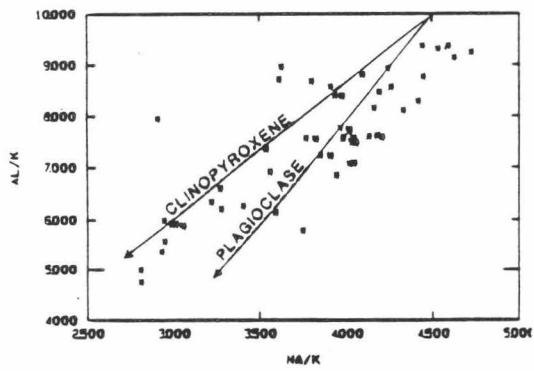
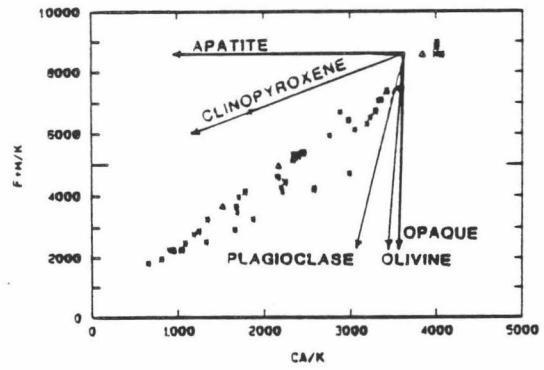
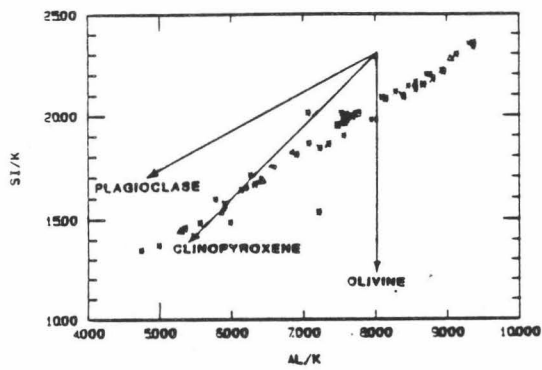
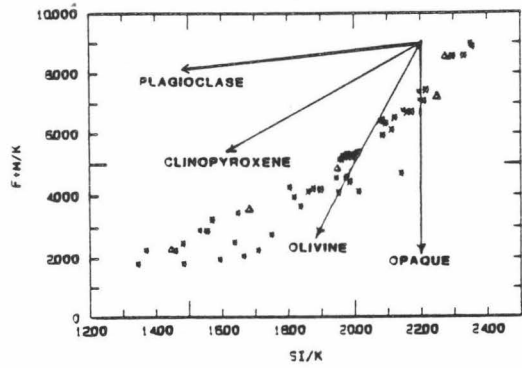
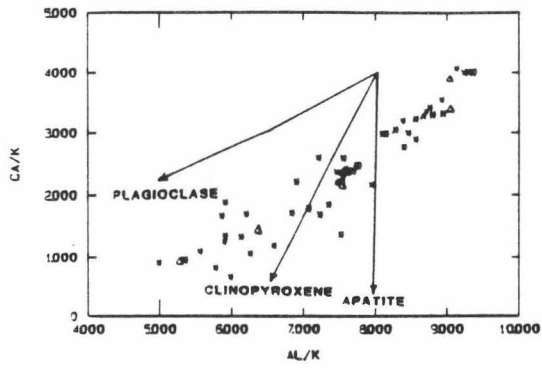
Figure 14. Major element variation diagrams for Hawi lavas. Triangular symbols are the compositions calculated by least-squares modelling using the observed phenocryst assemblage and a high pressure clinopyroxene composition (see Table 10 for modelled bulk rock compositions).



The use of molar ratio plots (Figure 15) gives one a quantitative means of evaluating various fractionating mineral components (Pearce, 1969). Potassium was used as the normalization factor for degree of fractionation due to its high relative incompatibility. Mineral chemical data of phenocryst phases were used to calculate the expected slope produced by fractionation. In the case of pyroxene, which is found only as a rare groundmass phase, a clinopyroxene composition from a Salt Lake crater xenolith (68 SAL-7 cpx) was used to evaluate potential variation due to high pressure clinopyroxene fractionation. This composition was chosen because it is probably the best approximation of the equilibrium composition of clinopyroxene in the sub-Hawaiian mantle (40-60 Km; Beeson and Jackson, 1970). The observed trends in these diagrams will equal the vector sum of the fractionating phase assemblage if fractionation is the sole process responsible for the variation.

The importance of plagioclase fractionation in the petrogenesis of these lavas is clearly illustrated in plots involving elements which reside predominately in plagioclase (eg. Al_2O_3 , Na_2O and to a lesser extent CaO). The plots of Si/K vs. Al/K and Ca/K vs. Al/K (Figure 15) are parallel to the trends calculated for plagioclase fractionation. The plot of $Fe+Mg/K$ vs. Ca/K parallels the expected trend for clinopyroxene fractionation, although this could merely be a by-product of the combined fractionation of plagioclase, apatite, olivine and magnetite. The effect of magnetite fractionation can be seen in the Ti/K vs. Fe/K plot. The observed trend appears to be largely controlled by opaque fractionation in conjunction with fractionation of another

Figure 15. Molar ratio plots for Hawi lavas. Trends drawn for mineral phases calculated from measured mineral compositions. Inflections in the trends for certain minerals reflects the change in mineral composition as a function of differentiation. Traingular diagrams are the same as described in Figure 14.



iron-bearing phase, presumably olivine. This is to be expected because of the large absolute amount of iron and titanium in magnetite (70 wt% and 23 wt% respectively) compared to olivine (27-40 wt% FeO) or clinopyroxene (8.08 wt% FeO and 0.97 wt% TiO₂). The plot of Fe+Mg/K vs. Si/K (Figure 15) gives a slope intermediate between that anticipated for opaque and olivine fractionation and the slope calculated for plagioclase fractionation. The observed "shallowing" of the slope at higher degrees of differentiation on this diagram and on the Ca/K vs. Al/K plot (towards the lefthand side of the diagrams) is consistent with the larger relative amounts of plagioclase fractionation needed to derive the more evolved lavas calculated by least squares modelling.

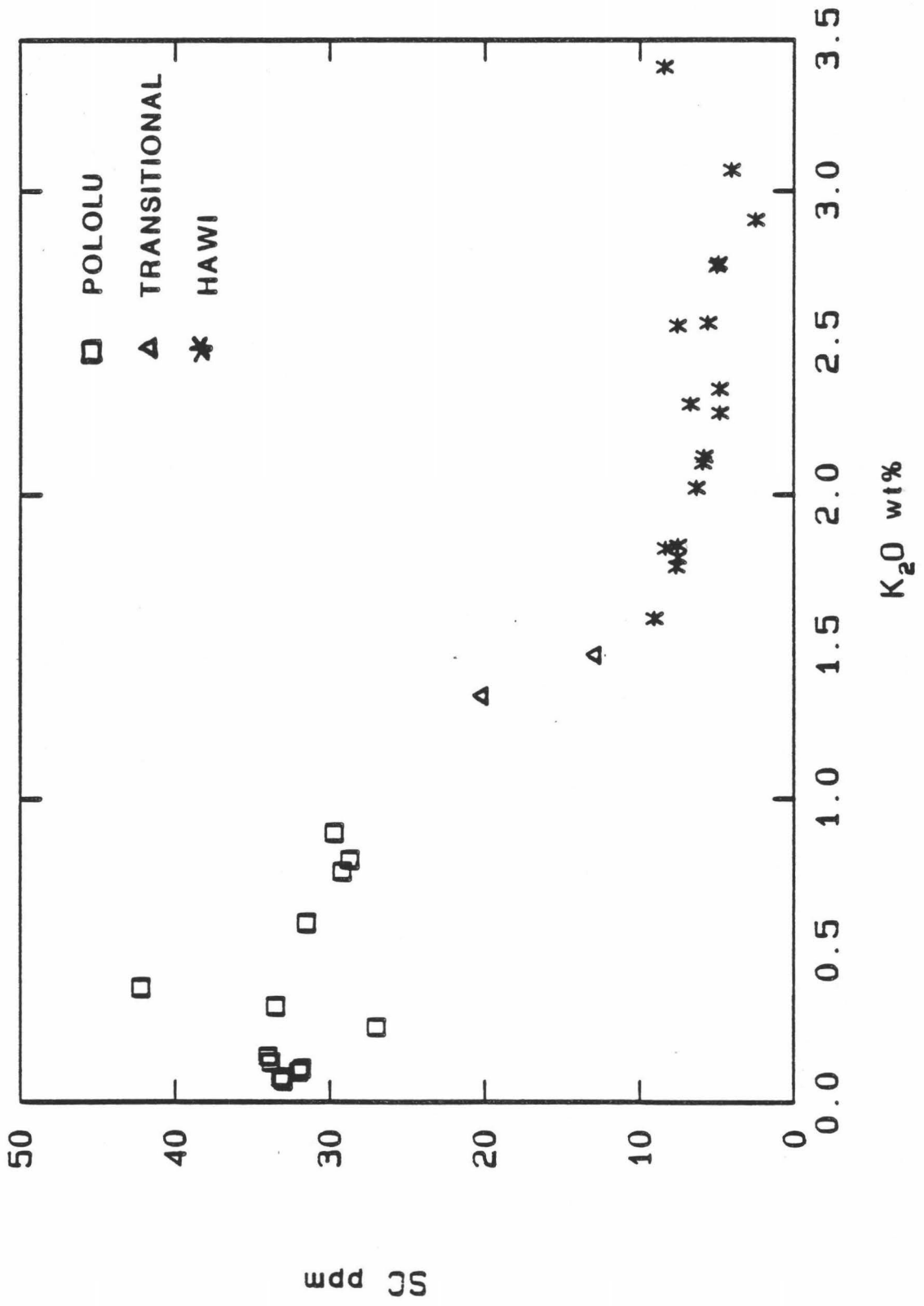
LEAST SQUARES MODELLING

Computer modelling of major element variation was carried out using the MIXING program written by M.J. Carr which is based on the least-squares mixing equations of Bryan et al. (1969). The "goodness" of fit of the modelling is reflected in the value of the sum of the squares of residuals. The absolute value of the residual is a function of the "size" of the fractionation step taken (ie. the % fractionation) as well as the number of mineral species used in the fractionation procedure. Because of the susceptibility of Na to weathering, it was assigned a weighting factor of 0.5 during the calculations, which minimizes its

importance in the fractionation calculations and on the magnitude of the calculated residuals.

The fractionation calculations were broken up into six intermediate steps, using rocks which had been analyzed for both major and trace element content. Plagioclase, apatite and magnetite were used in the fractionation calculations because of their clear fingerprints on the variation diagrams and their occurrence as phenocryst phases in the lavas. Olivine microphenocrysts and phenocrysts were found in most Hawi rocks and thus olivine was also used in the calculations. The plot of Sc vs K_2O shows that there is a dramatic drop in Sc abundance between the Pololu and Hawi samples (Figure 16). Low Sc abundances is a common characteristic of Hawaiian alkalic lavas. If the parental magma for these alkalic lavas had Sc contents typical of the alkalic basalts found in the upper Pololu (about 30 ppm), then clinopyroxene and/or magnetite fractionation must have taken place since clinopyroxene and magnetite are the only reasonable fractionating phases having partition coefficients for Sc greater than one (garnet fractionation is not important because of the observed increase in Yb content as a function of differentiation). Extensive magnetite fractionation probably did not occur in the derivation of the least evolved hawaiites as is evidenced by their relatively high titanium contents (up to 3 wt%). Because clinopyroxene is not a liquidus phase at low pressure (as evidenced by the paucity of cpx phenocrysts in these lavas and experimental work (Thompson, 1974)), fractionation apparently took place at high pressure. The question to be answered is whether the amount of high pressure fractionation was the same for all lavas erupted at the surface. To

Figure 16. Scandium content as a function of differentiation.
Note the discontinuity of measured levels in Pololu and Hawi lavas.



test this, fractionation calculations were performed using both the observed four mineral fractionation assemblage (plag, olv, opq, apt) and a five mineral fractionation assemblage (plag, olv, opq, apt, high P cpx). The use of amphibole and other accessory minerals found in the evolved lavas does not improve the quality of fit. As can be seen in Table 9, the quality of fit using the observed phenocryst assemblage (4 mineral) is relatively good on the whole with the exception of the step from H_g^{84-10} to H_p^{84-62} which corresponds roughly to the transition from mugearite to benmorite. The triangular symbols in the variation diagrams (Figure 14) and molar ratio plots (Figure 15) are the calculated least-square compositions. In each step, the greatest difference between calculated and observed values occurs with calcium and phosphorous. Because of the signs of the differences ($CaO +$, $P_2O_5 -$), it is apparent that the program is trying to account for the difference in calcium content by fractionating out excess apatite. This could possibly be due to the plagioclase composition used in the calculations not being as Ca-rich as it should be. However, even when a plagioclase composition found in the upper section of the Pololu is used, the same problem persists. The major improvement which is made upon adding the high pressure clinopyroxene composition to the fractionating assemblage is the reduction in these differences (Table 10). In addition, the improvement in "fit" is only seen for the first three fractionation steps from H_g^{84-11} (hawaiite) to H_g^{84-10} (mugearite). The relatively poor fit of the step from H_g^{84-10} to H_p^{84-62} is not greatly improved by addition of this extra component. Thus, the role of variable degrees of high-pressure fractionation in these lavas is

Table 9. Least squares modelling of chemical variation in the
Hawi using the observed phenocryst assemblage.

The Parent lava is Hg84-11

Coef	%									
0.045	0.186	OL1								
0.107	0.446	PLAG1								
0.057	0.238	OPQ1								
0.031	0.130	APT								
0.761	Hp84-25b is the daughter									
	SiO2	TiO2	Al2O3	FeO	MnO	MgO	CaO	Na2O	K2O	P2O5
Hg84-	51.73	2.18	16.91	10.71	0.24	3.29	5.93	5.42	2.02	1.57
Hg84-11										
OBS	47.21	3.00	15.77	13.09	0.23	4.55	7.50	4.81	1.58	2.26
CALC	47.19	3.08	15.90	13.06	0.25	4.59	7.28	4.72	1.59	2.54
DIF	0.02	-0.09	-0.13	0.04	-0.02	-0.04	0.22	0.04	-0.01	-0.28
Sum of squares of residuals= 0.155										

The Parent lava is Hp84-25b

Coef	%									
0.007	0.166	OL2								
0.018	0.448	PLAG2								
0.009	0.232	OPQ2								
0.006	0.154	APT								
0.960	Hg84-2 is the daughter									
	SiO2	TiO2	Al2O3	FeO	MnO	MgO	CaO	Na2O	K2O	P2O5
Hg84-	52.50	2.02	17.10	10.34	0.24	3.08	5.56	5.60	2.11	1.46
Hg84-25b										
OBS	51.73	2.18	16.91	10.71	0.24	3.29	5.93	5.42	2.02	1.57
CALC	51.71	2.13	16.96	10.72	0.24	3.30	5.85	5.48	2.03	1.67
DIF	0.01	0.05	-0.05	-0.01	-0.00	-0.01	0.08	-0.03	-0.01	-0.10
Sum of squares of residuals= 0.023										

The Parent lava is Hg84-2

Coef	%									
0.016	0.148	OL3								
0.057	0.531	PLAG2								
0.022	0.208	OPQ2								
0.012	0.113	APT								
0.896	Hg84-10 is the daughter									
	SiO2	TiO2	Al2O3	FeO	MnO	MgO	CaO	Na2O	K2O	P2O5
Hg84-	54.30	1.73	17.34	9.42	0.25	2.61	4.75	6.05	2.34	1.22
Hg84-2										
OBS	52.50	2.02	17.10	10.34	0.24	3.08	5.56	5.60	2.11	1.46
CALC	52.47	2.01	17.18	10.34	0.26	3.10	5.44	5.74	2.12	1.61
DIF	0.02	0.01	-0.08	0.00	-0.02	-0.02	0.11	-0.07	-0.01	-0.15
Sum of squares of residuals= 0.047										

The Parent lava is Hg84-10

Coef	%									
0.039	0.190	OL4								
0.121	0.586	PLAG3								
0.029	0.142	OPQ3								
0.017	0.082	APT								
0.793	Hp84-62 is the daughter									
	SiO2	TiO2	Al2O3	FeO	MnO	MgO	CaO	Na2O	K2O	P2O5
Hg84-	57.56	1.47	17.94	7.75	0.17	1.55	3.49	6.07	3.09	0.90
Hg84-10										
OBS	54.30	1.73	17.34	9.42	0.25	2.61	4.75	6.05	2.34	1.22
CALC	54.25	1.77	17.51	9.39	0.26	2.68	4.57	5.63	2.52	1.45
DIF	0.05	-0.04	-0.18	0.02	-0.01	-0.07	0.18	0.21	-0.18	-0.23
Sum of squares of residuals= 0.203										

The Parent lava is Hp84-62

Coef	%									
0.004	0.035	OL4								
0.083	0.715	PLAG3								
0.023	0.199	OPQ3								
0.006	0.051	APT								
0.887	Hp84-61 is the daughter									
	SiO2	TiO2	Al2O3	FeO	MnO	MgO	CaO	Na2O	K2O	P2O5
Hg84-	59.19	1.18	17.71	6.73	0.18	1.51	2.90	6.42	3.45	0.73
Hg84-62										
OBS	57.56	1.47	17.94	7.75	0.17	1.55	3.49	6.07	3.09	0.90
CALC	57.55	1.52	17.95	7.74	0.21	1.57	3.49	6.25	3.11	0.90
DIF	0.01	-0.05	-0.00	0.02	-0.04	-0.02	0.00	-0.09	-0.01	-0.00
Sum of squares of residuals= 0.012										

Table 10. Least squares modelling of chemical variation in the Hawi using the observed phenocryst assemblage and a high pressure clinopyroxene composition.

The Parent lava is Hg84-11

Coef	%									
0.027	0.107	OL1								
0.090	0.337	PLAG1								
0.058	0.232	OPQ1								
0.026	0.103	APT								
0.050	0.200	PYXF								
0.747	Hg84-25b is the daughter									
	SiO2	TiO2	Al2O3	FeO	MnO	MgO	CaO	Na2O	K2O	P2O5
Hg84-	51.72	2.18	16.91	10.71	0.24	3.29	5.93	5.42	2.02	1.57
Hg84-11										
OBS	47.21	3.00	15.77	13.09	0.23	4.55	7.50	4.81	1.58	2.26
CALC	47.23	3.13	15.76	13.05	0.23	4.56	7.47	4.84	1.55	2.29
DIF	-0.01	-0.13	0.01	0.05	-0.01	-0.01	0.03	0.09	0.02	-0.03
Sum of squares of residuals= 0.030										

The Parent lava is Ho84-25b

Coef	%									
0.000	0.002	OL2								
0.013	0.271	PLAG2								
0.010	0.205	OPQ2								
0.004	0.087	APT								
0.020	0.434	PYXF								
0.953	Hg84-2 is the daughter									
	SiO2	TiO2	Al2O3	FeO	MnO	MgO	CaO	Na2O	K2O	P2O5
Hg84-	52.50	2.02	17.10	10.34	0.24	3.08	5.56	5.60	2.11	1.46
Ho84-25b										
OBS	51.73	2.18	16.91	10.71	0.24	3.29	5.93	5.42	2.02	1.57
CALC	51.72	2.14	16.91	10.72	0.23	3.29	5.93	5.44	2.01	1.57
DIF	0.00	0.04	-0.00	-0.01	0.01	0.00	-0.00	-0.01	0.01	0.00
Sum of squares of residuals= 0.002										

The Parent lava is Hg84-2

Coef	%									
0.005	0.048	OL3								
0.047	0.417	PLAG2								
0.022	0.199	OPQ2								
0.009	0.078	APT								
0.029	0.258	PYXF								
0.888	Hg84-10 is the daughter									
	SiO2	TiO2	Al2O3	FeO	MnO	MgO	CaO	Na2O	K2O	P2O5
Hg84-	54.30	1.73	17.34	9.42	0.23	2.81	4.73	5.05	2.34	1.22
Hg84-2										
OBS	52.50	2.02	17.10	10.34	0.24	3.08	5.56	5.60	2.11	1.46
CALC	52.49	2.03	17.10	10.34	0.24	3.09	5.56	5.69	2.10	1.46
DIF	0.00	-0.01	0.00	0.00	-0.01	-0.00	-0.00	-0.05	0.01	0.00
Sum of squares of residuals= 0.002										

The Parent lava is Hg84-10

Coef	%									
0.022	0.106	OL4								
0.100	0.490	PLAG3								
0.032	0.156	OPQ3								
0.012	0.061	APT								
0.038	0.187	PYXF								
0.793	Ho84-62 is the daughter									
	SiO2	TiO2	Al2O3	FeO	MnO	MgO	CaO	Na2O	K2O	P2O5
Hg84-	57.56	1.47	17.94	7.75	0.17	1.55	3.49	5.07	3.09	0.90
Hg84-10										
OBS	54.30	1.73	17.34	9.42	0.23	2.81	4.73	5.05	2.34	1.22
CALC	54.28	1.86	17.41	9.37	0.23	2.87	4.72	5.56	2.52	1.25
DIF	0.02	-0.13	-0.08	0.04	0.02	-0.06	0.03	0.24	-0.18	-0.04
Sum of squares of residuals= 0.012										

The Parent lava is Ho84-e2

Coef	%									
0.004	0.033	OL4								
0.082	0.712	PLAG3								
0.023	0.199	OPQ3								
0.006	0.051	APT								
0.001	0.005	PYXF								
0.387	Ho84-61 is the daughter									
	SiO2	TiO2	Al2O3	FeO	MnO	MgO	CaO	Na2O	K2O	P2O5
Hg84-	59.19	1.18	17.71	5.73	0.18	1.51	3.90	5.42	3.45	0.73
Ho84-e2										
OBS	57.56	1.47	17.94	7.75	0.17	1.55	3.49	5.07	3.09	0.90
CALC	57.55	1.52	17.95	7.74	0.21	1.57	3.49	5.25	3.11	0.90
DIF	0.01	-0.05	-0.00	0.02	-0.04	-0.02	0.00	-0.09	-0.01	-0.00
Sum of squares of residuals= 0.012										

suggested, but certainly not proved, by the improvement in the magnitude of the residuals for the hawaiite to mugearite differentiation trend.

Figure 17 shows the relative proportions of fractionating phases throughout the differentiation suite using sample H_g84-11 as the parent and doing least squares fractionation calculations for all lavas analyzed for trace elements in this study. The most conspicuous feature of the diagram is that the relative percentage of plagioclase fractionation required increases more or less steadily in the more evolved lavas. The amount of olivine fractionation decreases greatly in the more evolved lavas while the amounts of magnetite and apatite fractionation decrease slightly.

If one assumes that the variation in phosphorous content is due solely to the magma reaching saturation in apatite, then an independent check on the amount of apatite fractionation can be made if one can estimate the total fraction of crystals removed from the parental liquid to produce the differentiated magmas under consideration. Using the major element variation and the change in concentration of the most incompatible elements (ie. Rb), the total amount of fractionation can be estimated. The average calculated amount of fractionation to derive trachyte H_p84-62 from hawaiite H_g84-11 is roughly 60%. Based on this result, the calculated amount of apatite fractionation is 4.7%. This is slightly less than the 4.9% determined by the six-step least squares fractionation calculation. This difference could be due to an incorrect assumption of apatite saturation or, more likely, simply reflects the general uncertainty (5%) in fractionation modelling of suites of lavas over large ranges of chemical variation.

Figure 17. Relative proportions of modelled fractionating mineral phases as a function of weight percent residual liquid. Sample H_g84-11 was used as the "parental" composition to which more evolved Hawi lavas were modelled.

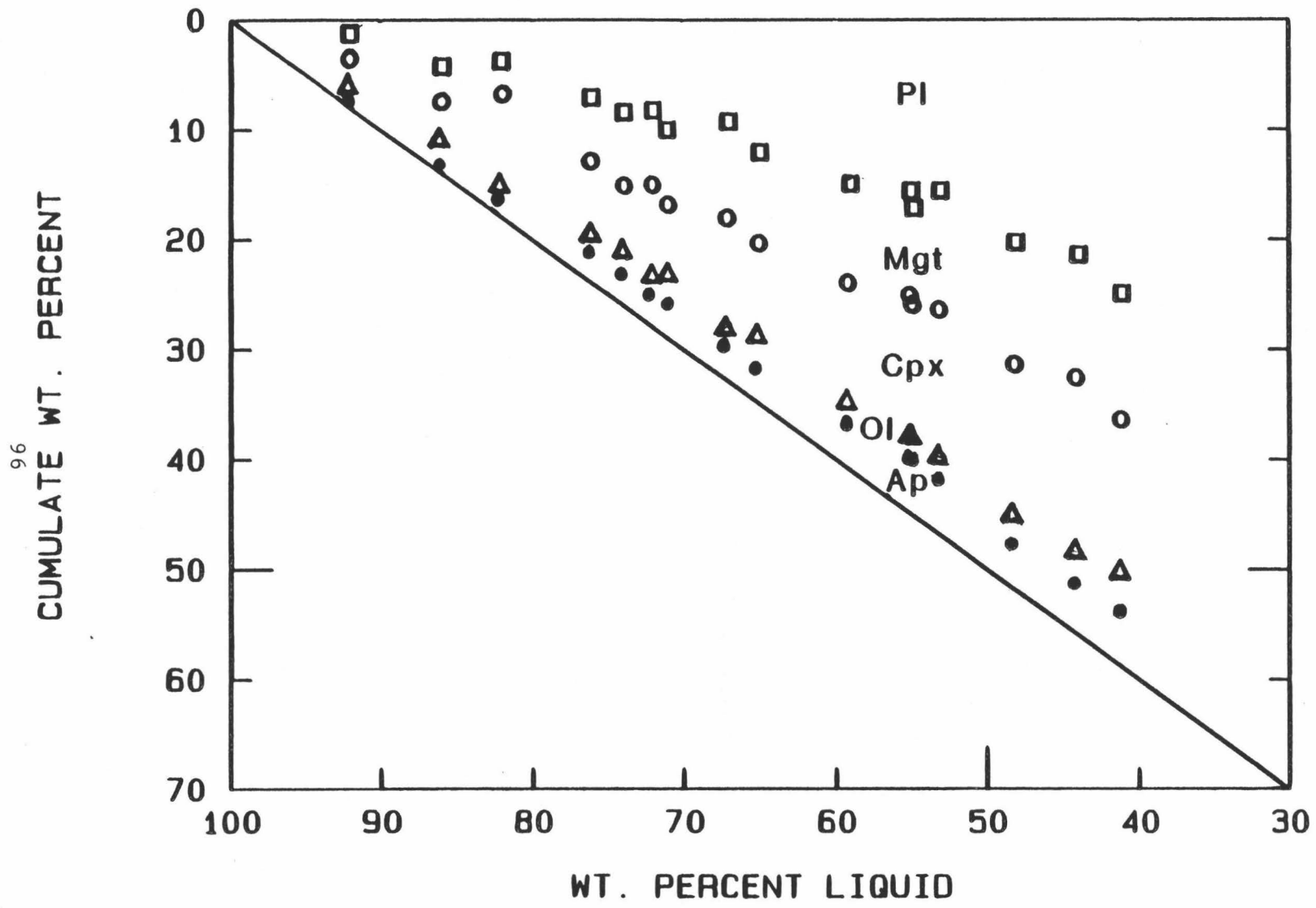
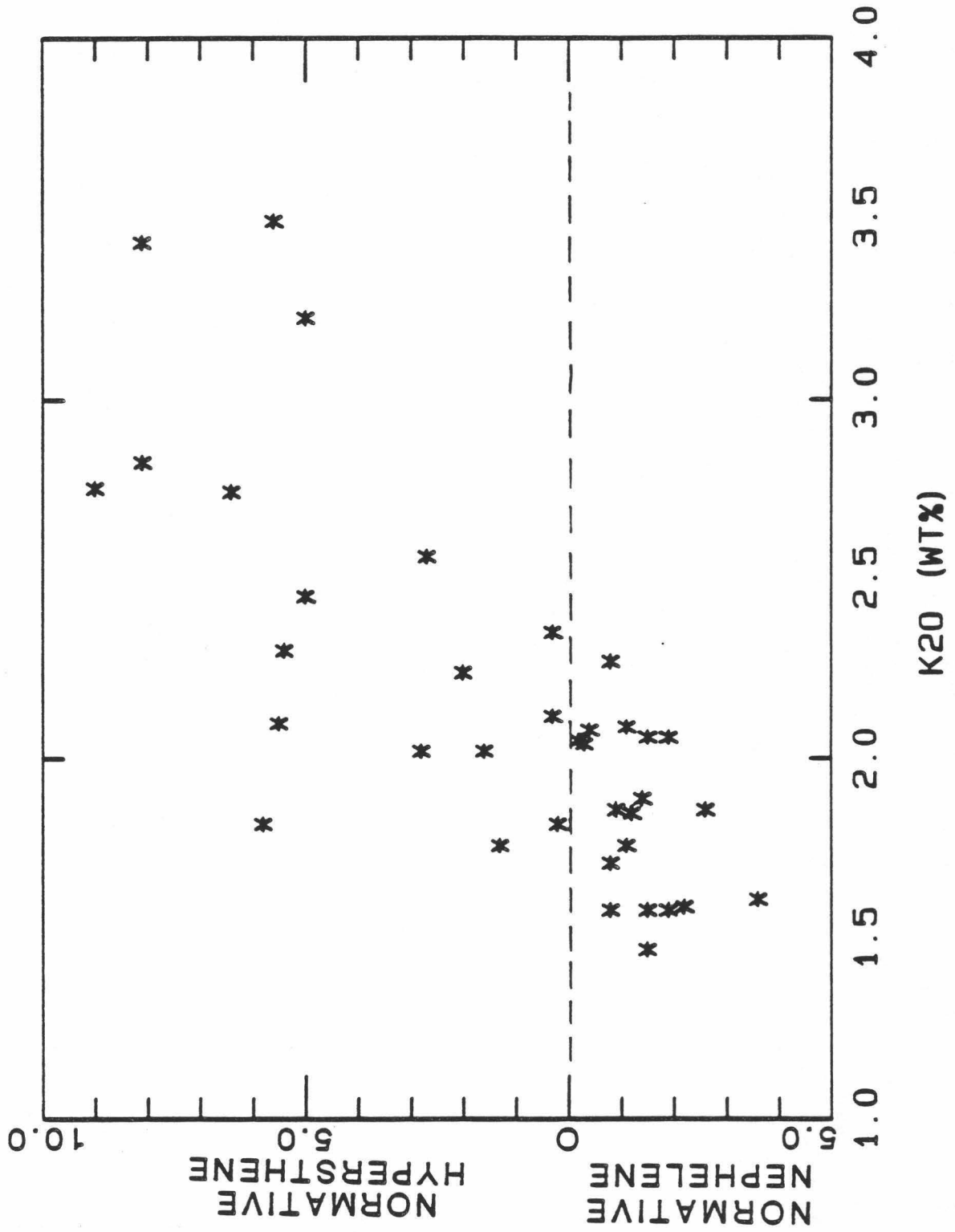


Figure 18 is a plot of the change in normative nepheline-hypersthene as a function of K_2O content for Hawi lavas. The general trend observed as differentiation proceeds crosses the normative nepheline/hypersthene boundary. Because of the uncertainty in the exact location of the thermal divide for these evolved rocks, caution must be taken in attaching too much significance to this trend. But if the compositions do actually cross the thermal divide, this would indicate that the more evolved rocks had indeed undergone greater amounts of high pressure fractionation as compared to the hawaiites.

TRACE ELEMENTS

Because certain trace elements (notably the transition elements) are highly selective of the mineral phase they enter, observed variations in these elements can often be used to fingerprint the identity of fractionating phases in a suite of rocks. In general, the more incompatible trace elements (Zr, Nb, Rb, Ta, Th) all show varying degrees of uniform enrichment throughout the Hawi while the ferromagnesian compatible trace elements show a general decrease with differentiation. The low content of Ni in the least evolved hawaiites (5-9 ppm) suggests that the Hawi lavas had undergone extensive olivine and/or clinopyroxene fractionation prior to eruption at the surface. The low abundance of chrome throughout the Hawi (>6 ppm) can be explained by its removal at deep levels by clinopyroxene fractionation

Figure 18. Variation in normative nepheline/hypersthene composition of Hawi lavas as a function of differentiation (K_2O content). Note that Hawi lavas normative compositions cross the low pressure thermal divide separating normative nepheline from normative hypersthene compositions. This suggests that fractionation at shallow depths alone could not give rise to the observed trend.



($D = 4.7-20$; Henderson, 1982) or by fractionation of Cr-rich spinel at pressure of less than 10 Kb. The low abundance of cobalt in Hawi lavas (2-16 ppm) is consistent with either clinopyroxene fractionation ($D = 6-11$) or appreciable amounts of olivine fractionation ($D = 2.8-5.2$). The decrease in Sc content from the hawaiites (9 ppm) to trachyte (3.5 ppm) requires the fractionation of a mineral phase having a partition coefficient for Sc of greater than one (ie clinopyroxene or magnetite). The strong depletion of Sr can be accounted for by both apatite ($D_{\text{apt}} = 2.2-2.4$) and plagioclase ($D_{\text{plag}} = 3.0-4.3$) fractionation. The decrease in V is predominately controlled by opaque fractionation and to a much lesser degree by clinopyroxene fractionation ($D_{\text{opq}} = 13, D_{\text{cpx}} = 1.3$).

The rare earth element concentrations are presented in Table 8 and the range of chondrite-normalized REE variations observed in Kohala lavas are illustrated in Figure 19. The lavas all show strong REE enrichment which is typical of ocean island basalts (e.g. Schilling and Winchester, 1969; Zielinski and Frey, 1970). The rare earth elements as a group typically increase in abundance as differentiation proceeds due to their large ionic radius. However, in the Hawi suite, a slight decrease in abundance is observed for the middle rare earths (Nd, Sm, Eu) as differentiation proceeds. This is due to the fractionation of apatite which preferentially incorporates middle rare earth elements. This is clearly illustrated in Figure 20, which is a plot of various evolved rocks normalized REE abundances divided by the normalized REE abundance (K_2O content is used as the normalization divisor to account for different degrees of fractionation) of the least evolved Hawi lava, H_g 84-11. The resulting curves can be compared with that on Figure 21

Figure 19. Chondrite normalized rare earth element patterns for Kohala lavas. Shaded field represents the range of compositions found in Pololu lavas. The rare earth element content of Hawi lavas are very uniform (except for anomalously high concentrations observed in sample H_p84-89) due to the buffering of concentrations by apatite fractionation.

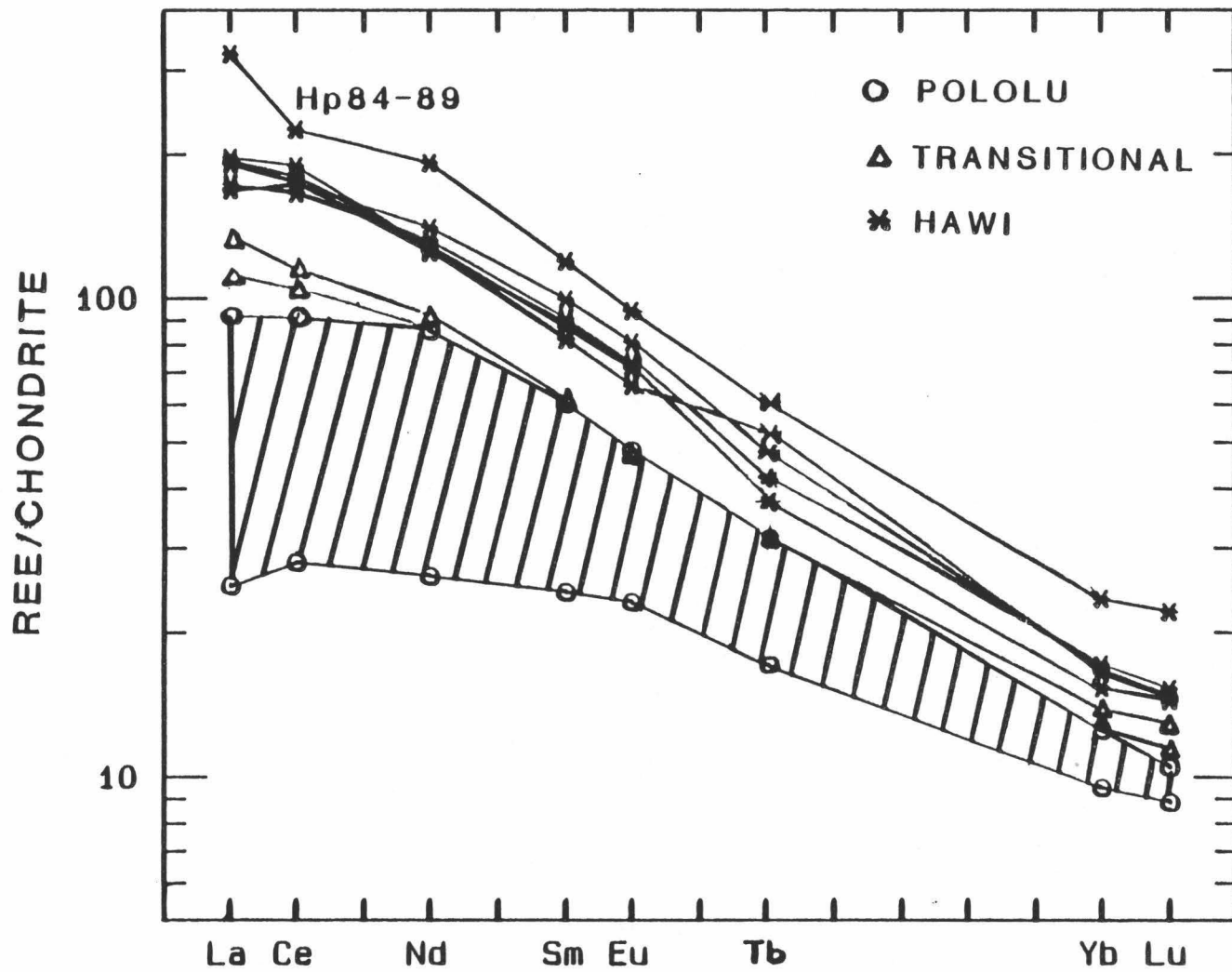


Figure 20. Variation in normalized (divided by whole rock K_2O content) rare earth element abundances of various Hawi samples divided by the normalized abundance of the least differentiated Hawi sample (H_g84-11). This diagram illustrates the relative decrease in rare earth element content as a result of removal by the fractionating phase assemblage.

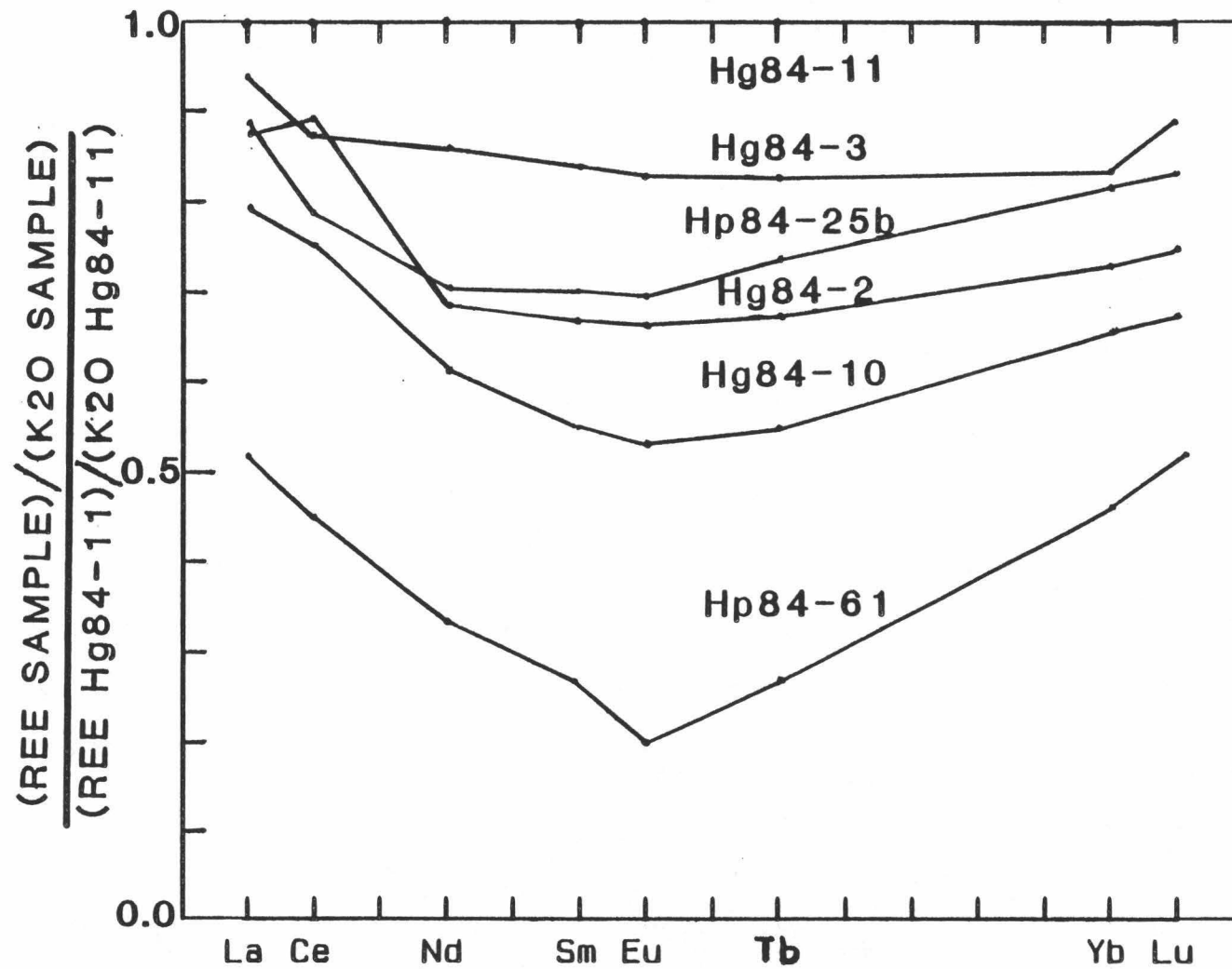
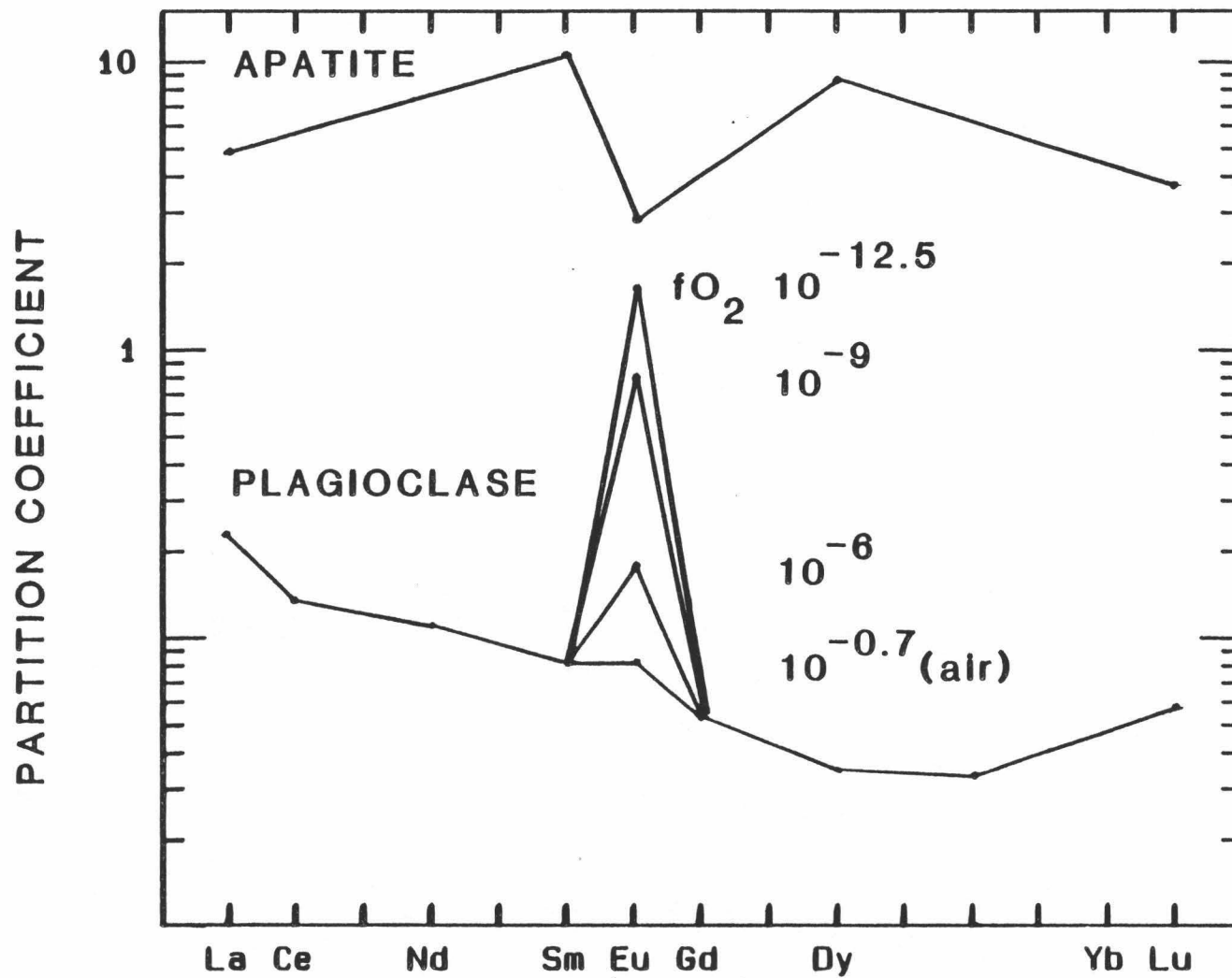


Figure 21. Experimentally determined partition coefficient values for apatite and plagioclase. The values for apatite were determined for apatite in equilibrium with a melt of nepheline normative hawaiite composition (Watson and Green, 1981). The values for plagioclase were determined at temperatures between 1290-1300°C, under various oxygen fugacities as labelled (Drake and Weill, 1975).



which is of the measured distribution coefficients determined by Watson (1981) for apatite co-existing with a host of nepheline normative hawaiite composition. The mirror image like nature of these two curves (except for Eu) is what is anticipated if apatite fractionation controlled the REE abundances in the lavas. Europium has a lower partition coefficient in apatite than the other middle rare earths due to its ability to exist in a divalent oxidation state in magmas of low oxygen fugacities. Despite this, its abundance also decreases as fractionation proceeds. This is readily explained by the predominance of plagioclase fractionation in this suite. The partition coefficient of europium in plagioclase is greater than one in lavas of intermediate composition (range 0.82-4.2; Henderson, 1982). Thus the fractionation of plagioclase preferentially removes europium from the melt decreasing its absolute concentration as differentiation proceeds. No negative europium anomaly is observed in the hawaiite and mugearite REE patterns despite extensive plagioclase fractionation, because the decrease in europium abundance is most probably masked by the concomitant decrease in the other middle rare earth abundances due to apatite fractionation. Sample H_p 84-61 does show a slight Eu anomaly, consistent with the higher degrees of plagioclase fractionation and smaller amounts of apatite fractionation calculated for its derivation from a less evolved benmorite.

A quantitative check on the absolute amount of the rare earth elements removed from the melt can be carried out by using molar ratio plots. If one assumes that all the variation in phosphorous content and rare earth element content (except europium) is controlled by apatite

fractionation, then a plot of P/K vs. REE/K allows one to calculate the weight percent of rare earth element removed to cause the observed trend. Figure 22 shows the variation anticipated for removal of various concentrations of La, Ce and Nd in apatite. The trends of the data are broadly consistent with the crudely measured amounts (by microprobe) of La and Nd in apatites found in the hawaiites and mugearites while the observed amount of Ce removed is slightly greater than the amount measured in the apatites (Table 6).

Log-log plots are useful for delineating the variation in bulk partition coefficient for trace elements in a suite of lavas whose chemical variability is controlled by fractional crystallization following the Rayleigh law. The concentration of a highly incompatible element is used as a measure of the weight fraction of residual liquid and is plotted against the concentration of another trace element. The resulting plot will give a straight line of slope $(1-D_i)$ for incompatible elements and a line of slope (D_c-1) for compatible elements if the bulk partition coefficient of the element plotted remains constant throughout the suite. Changes in the slopes of these diagrams can reflect either a change in the fractionating phase assemblage, a change in the relative fractionating proportions of the phase assemblage or a change in the partitioning behavior as a function of the degree of polymerization of the melt. Rb was chosen as the highly incompatible element against which other elements were plotted because it shows the largest variation in concentration. Figure 23 shows the log-log plots for various trace elements with lines drawn in for various values of D.

Figure 22. Molar ratio diagrams depicting the absolute amount of light rare earth elements (La, Ce and Nd) removed by apatite to account for the observed chemical variation of these elements.

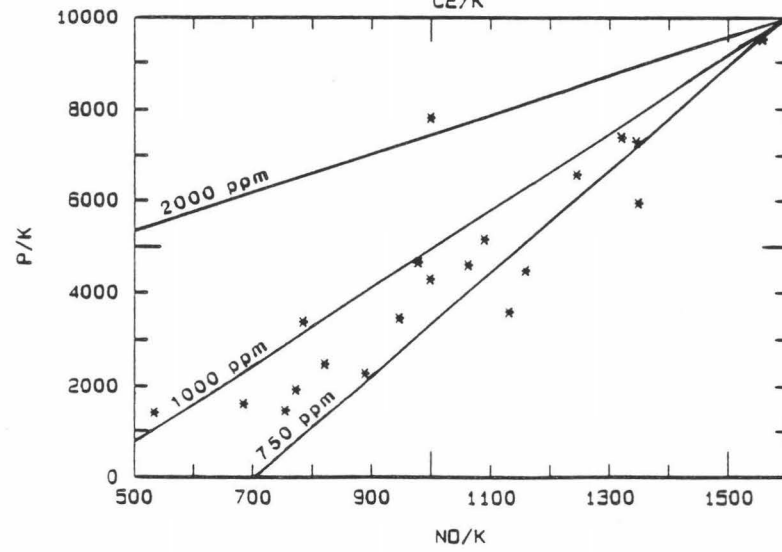
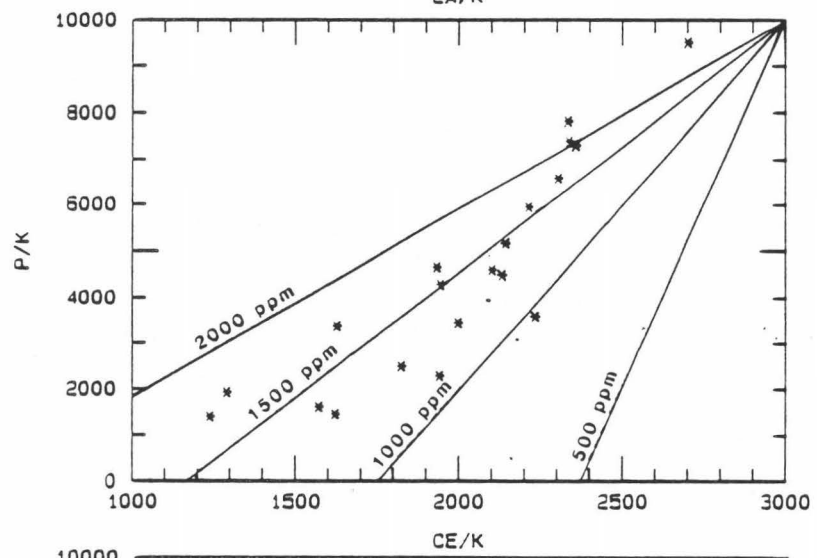
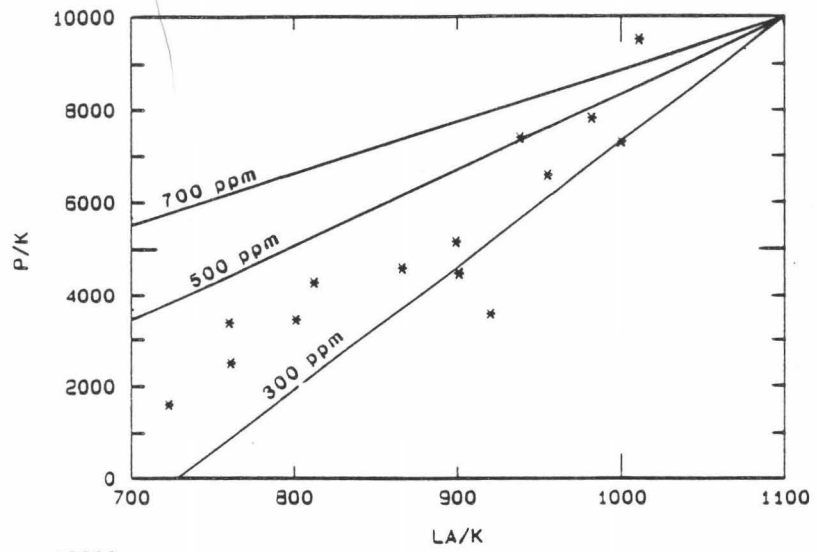


Figure 23. Log-Log plots for various trace elements. The drawn lines are the trends for the labelled bulk partition coefficients.

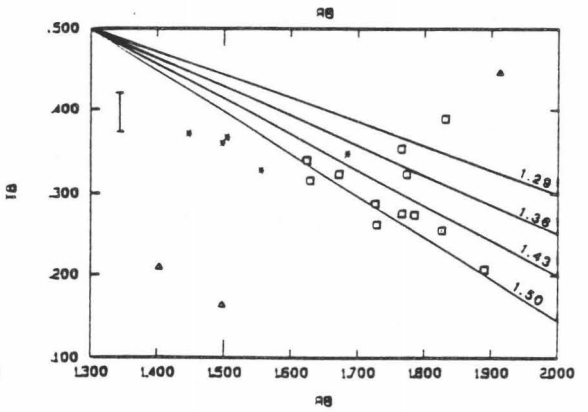
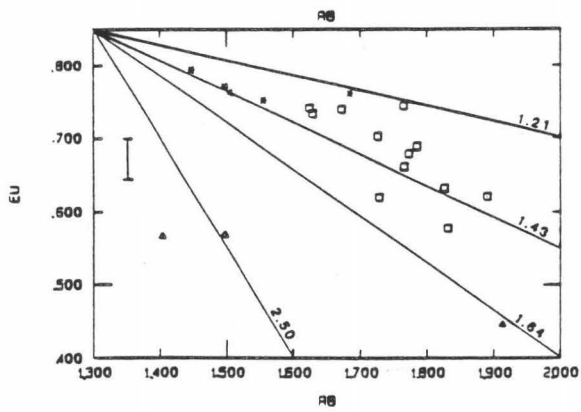
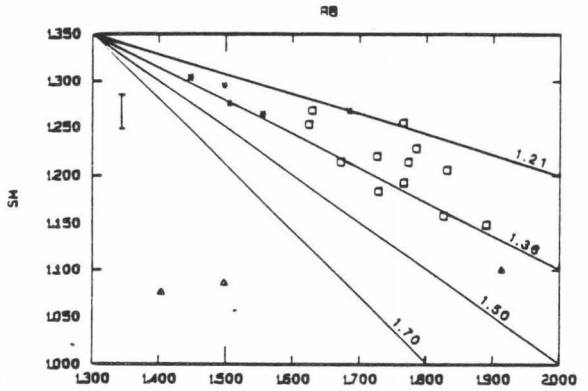
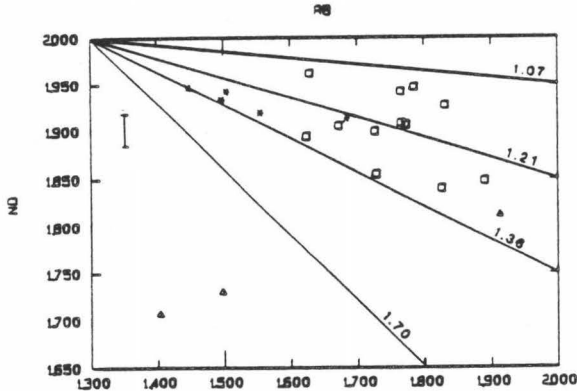
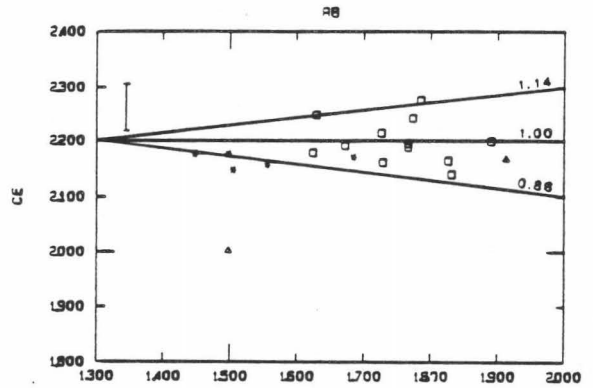
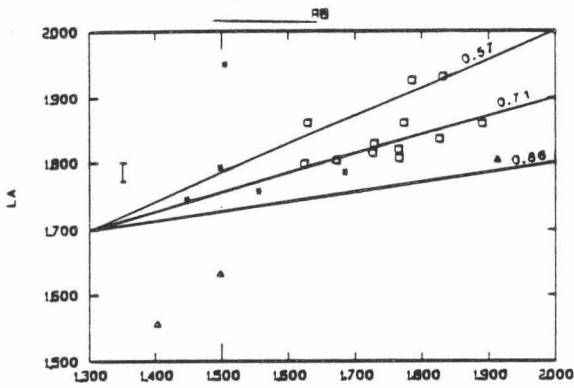
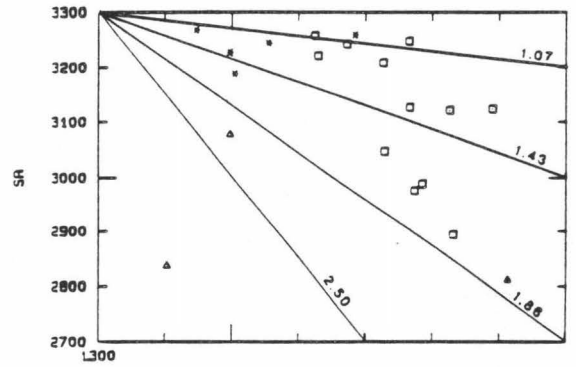
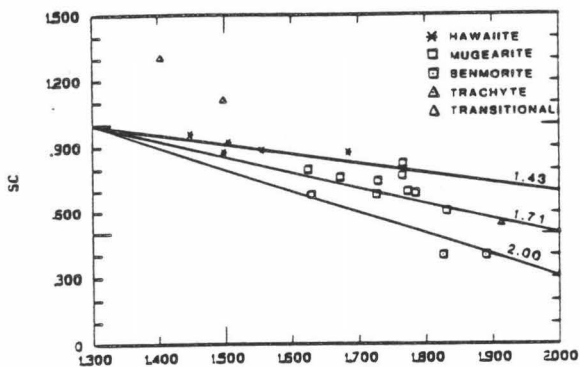
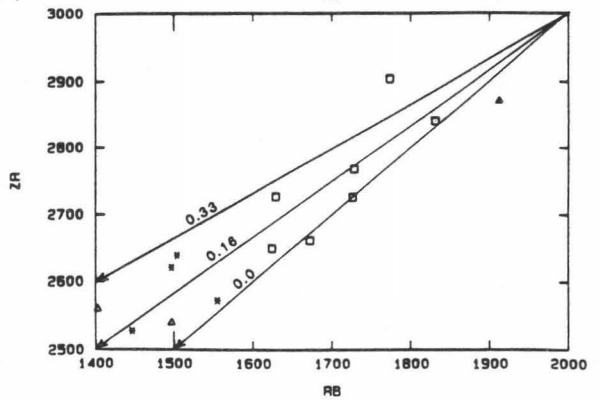
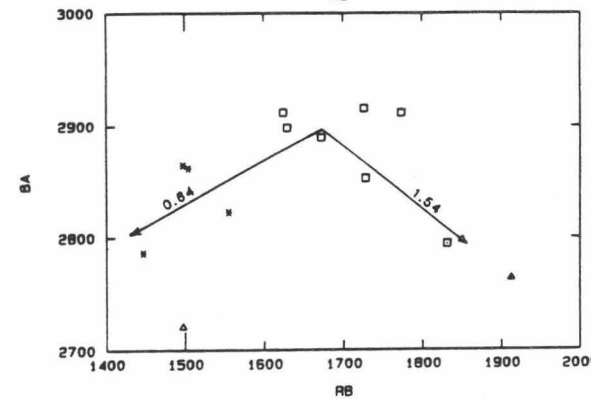
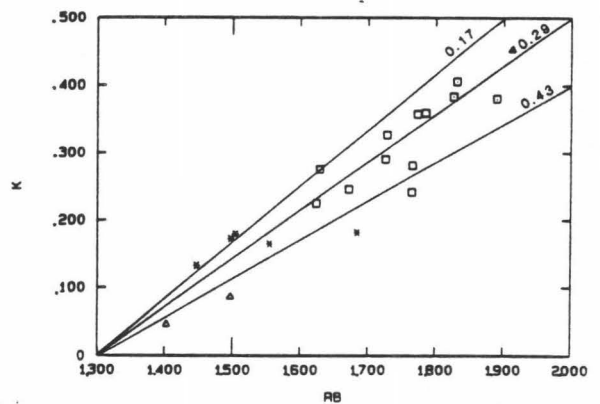
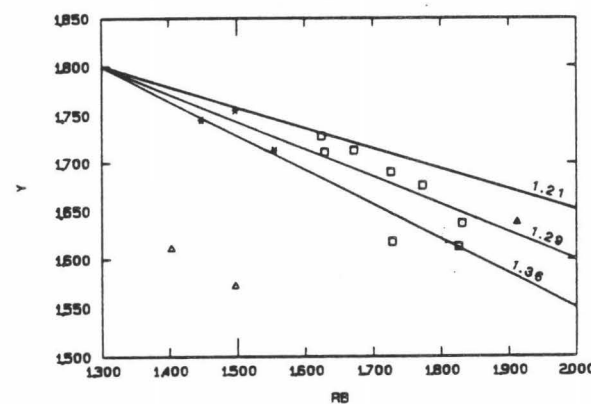
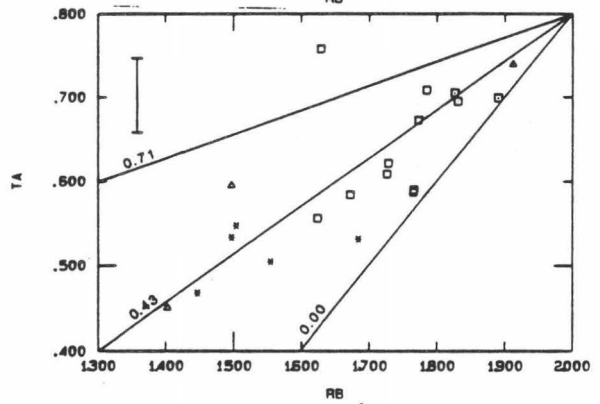
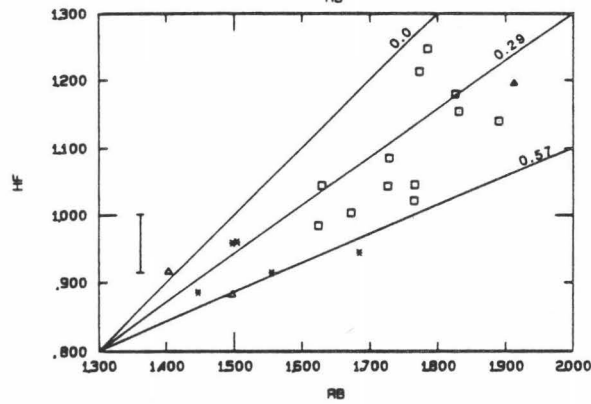
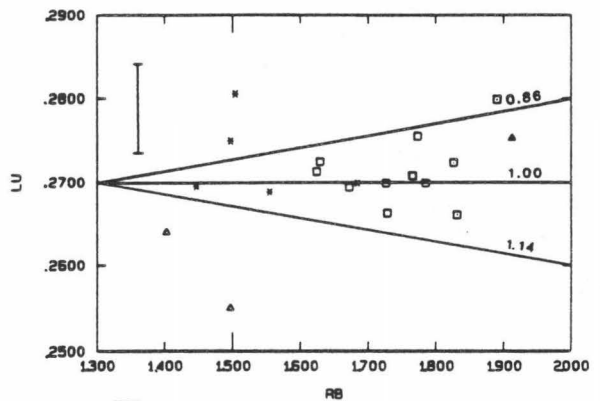
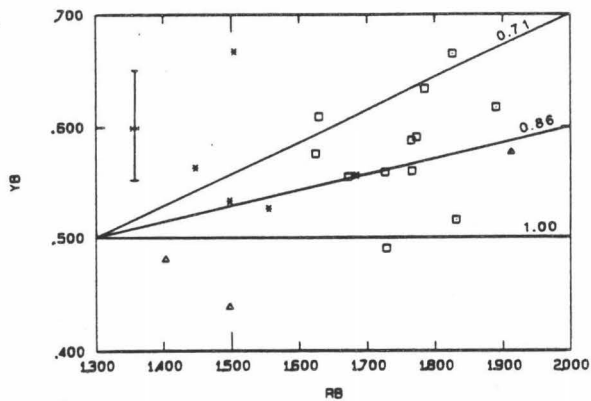


Figure 23 continued



These plots can be used to place constraints on model partition coefficient values.

A matrix of mineral partition coefficient values for each element can be produced using the relative percentages of fractionating mineral phases determined from least squares modelling for a given fractionation step using measured and experimental partition coefficient values determined for magmas of similar bulk composition as constraints on the absolute values of the individual partition coefficients. The solution to this matrix is unfortunately underdetermined due to the contribution of several mineral partition coefficient values on the determination of the matrix. For elements which are predominantly controlled by a single mineral phase (ie. the rare earths in apatite), the effect of other fractionating phases is minimal and a good value can be calculated. For certain elements (Sr and Ba), the measured partition coefficient values for Hawi lavas were used (Sibray 1977). For other elements, the value was constrained to be within the range of values obtained by experimental studies (Dudas et al, 1971; Goodman 1972; Green and Pearson 1985; Hart and Brooks 1974; Higuchi and Nagasawa 1969; Nagasawa and Schnetzler 1970; Schnetzler and Philpotts 1968, 1970; Watson 1981) and those determined for other alkalic series (Villemant et al. 1981).

Because of fluctuations observed in the trace element content of individual lavas of similar major element composition (Table 8), it was decided to average the existing analyses of hawaiiites(6), mugearites(9) and benmorites/trachytes(3) in order to model individual mineral partition coefficient values. Table 11 shows the results of the least squares calculations. The size of the residuals for both fractionation

Table 11. Results of least squares calculations for deriving the average mugearite (based on 9 analysis) from the average hawaiiite (based on 6 samples) and the average benmorite (3 samples) from the average mugearite (6 samples). The bulk partition values were calculated using the Rayleigh equation, using the amount of fractionation modelled by major element variation for the value of F. Those trace elements with no tabulated bulk D value showed an increase in abundance greater than could be produced by fractionation alone (based on the modelled major element variation).

The Parent lava is the average hawaiite

gms removed per 1.0 gm	Absolute Value Removed	
0.018	0.064	Olivine
0.110	0.401	Plagioclase
0.060	0.217	Opaque
0.024	0.087	Apatite
0.064	0.231	High-P Clinopyroxene
0.723	The average mugerite is the daughter	

	SiO ₂	TiO ₂	Al ₂ O ₃	FeO	MnO	MgO	CaO	Na ₂ O	K ₂ O	P ₂ O ₅
Avg Mug	53.61	1.84	17.23	9.81	0.24	2.76	5.14	5.62	2.36	1.30
Avg Haw	48.78	2.71	16.49	12.20	0.23	4.00	6.97	4.91	1.73	1.97
Calc	48.78	2.63	16.50	12.22	0.23	3.99	6.97	4.80	1.76	1.97
Dif	0.00	0.08	-0.01	-0.02	0.00	0.01	0.00	0.11	0.02	0.00

Sum of squares of residuals = 0.011

	Sc	Rb	Sr	La	Ce	Nd	Sm	Eu	Tb	Yb	Hf	Ta
Avg Mug	5.54	52.8	1442	68.7	162.8	82.1	17.0	5.04	1.99	3.76	12.16	4.33
Avg Haw	8.13	31.8	1708	58.4	144.8	86.1	19.2	5.85	2.25	3.64	8.47	3.25
Bulk D	2.21		1.54	0.52	0.66	1.16	1.40	1.48	1.40	0.92		0.13

The Parent lava is the average mugerite

gms removed per 1.0 gm	Absolute Value Removed	
0.018	0.061	Olivine
0.142	0.485	Plagioclase
0.051	0.174	Opaque
0.018	0.063	Apatite
0.063	0.217	High-P Clinopyroxene
0.709	The average benmorite-trachyte is the daughter	

	SiO ₂	TiO ₂	Al ₂ O ₃	FeO	MnO	MgO	CaO	Na ₂ O	K ₂ O	P ₂ O ₅
Avg Ben-T	58.56	1.23	17.94	7.19	0.20	1.43	3.06	6.45	3.16	0.78
Avg Mug	53.61	1.84	17.32	9.81	0.24	2.76	5.14	5.62	2.36	1.30
Calc	53.61	1.98	17.31	9.77	0.26	2.79	5.11	5.63	2.32	1.34
Dif	0.00	-0.12	0.01	0.04	-0.02	-0.03	0.03	-0.01	0.04	-0.04

Sum of squares of residuals = 0.025

	Sc	Rb	Sr	La	Ce	Nd	Sm	Eu	Tb	Yb	Hf	Ta
Avg Ben-T	3.4	75.7	919	73.8	147.6	73.2	14.3	3.58	1.65	3.73	14.57	5.14
Avg Mug	5.54	52.8	1442	68.7	162.8	82.1	17.0	5.04	1.99	3.76	12.16	4.33
Bulk D	2.46		2.31	0.79	1.28	1.33	1.51	2.00	1.54	1.02	0.47	0.50

steps are very small, with most of the differences lying within analytical uncertainty. Table 12 is a matrix of partition coefficients for the fractionating mineral assemblage which would produce the observed trace element variation. As can be seen, many elements which normally behave incompatibly within volcanic suites have relatively high bulk distribution coefficients. In the case of the rare earth elements this behavior is due to apatite fractionation and for other typically "hygromagmatophile" elements (ie. Ta, Hf), it is due to the fractionation of titanomagnetite (Villemant et al. 1981). The D values determined for apatite in the hawaiite to mugearite differentiation step are very similar to experimental values obtained by Watson and Green (1981) on a nepheline normative hawaiite (La=4.9, Sm=10.5, Dy=8.9, Lu=3.8). The D values calculated for Sr in plagioclase and apatite are consistent with values measured by Sibray(1977) in Hawi lavas (see Figure 6). The D values for Sc in clinopyroxene are intermediate between literature values for rocks of basaltic to andesitic composition (1.7-3.2) and values for rocks of dacitic to rhyolitic composition (18-28). The need for a mineral with a high partition coefficient for Sc is further evidence that variable degrees of high pressure clinopyroxene fractionation played an important role in the petrogenesis of Hawi lavas. Opaque fractionation alone could not create the observed decrease in Sc content. The high D value for Ta in opaques for the mugearite to benmorite-trachyte fractionation step is somewhat arbitrary. No published D values for Ta in apatite were found in the literature. However, Ta is pentavalent and might, despite its larger

Table 12. Matrix of individual partition coefficients calculated to explain the observed variation in trace element content in the Hawi. These values are constrained to be consistent with experimentally determined values and values measured in lavas of similar, evolved compositions (i.e. Villemant et. al., 1981).

MODEL D VALUES FOR AVG HAWAIIITE TO
AVG MUGEARITE DIFFERENTIATION STEP

Element	Olivine	Plagioclase	Opaque	Apatite	Clinopyroxene
Sc	0.22	0.05	3.00	0.10	6.60
V	0.10	0.10	13.00	0.10	1.30
Sr	0.01	2.50	1.50	2.20	0.10
La	0.01	0.20	0.50	3.70	0.10
Ce	0.01	0.18	0.50	4.80	0.30
Nd	0.01	0.16	0.70	9.20	0.60
Sm	0.01	0.11	0.80	10.30	1.00
Eu	0.01	0.70	1.60	7.00	0.90
Tb	0.01	0.11	1.70	8.00	1.10
Yb	0.01	0.11	1.55	4.00	0.80
Ba	0.01	1.05	0.50	0.40	0.10
Ta	0.01	0.05	0.30	0.10	0.20

MODEL D VALUES FOR AVG MUGEARITE TO
AVG BEN-TRAC DIFFERENTIATION STEP

Element	Olivine	Plagioclase	Opaque	Apatite	Clinopyroxene
Sc	0.40	0.10	5.20	0.10	6.60
V	0.20	0.10	13.00	0.20	1.30
Sr	0.01	3.50	2.80	2.40	0.10
La	0.01	0.30	1.00	7.90	0.10
Ce	0.01	0.25	1.50	13.50(?)	0.30
Nd	0.01	0.20	1.80	12.40	0.60
Sm	0.01	0.15	2.00	13.30	1.00
Eu	0.01	1.50	2.50	10.00	0.90
Tb	0.01	0.15	2.80	11.90	1.10
Yb	0.01	0.15	2.20	6.30	0.80
Ba	0.01	3.20	0.80	0.50	0.10
Ta	0.01	0.10	2.25	0.20	0.20

ionic radius, substitute in a limited manner for phosphorous in apatite, especially as its concentration increased in the melt.

The element which shows the largest variation, and thus presumably has the lowest bulk distribution coefficient, is Rb. Because of the infamous mobility of Rb as a result of alteration or late stage hydrothermal fluid migration, this variation might be looked upon as suspect. However, the rocks used in the modelling calculations were exceedingly fresh in hand sample, showed no sign of alteration in thin section (except for the evolved benmorite and trachyte samples which showed reaction rims around kaersutite and olivine (iddingsite)), and had low bulk water contents (loss on ignition). The observed amount of enrichment of Rb is consistently higher than the degree of fractionation calculated by least squares modelling for each incremental step, even when a bulk distribution coefficient of 0 is assumed. This consistent enrichment is especially well demonstrated in Figure 24 which plots the abundances of various "incompatible" trace elements normalized to the abundances in the "parental" hawaiite H_g84-11 versus the weight fraction of residual liquid (F) calculated by least squares modelling of major element data. The curve in the diagrams is the trend calculated for an element with a bulk partition coefficient of 0. While the other trace elements plot around or below the curving trend, the Rb values plot consistently above the curve. Such a trend might be obtained if the Rb content of the parental lava (H_g84-11) was low due to alteration. The fresh character of the analyzed sample and the low water content (0.01 wt %) suggest that alteration was not a factor. Table 13 compares the amount of fractionation calculated by least squares for six steps and

Figure 24. Observed enrichment observed for various incompatible elements. Drawn curve is shape of variation expected for a perfectly incompatible element ($D = 0$).

HAWAII

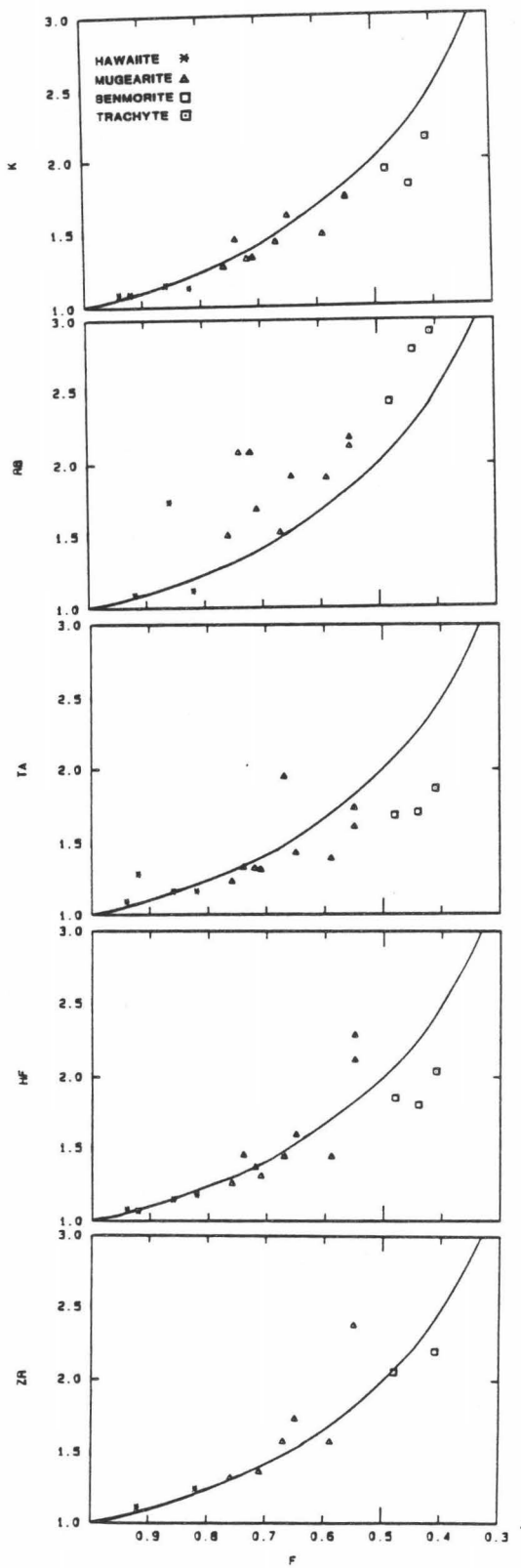


Table 13. Greater percent of fractionation predicted by observed variation in Rb content (assuming $D=0$) than calculated by least squares modelling of major element variation.

FRACTIONATION STEP	CALCULATED MAJORS	PERCENT FRACTIONATION Rb (D=0)
H _g 84-11	.265	.335
H _p 84-25b	.049	.104
H _g 84-2	.116	.117
H _g 84-10	.203	.215
H _p 84-62	.119	.169
H _p 84-61		

the amount calculated based on the variance of Rb concentration with D assumed to be 0. This table shows that this enrichment is observed throughout the suite and is not dependent on the freshness of a particular sample. If more reasonable bulk partition coefficient values for Rb of between 0.1 and 0.2 are used, then the absolute amount of Rb "enrichment" is even greater. A similar enrichment in incompatible element content over that predicted by major element variation has also been observed on Mauna Kea. West et al. (in prep.) attributed this enrichment to being the product of an open system magma chamber having undergone repeated episodes of recharge and discharge. If this type of process actually went on in Kohala during the alkalic stage, then the partition coefficient values listed in Table 12 are slightly high for the compatible elements ($D > 1$) and slightly low for incompatible elements ($D < 1$), assuming that the same relative proportion of phases fractionated (but a larger absolute amount) as calculated by the least squares program. The anticipated preferential enrichment of highly incompatible elements over moderately incompatible elements would be difficult to detect in the Hawi suite because it would be masked by the moderately incompatible behavior of all analyzed elements with respect to the fractionating phase assemblage. Thus, no attempt was made to model the observed variation using the equations applicable to an open system magma chamber derived by O'Hara and Mathews (1981). Whether or not such a system involving continuous replenishment could actually maintain itself during this waning stage of volcanism, when the magma supply rate is low, is open to speculation. In fact, the long duration and infrequency of eruptive activity within the Hawi (average of one

eruption every 3000 years) and the need for variable amounts of high pressure clinopyroxene fractionation suggest that individual eruptive events during the Hawi were the final products of discrete "squirts" of magma rising from the area of initial melting which then differentiated at deep and shallow levels independently of one another.

EXPERIMENTAL EVIDENCE ON CRYSTAL FRACTIONATION IN HAWAIITE

Melting experiments have been performed on rocks of hawaiite composition by Thompson (1974), Knutson and Green (1975), and French and Cameron (1981). The compositions of the hawaiites used in these studies are broadly similar to Kohala hawaiites (except for slightly lower P_2O_5 contents). At atmospheric pressure, French and Cameron (1981) observed that plagioclase appeared first at $1144^{\circ}C$, followed by clinopyroxene at $1128^{\circ}C$ and then olivine at $1082^{\circ}C$ in a hawaiite from the Marquesas Islands. Thompson (1974) studied an aphyric hawaiite from the Isle of Skye and also found that plagioclase is on the liquidus at atmospheric pressure but that it was followed by olivine and then clinopyroxene. This is the apparent sequence of crystallization observed in Hawi lavas based on petrographic analysis. Knutson and Green (1975) performed experiments at elevated pressures on a hawaiite from the mid-north coast of New South Wales, Australia. At intermediate pressures (5.0-7.5 Kb) and anhydrous conditions, olivine and plagioclase are the near-liquidus phases at 5 kb while olivine, clinopyroxene and plagioclase are the

near-liquidus phases at 7.5 kb. In hydrous runs (2% H₂O) at intermediate pressures, olivine is the liquidus phase at 5 and 7.5 kb. Amphibole was not present in runs with 2% H₂O, but appeared as an important near-liquidus phase in runs with 5% H₂O at 5 kbar. Ilmenite of similar composition to that occurring in Hawi samples as well as apatite were found in the experimental runs at 5 and 6.5 kbar (2% H₂O) which is consistent with their early appearance in the crystallization sequence at elevated pressures. At pressures of 10 kbar and greater, clinopyroxene is the liquidus phase under hydrous and anhydrous conditions (Knutson and Green 1975). Thompson (1974) also showed that clinopyroxene is on the liquidus at pressures greater than 18 kbar.

The experimental work is thus consistent with the "high pressure" fractionation scheme used in the modelling section. High pressure fractionation of clinopyroxene and olivine (as evidenced by low Ni and Cr abundances of least differentiated hawaiites) was followed by later fractionation of plagioclase, magnetite and apatite as the magma rose to shallower depths. The need for larger relative amounts of plagioclase fractionation to derive the more evolved lavas suggests that much of the differentiation processes that formed the evolved mugearites, benmorites and trachytes took place at relatively shallow levels. The absence of clinopyroxene and the paucity of olivine in the lavas attests to the efficiency of the fractionation mechanism at depth. Fractionation of these phases may have occurred at or near the base of the crust (7-10 Kb) where removal of the crystallizing phase assemblage would have been facilitated by the low yield strength of the magma. As the magma ascended and reached more evolved compositions, the yield strength of

the magma increased which hindered the gravitational removal of the crystallizing, low pressure phase assemblage.

The density variation of plagioclase as a function of composition was calculated using the experimental data of Grundy and Brown (1967), who determined the molar volume of plagioclase from the unit cell parameters for a number of compositions at temperatures between 25°C and 950°C. This data was then extrapolated to 1100°C (the estimated eruption temperature for the hawaiites) to obtain the lower curve in Figure 25. From this curve the densities of plagioclase found in lavas of different degrees of differentiation were calculated and plotted with 1 atmosphere melt densities calculated using the equations of Bottinga and Weill (1970) at 1200°C (Figure 26). Because the whole rock calculations were performed for a higher temperature value than the phenocryst data, their values are somewhat low. Nelson and Carmichael (1979) determined the partial molar volumes of oxide components over a wider range of temperatures than Bottinga and Weill and found that on average the decrease in density as a function of temperature is on the order of 1-2 g/cm³/100°C. Thus, the difference between the actual values at 1200°C and 1100°C is quite small. In figure 26 it can be seen that plagioclase is less dense than the melts of hawaiitic composition in which they are found and becomes slightly more dense than the co-existing melt somewhere in the intermediate mugearite range. If fractionation occurred at higher than atmospheric pressure, then this density contrast would be even greater for the hawaiites and the cross-over in densities shifted to more evolved compositions due to the greater compressibility of liquids as compared to the mineral phase.

Figure 25. Plagioclase density as a function of anorthite content and temperature. Measured values from Grundy and Brown (1967).

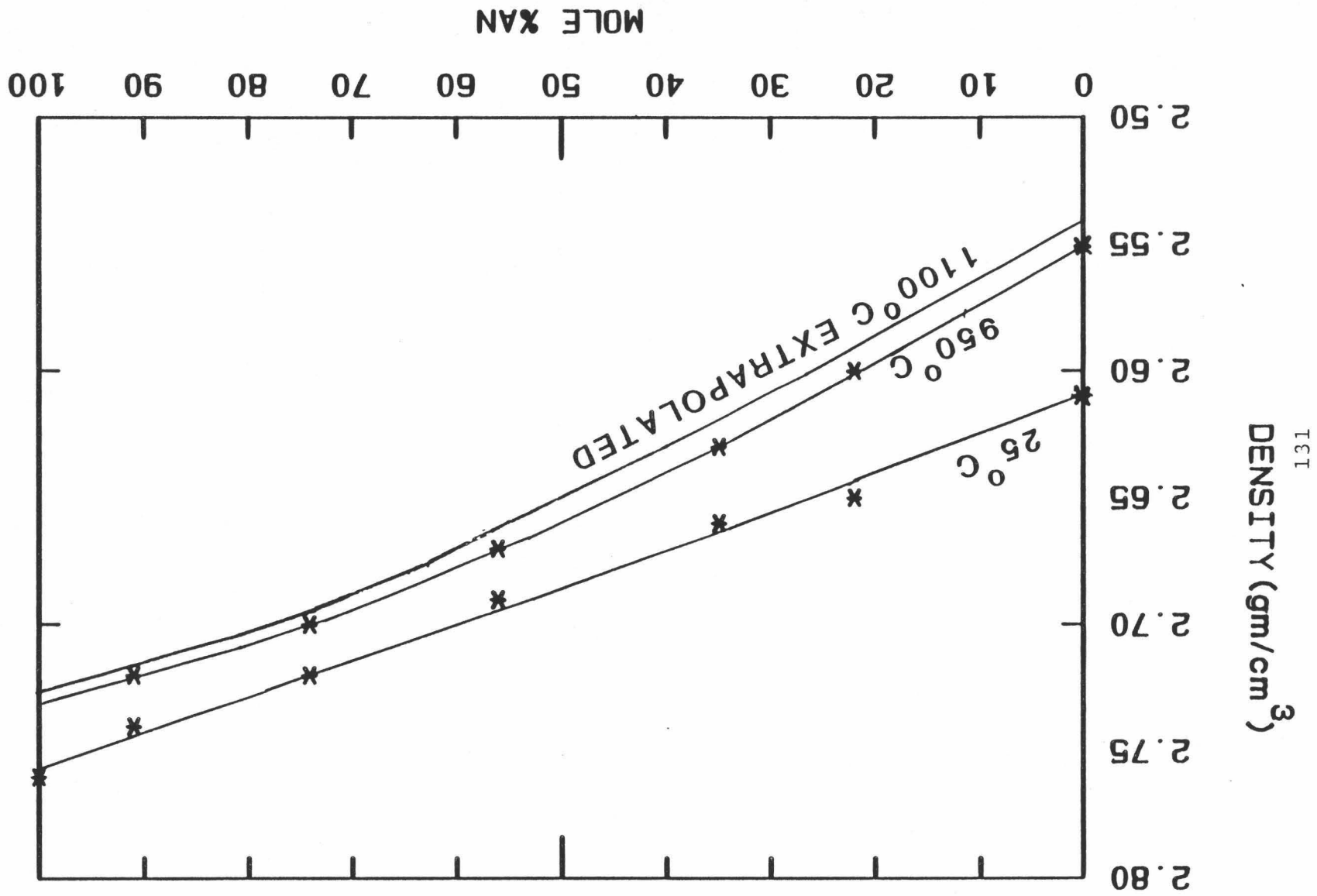
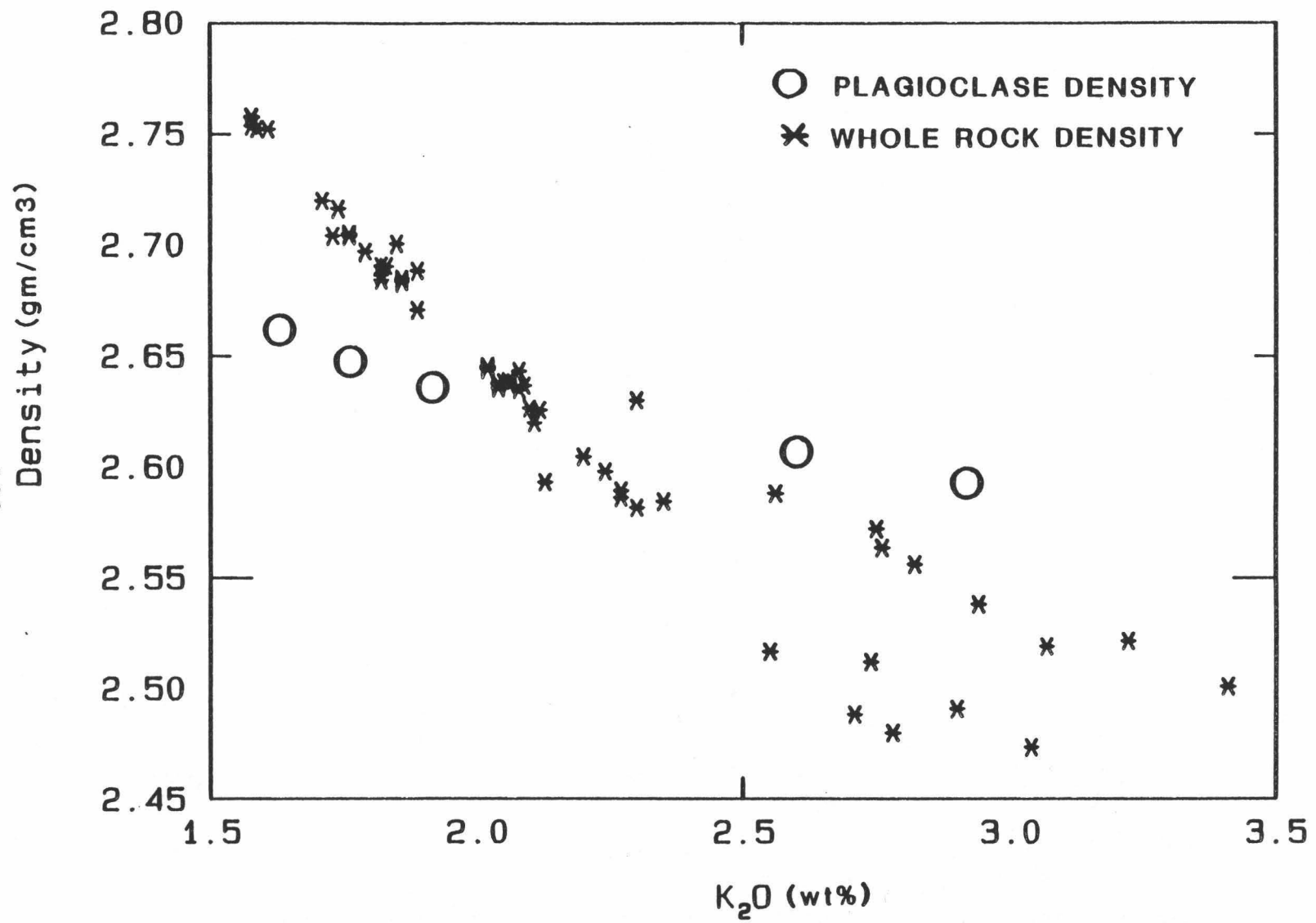


Figure 26. Densities of Hawi lavas, calculated using the equations of Bottinga and Weill (1970), as a function of differentiation (K_2O content). The circular symbols are densities of plagioclases (as determined by inspection of Figure 27) found in Hawi lavas of different compositions.



Thus lavas of hawaiite and moderately evolved mugearite composition which show geochemical evidence of plagioclase fractionation did not differentiate by gravitational settling.

The nature of the flow in a conduit can be predicted from the value of the Reynolds number. Huppert et al. (1984) have shown that for an ascending magma driven upwards by the density contrast between it and the surrounding lithosphere, the Reynolds number is given by

$$Re = g p / k p_m^{1/2} d^{3/2} v^{-1}$$

where p_m is the density of the magma, k is a friction coefficient dependent upon surface roughness of the dyke, d is the width of the dyke, v is the kinematic viscosity and p is the average density difference between the ascending magma and its wall rocks. The flow is turbulent if Re exceeds a critical value which is approximately 2000. Campbell (1985), using the above equation, showed that the flow of primitive magma in dykes with widths greater than 3 meters will be fully turbulent.

Kushiro et al. (1976) have shown that the viscosity of a melt increases with decreasing pressure even under isothermal conditions. Increasing the viscosity of the magma upon ascent will lower the Reynolds number of the flow and may lead to a change from turbulent flow at depth to laminar flow at shallower levels. The crystallization of relatively large amounts of clinopyroxene and olivine at depth would further facilitate this transition by increasing the viscosity of the residual magma. Because of the rapid formation of a chilled margin at

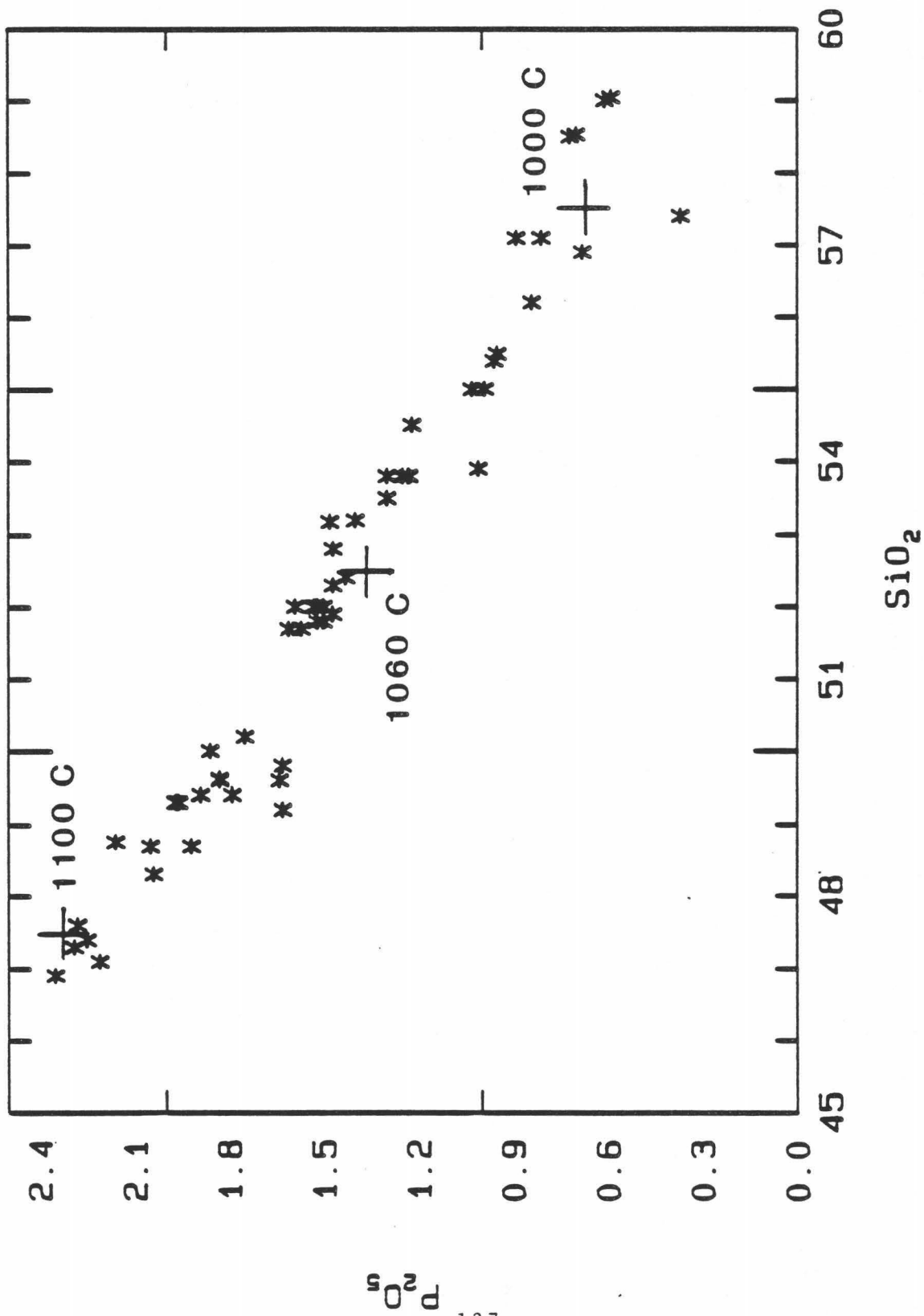
the boundary of the conduit in laminar flow regimes, the amount of assimilation of wall rock at shallower levels is greatly decreased. Laminar flow also leads to a favorable environment for crystallization along the conduit walls in a manner similar to that envisioned by Irving (1980)(dynamic flow crystallization). A plating mechanism of this type can explain how buoyant crystallizing phases such as plagioclase could be removed from a relatively evolved magma with an appreciable yield strength.

PHYSICAL CONDITIONS OF ERUPTION

By using the empirical equation relating apatite solubility to absolute temperature and silica content derived by Harrison and Watson (1981), one can estimate the temperature of the magma if one assumes equilibrium existed between apatite and the melt. The resulting temperatures range from 1100°C for the hawaiites to 1000°C for the benmorites (Figure 27). Temperature values calculated based on the composition of plagioclase and the co-existing melt using the equations of French and Cameron (1981) yield results of between 1120-1080°C. Both of these temperature ranges are close to measured values for Etna hawaiites, which range from 1070-1090°C, suggesting that they are realistic values.

The presence of dunitic xenoliths of up to 15 cm in diameter suggests that the Hawi lavas possessed a yield strength . Sparks et al.

Figure 27. Variation of P_2O_5 versus SiO_2 for Hawi lavas. The values of P_2O_5 required for apatite saturation in a magma containing 47.5, 52.5 and 57.5% SiO_2 were calculated at the temperatures indicated using the equation found in Harrison and Watson (1984). The close correlation between these calculated values and the observed trend is consistent with the variation being due to the change in apatite saturation as the magma evolved.



(1977) measured values of between 250-400 N/m^2 for an Etna hawaiite which is probably a reasonable value for Hawi hawaiites upon extrusion at the surface. Wilson and Head (1981) presented an equation relating the minimum conduit radius required to allow eruption of a magma with a yield strength. Using a value of 200 Kg/m^3 for the density contrast between wall rock and magma, a minimum conduit radius of 0.4 meters would be required for a magma to rise having a yield strength of 400 N/m^2 . Dikes are found on Kohala exposed at the heads of the great canyons and in the tributaries of the larger valleys. Dikes belonging to the Pololu Formation range in width from a few inches to ten feet and average about 2 feet (Stearns and Macdonald, 1946). Dikes associated with Hawi activity are wider, and tend to increase in dimension as a function of differentiation (hornblende bearing dikes with widths in excess of 25 feet have been observed). This increase in dike dimension in going from the tholeiitic and mildly alkalic lavas of the Pololu to the evolved lavas of the Hawi is almost certainly due in part to the increasing yield strength of the lavas.

WHY ARE SUCH HIGH PHOSPHOROUS CONTENTS OBSERVED IN HAWI LAVAS?

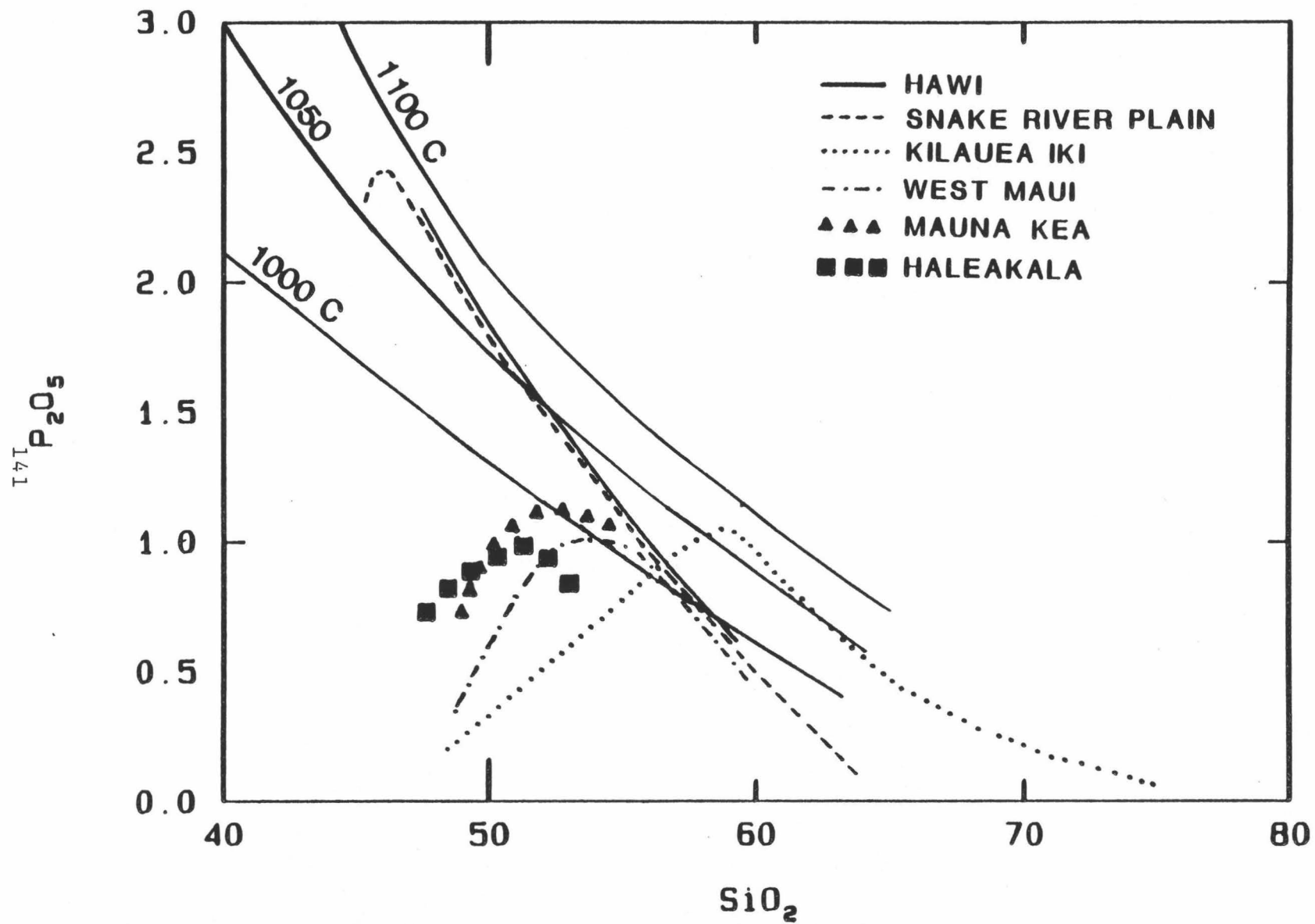
The hawaiites found in the Hawi have much higher phosphorous contents than any other alkalic lava found in Hawaii. In fact, with the exception of some alkali and phosphorous-rich ferrobasalts found around

the margins of the Snake River Plains (Leeman et al., 1976), they have the highest phosphorous contents of any analyzed volcanic lava.

Figure 28 shows the differentiation trends observed within various Hawaiian alkalic suites, as well as alkalic lavas from the Snake River Plain (Leeman et al., 1976) and tholeiites of the Kilauea Iki lava lake (Helz, 1981). The isotherms were calculated using the empirical relationship relating apatite saturation as a function of temperature and SiO_2 content given in Harrison and Watson (1981). As can be seen from the plot, the trends for Hawi lavas is paralleled by lavas from the Snake River Plain, Mauna Kea and West Maui. The trend for Haleakala seems to "turn" over at lower SiO_2 contents than the other suites but this trend is not well defined due to the paucity of evolved compositions. The trend for West Maui is well defined for both limbs of the curve, but due to the near absence of intermediate compositions, the exact location of the turn over point is not well defined. The trend for Kilauea Iki lavas turns over at higher SiO_2 contents, due to the higher liquidus temperatures (measured bore hole temperatures 1070-1170°C (Luth, 1981) at a given SiO_2 content for magmas evolving along a tholeiitic differentiation trend as compared to an alkalic differentiation trend. From this diagram one can infer that the observed systematic decrease in P_2O_5 content reflects the variation in apatite solubility as a function of increasing SiO_2 contents and decreasing liquidus temperatures (1100-1000°C) in going from hawaiite to benmorite.

Because phosphorous and neodymium typically have similar bulk partition coefficients in basaltic suites of lavas which have not

Figure 28. Variation of SiO_2 vs. P_2O_5 for natural melt series. The curved projections drawn are the variation of apatite solubility as a function of SiO_2 content at temperatures of 1100°C , 1050°C and 1000°C . This diagram illustrates that the turning over in phosphorous abundance in most melt series is clearly controlled by the solubility of apatite in the melt.



undergone apatite fractionation, the abundance ratio of these two elements can give information regarding the source ratio. Figure 29 shows the observed trends for various Hawaiian volcanoes, where the numerical values are a measure of the quality of fit (r) of the drawn line through the (n) data points. In actuality most of the drawn projections aren't strictly linear but rather tend to curve upwards as the degree of differentiation increases, presumably because phosphorous behaves more incompatibly than neodymium in the more evolved compositions. This curvature is, however, small and does not significantly affect the drawn slopes which were calculated by linear regression analysis (the value r is a measure of the quality of fit of the line to the data). Superimposed on these linear lines are the individual data points for the Hawi. The hawaiites plot well above the typical Hawaiian trends (ie. have higher P_2O_5/Nd ratios), while the more evolved mugearites and benmorites, which have fractionated apatite, plot roughly within the extension of these lines. Figure 30 illustrates the discontinuity in P_2O_5/Nd values between Pololu and Hawi lavas. If apatite fractionation had also occurred in the petrogenesis of the least differentiated hawaiites, then some less-evolved lavas may have had even higher P_2O_5/Nd ratios. These abnormally high ratios lead one to speculate why phosphorous is not well correlated with neodymium and other incompatible elements in the Hawi.

One possible explanation is that the high P_2O_5 contents were produced by disequilibrium melting of apatite. The REE content of the resulting melt would then be strongly controlled by the REE content in the apatite due to the high absolute concentrations of rare earths in

Figure 29. P_2O_5/Nd ratios observed for various Hawaiian volcanoes. The r values is a quality of fit factor for the drawn trends and n is the number of data points available. Individual data points plotted are for Hawi lavas, the decreasing ratios being due to progressive apatite fractionation in going from hawaiite to benmorite. Note the abnormally high P_2O_5/Nd values for the least differentiated hawaiites.

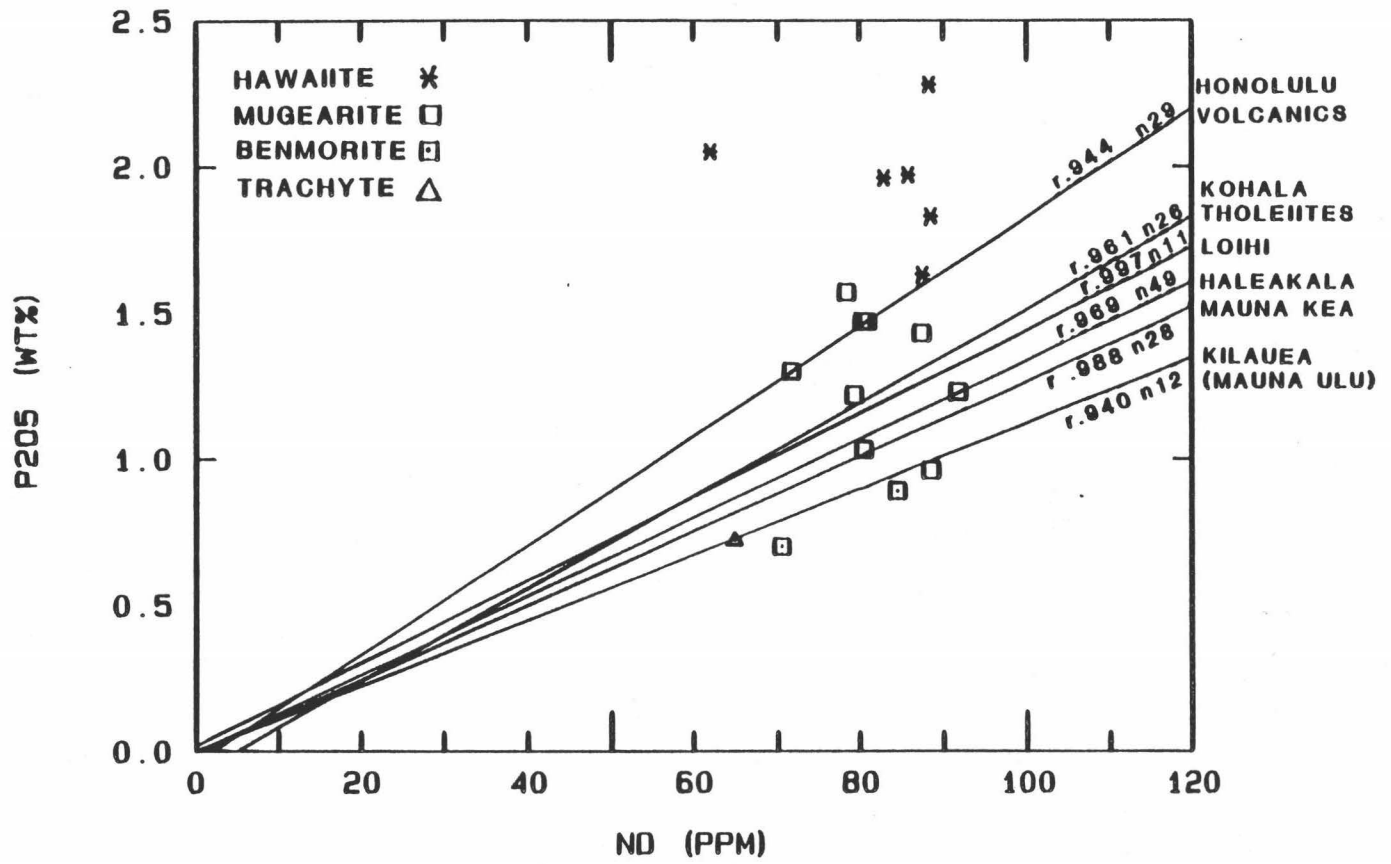
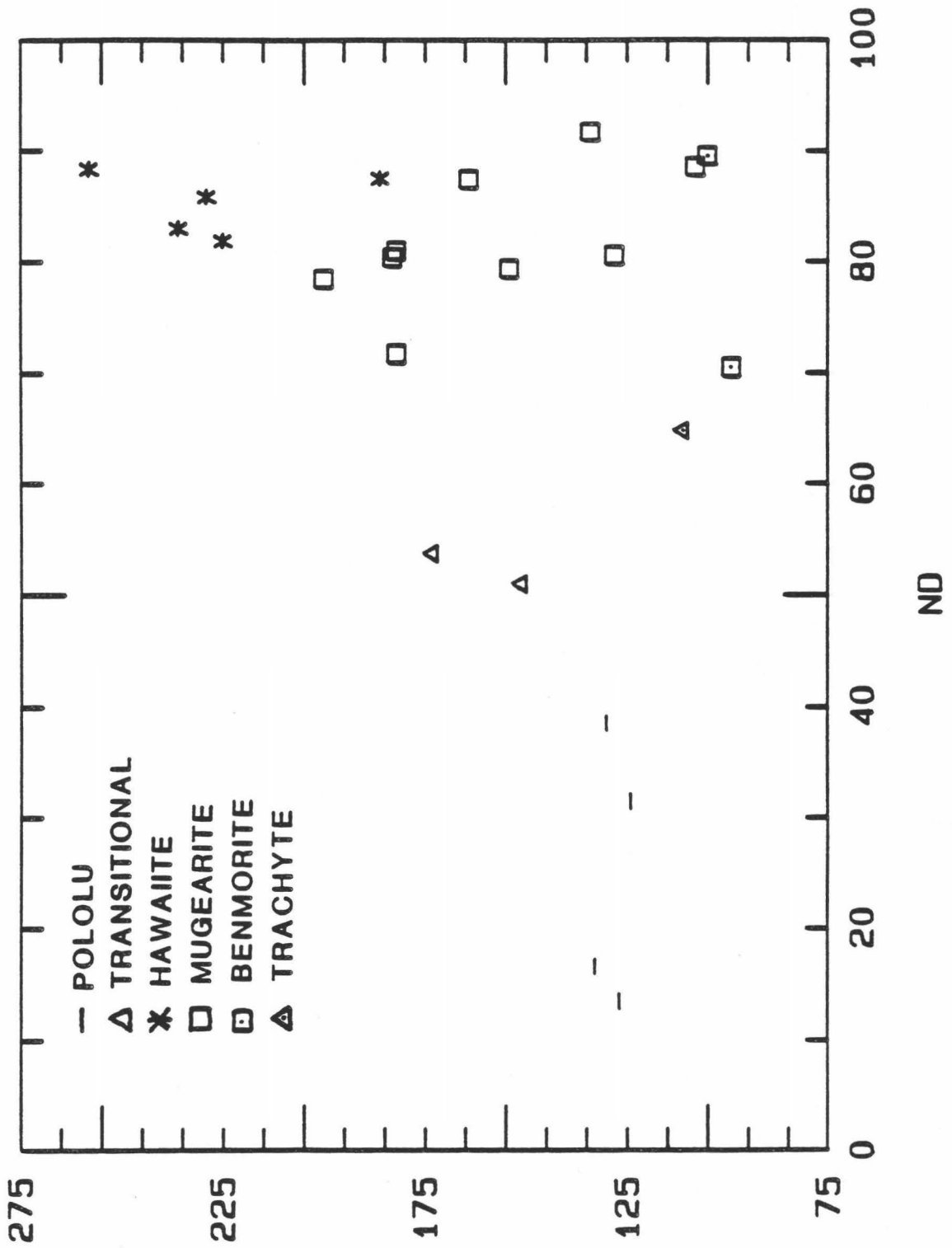


Figure 30. Discontinuous increase in P_2O_5/Nd ratio between Pololu lavas and the least evolved hawaiiite lavas observed in the Hawi.



apatite. An initial disequilibrium melt containing relative rare earth abundances proportional to apatite partition coefficients (K_d Ce<Nd<Sm>Dy>Yb) that underwent appreciable clinopyroxene fractionation (K_d Ce<Nd<Sm<Dy=Er=Yb), does not produce a product magma with relative rare earth contents similar to those observed in the Hawi (Figure 31). A major problem with a disequilibrium process is the experimental observation that it is possible to reach equilibrium rather quickly in the laboratory at mantle-type conditions. Since the process of melt extraction must take some time, especially under waning thermal conditions with the production of small degree partial melts, it almost seems inescapable that equilibrium would be at least been approached during melting within the mantle.

Figure 32 shows the relative abundances of various incompatible elements for a hawaiite from Kohala (H_g84-3) and from Mauna Kea (PH-1; West, 1987) which have undergone roughly similar amounts of fractionation (based on similar K₂O, Nb and Ba contents). The relative enrichment of the REE's observed in the Hawi increases roughly in the same relative order as the partition coefficient values of these REE's in apatite (Watson and Green, 1981). By first calculating how much apatite (41.5 wt% P₂O₅) must be added to the Mauna Kea lava to reach the high P₂O₅ abundances observed in the Hawi lava, one can then calculate the concentration of REE's which would be required to produce the observed difference in REE content between the two lavas. Adding 2.9 grams of apatite to PH-1 would raise the P₂O₅ content to that found in H_g84-3. The concentration of the the various REE's required to produce the observed enrichment are roughly similar to measured microprobe

Figure 31. Possible rare earth element pattern resulting from disequilibrium melting of apatite bearing source with chondritic relative abundances of rare earths (squares). Fractionation of 75% clinopyroxene from this primary melt results in the triangle pattern. Least differentiated hawaiiite (H_g 84-11) is shown for comparison. Partition coefficient values calculated in Table 12 were used for clinopyroxene. Partition coefficient data found in Watson and Green (1981) were used for apatite.

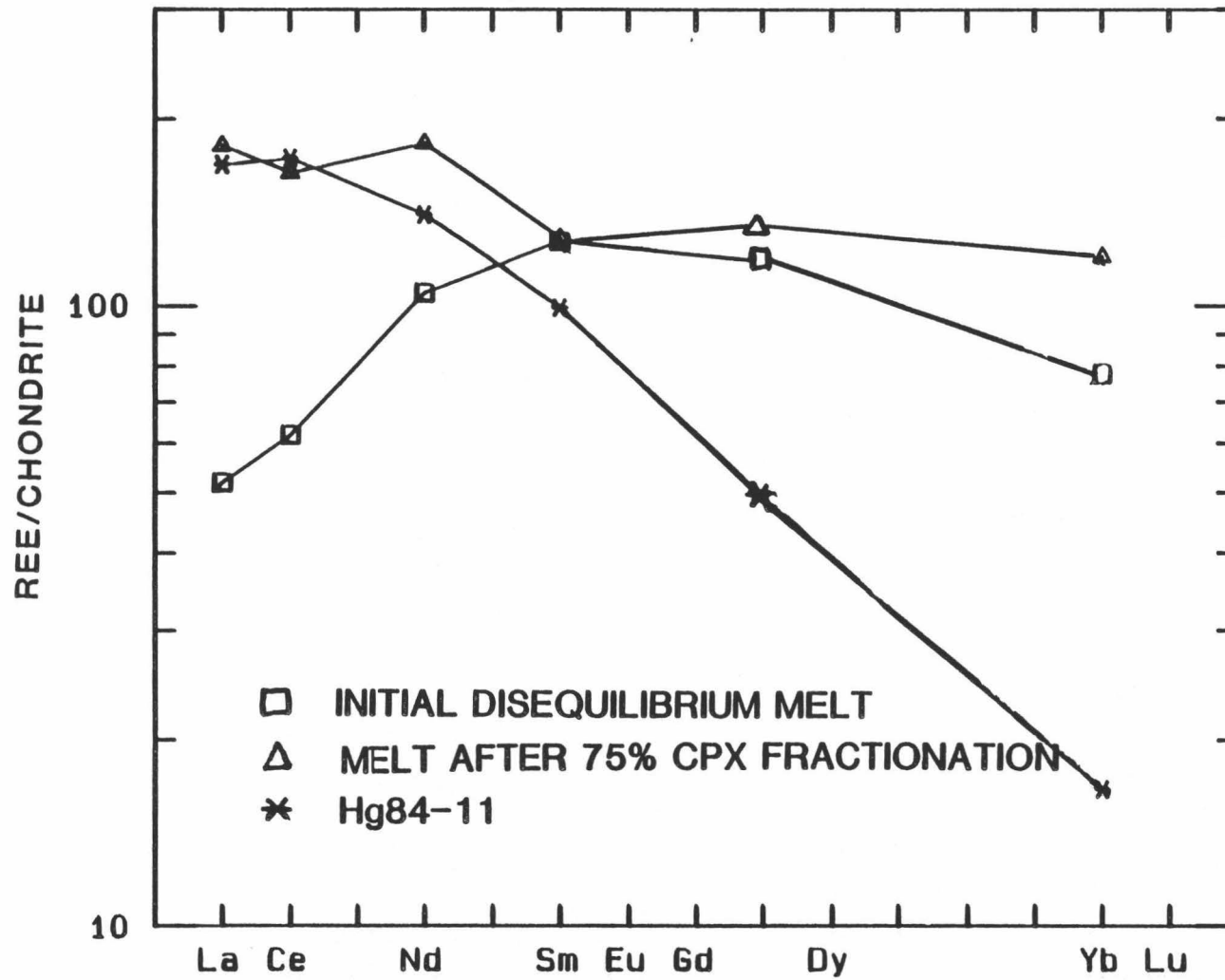
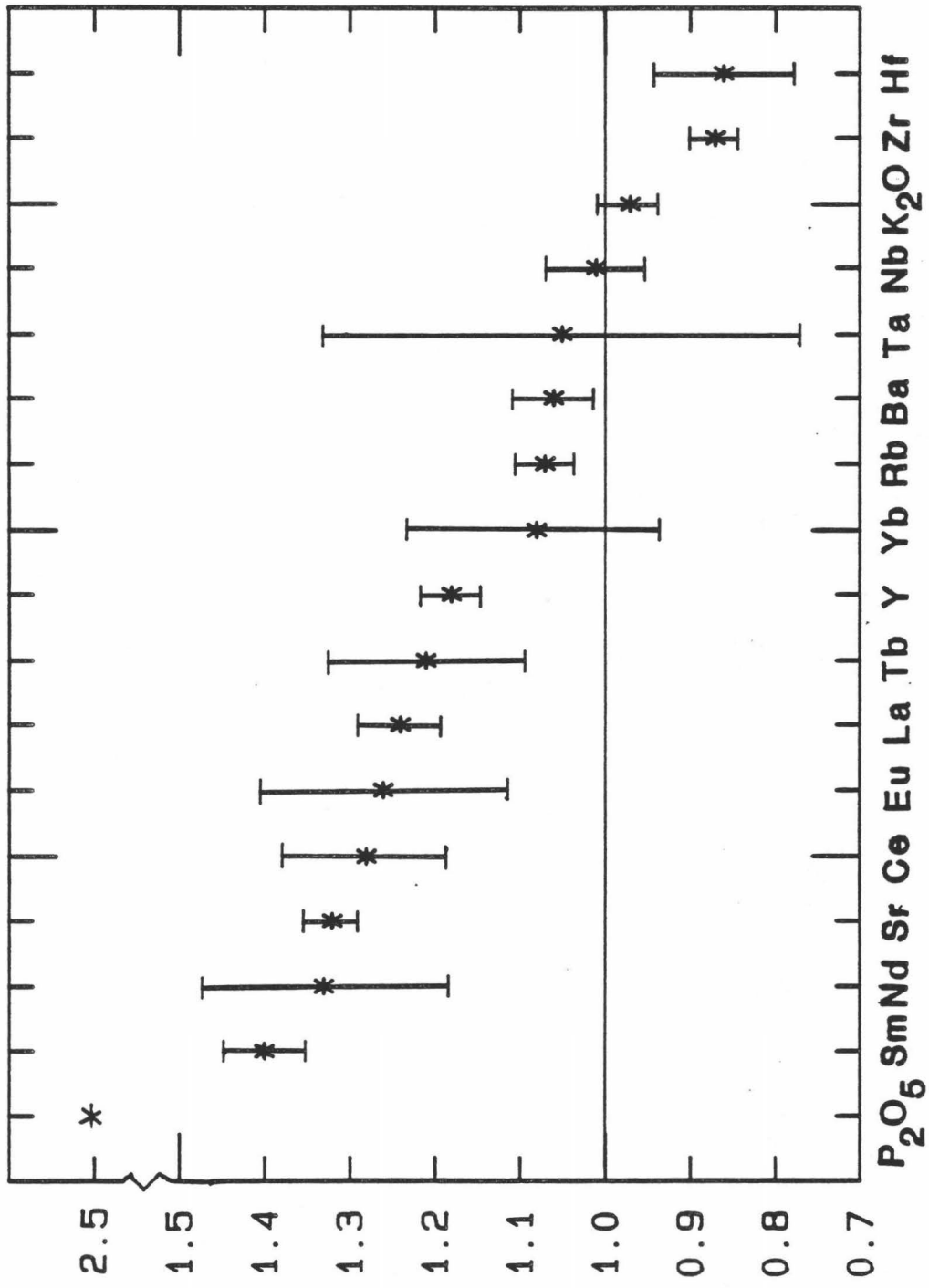


Figure 32. Relative enrichment of various incompatible elements in a Hawi hawaiiite (H_g84-3) over a Mauna Kea hawaiiite (PH-1; West, 1987) of roughly similar degrees of differentiation (based on similar K₂O, Ba, Nb and Rb contents).

Hg84-3/PH-1

151

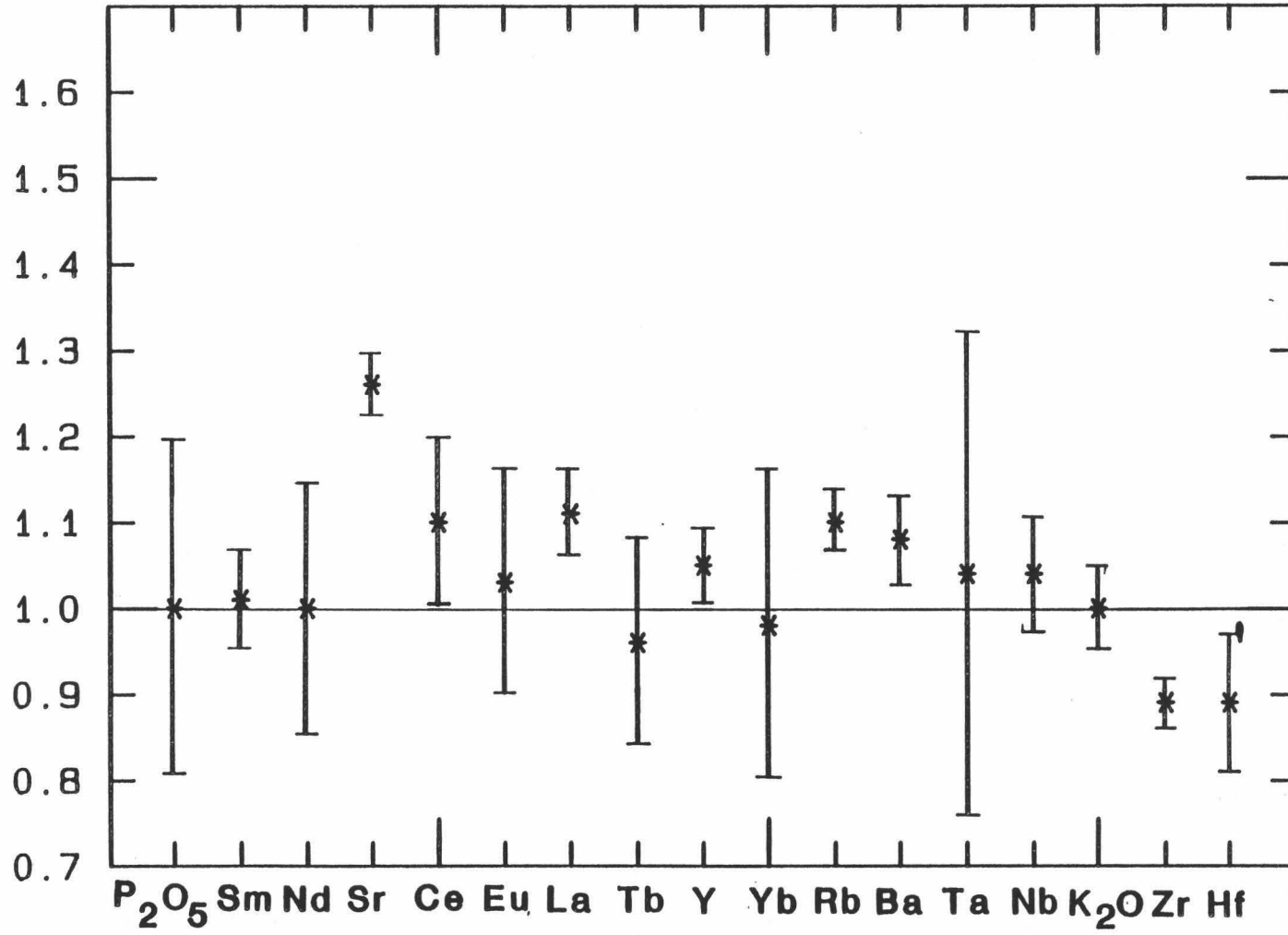


values (Table 6) as well as to estimates from the REE/K₂O vs. P₂O₅/K₂O plots (Figure 22) for Hawi lavas (which graphically display the concentration of REE's needed in apatite to explain the observed chemical variability assuming that apatite alone controls the variation in both REE and P₂O₅ content within the Hawi suite). The differences in elemental abundance between these two hawaiites upon adding 2.9 grams of apatite to the Mauna Kea lava is plotted in Figure 33. The concentration of Sr and Nd in apatite used in the calculations were averages of measured values (Sibray, 1977 and this study, Table 6) while the concentration of other rare earth elements were calculated using the model K_d abundances for apatite (Table 12) for the hawaiite to mugearite step and an average abundance of rare earths in rocks of hawaiite to mugearite composition. Most elements approach ratios of one upon addition of the apatite suggesting that the anomalously high P₂O₅ contents are the result of assimilation of apatite during the ascent of Hawi magmas. Apatite accumulation is not responsible for the observed enrichments as is evidenced by apatites consistently low modal abundance in the rocks (Table 1). Since the modelled concentrations of the rare earth elements are similar to those observed in apatites crystallized from Hawi lavas, the magma from which the assimilated apatites crystallized must have been of generally similar composition to Hawi lavas. The source of these apatites might have been from ascending precursors of Hawi activity which stalled prior to reaching the surface. These trapped lavas would have slowly cooled producing a residual magma which would have eventually crystallized apatite. How apatite was then selectively assimilated into Hawi lavas without a concomitant enrichment

Figure 33. Difference in various incompatible element contents in H_g84-3 and PH-1 after the addition of 2.9 grams of apatite to the Mauna Kea composition. See text for details of calculations.

75T

Hg84-3/ (PH-1+APT)



in other highly incompatible elements is not clear. While strontium abundances are anomalously high in H_g84-3 (and in other Hawi hawaiites), typically hygromagmatophile elements such as Zr and Hf are somewhat depleted which is perhaps indicative of differences in source composition.

RELATIONSHIP TO THE POLOLU

The Sr and Nd isotopic data presented in Lanphere and Frey (1986) and Hofmann et al. (1986) demonstrate a small but distinct difference in Sr isotopic composition and an overlap in Nd isotopic composition between lavas of the Pololu and Hawi (Figure 7). Additional isotopic analysis of "transitional" rocks collected during this study indicate that these lavas lie in the Hawi isotopic field despite having major and trace element characteristics more akin to evolved Pololu lavas. Attempts to derive the least evolved hawaiite (H_g84-11) from the most evolved "transitional" lava (T_g85-16) by fractional crystallization modelling would require large amounts of plagioclase and clinopyroxene fractionation in conjunction with the assimilation of small amounts of apatite (Table 14). The combination of relatively large amounts of plagioclase fractionation (high K_d for Eu compared to other rare earths) in conjunction with the assimilation of small amounts of apatite (lower K_d for Eu than other middle rare earths) would produce a residual lava with a pronounced negative europium anomaly, which is not observed in

Table 14. Least-squares calculations attempting to relate the transitional lava T_g85-16 to the least differentiated hawaiite (H_g84-11) and to an evolved upper Pololu lava (72M037)(sample from Lanphere and Frey (1986)).

The Parent Lava is Sample T_g85-16

gms removed per 1.0 gm	Absolute Value Removed	
-0.003	-0.009	Olivine
0.170	0.530	Plagioclase
0.046	0.145	Opaque
-0.014	-0.043	Apatite
0.121	0.378	Pyroxene

0.677 Sample H_g84-11 is the daughter

	SiO ₂	TiO ₂	Al ₂ O ₃	FeO	MnO	MgO	CaO	Na ₂ O	K ₂ O	P ₂ O ₅
H _g 84-11	47.21	3.00	15.77	13.09	0.23	4.55	7.50	4.81	1.58	2.26
T _g 85-16	47.30	3.52	16.70	13.10	0.19	4.99	7.66	4.14	1.47	0.93
Calc	47.31	3.30	16.67	13.18	0.18	4.94	7.66	4.40	1.15	0.93
Diff	-0.01	0.22	0.03	-0.08	0.01	0.05	0.00	-0.13	0.32	0.00

Sum of squares of residuals = 0.180

	Sc	Rb	Sr	La	Ce	Nd	Sm	Eu	Tb	Yb	Zr	Hf	Ta	Nb
H _g 84-11	9.1	28.0	1854.4	55.6	149.5	88.3	20.15	6.22	2.35	3.66	337.4	7.7	2.93	52.0
T _g 85-16	12.9	31.4	1193.9	42.8	100.5	53.7	12.19	3.70	1.46	2.74	347.9	7.6	3.94	48.4

The Parent Lava is Sample 72M037

gms removed per 1.0 gm	Absolute Value Removed	
-0.185	2.412	Plagioclase
0.178	-2.320	Pyroxene
-0.070	0.908	Olivine

1.096 Sample T_g85-16 is the daughter

	SiO ₂	TiO ₂	Al ₂ O ₃	FeO	MnO	MgO	CaO	Na ₂ O	K ₂ O	P ₂ O ₅
T _g 85-16	47.30	3.52	16.70	13.10	0.19	4.99	7.66	4.14	1.47	0.93
72M037	48.25	3.58	13.78	14.87	0.21	5.21	9.90	2.81	0.89	0.50
Calc	48.46	4.18	13.56	14.18	0.23	5.45	9.50	3.83	1.56	1.02
Diff	-0.21	-0.61	0.22	0.69	-0.02	-0.24	0.40	-0.51	-0.67	-0.52

Sum of squares of residuals = 2.132

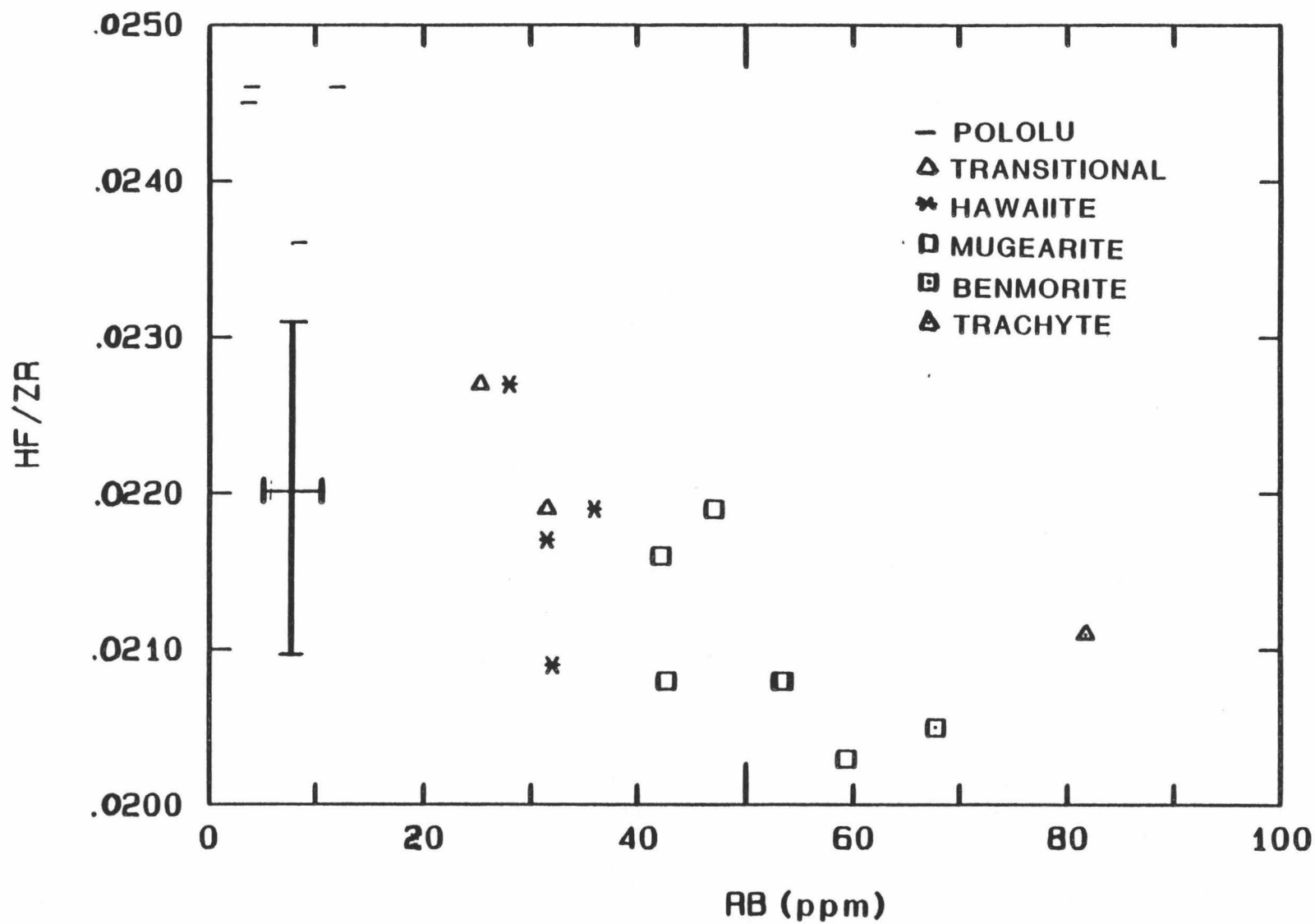
	Sc	Rb	Sr	La	Ce	Nd	Sm	Eu	Tb	Yb	Zr	Hf	Ta	Nb
T _g 85-16	12.9	31.4	1193.9	42.8	100.5	53.7	12.19	3.70	1.46	2.74	347.9	7.6	3.94	48.4
72M037	29.7	18.6	542.0	26.1	65.8	40.7	9.04	3.06	1.37	2.76	-	6.6	1.67	-

sample H_g84-11. In addition, since these lavas have similar contents of highly incompatible elements such as Zr, Nb, Hf and Rb (Table 14), large amounts of fractionation can not be used to relate one lava to the other. Simple assimilation of apatite to the transitional lava T_g85-16 to derive H_g84-11 does not work because of large differences in TiO₂, Al₂O₃ and Na₂O contents and since T_g85-16 actually has a higher CaO content than H_g84-11. The above evidence precludes a simple genetic relationship between these relatively aphyric lavas. In addition, attempts at modelling the derivation of the transitional lavas by fractional crystallization from evolved alkalic rocks found within the upper Pololu section also failed (Table 14). The distinctive character of Pololu and Hawi lavas is also seen in the discontinuous decrease in the incompatible element ratio of Hf/Zr between Pololu and transitional lavas (Figure 34; note that the difference does, however, lie within analytical uncertainty).

From the above considerations, it is obvious that the use of inverse modelling for all lavas found on Kohala, as was attempted in the study of Feigenson et al (1983), is invalid. Because of their distinct compositional and isotopic characteristics, Hawi and transitional lavas can not be used in modelling calculations to constrain the source composition for the Pololu lavas (Hofmann, 1986; Lanphere and Frey, 1986). The observed range in isotopic content for Pololu lavas is larger than analytical uncertainty, implying that the source region for these lavas is isotopically heterogeneous (Figure 10). The fact that the Pololu, Transitional and Hawi lavas have distinct isotopic and compositional characteristics shows that at least three distinct source

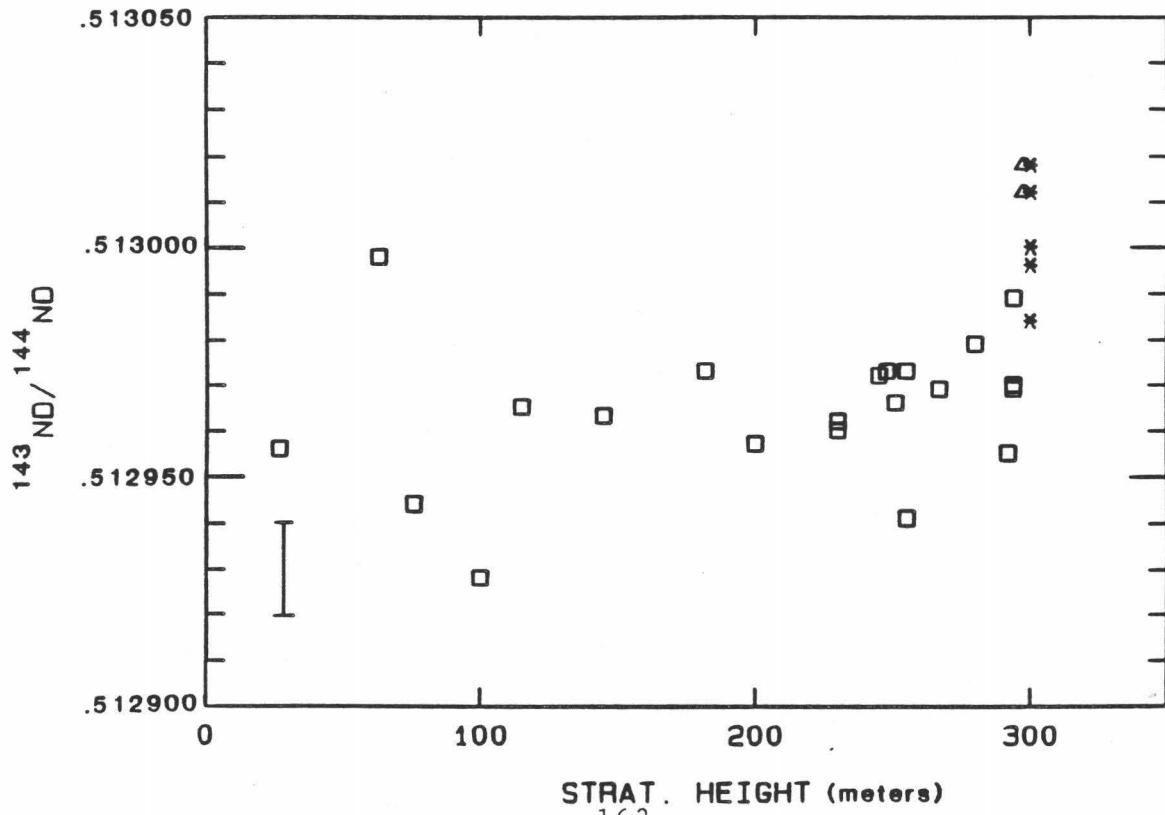
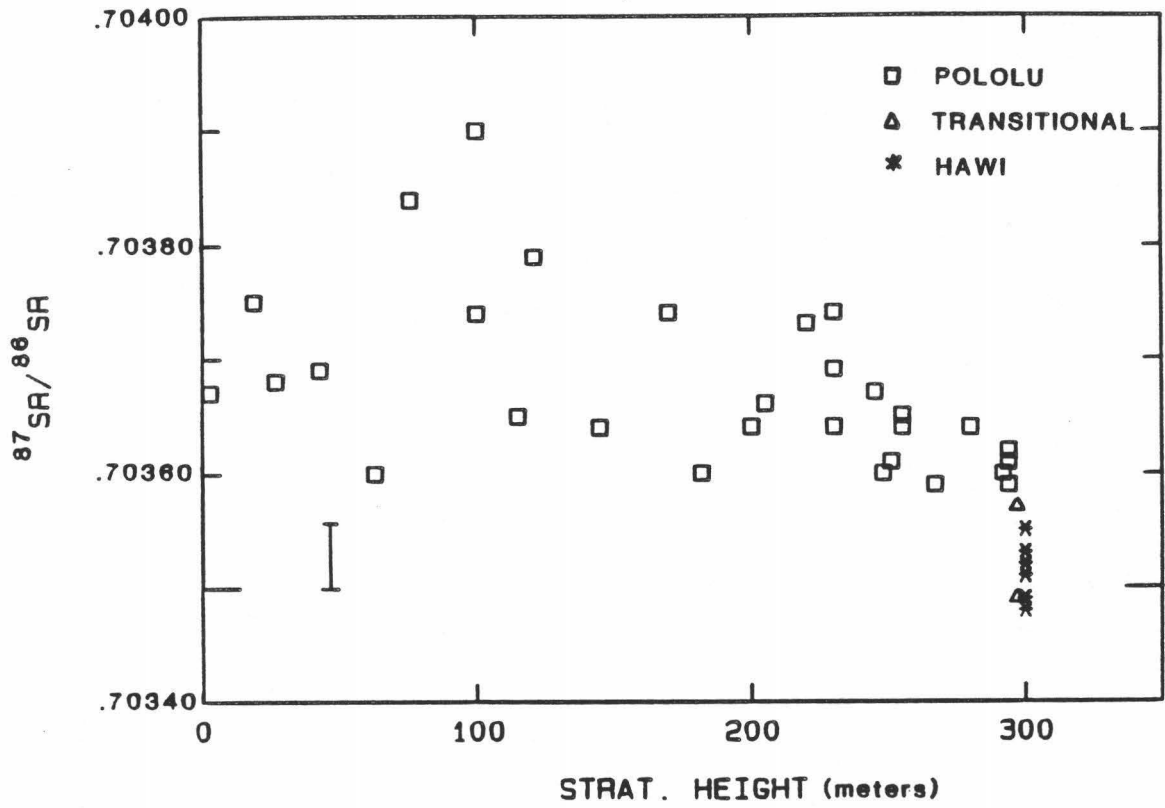
Figure 34. Ratio of two highly incompatible elements (Hf and Zr) showing small discontinuity between Pololu and Hawi values. The observed decrease in this ratio as differentiation proceeds within the Hawi is due to the greater incompatibility of Zr.

160



regions are involved. Studied stratigraphic sections from Haleakala have shown that the isotopic ratios of Sr and Nd change systematically as a function of eruptive age (Chen and Frey, 1983). On Kohala, however, there is not a strong correlation between $^{87}\text{Sr}/^{86}\text{Sr}$ - $^{143}\text{Nd}/^{144}\text{Nd}$ content and eruptive age except for the small gap between $^{87}\text{Sr}/^{86}\text{Sr}$ values found in the Pololu and Hawi (Figure 35). The general inverse correlation between parent/daughter abundance ratios and the corresponding radiogenic isotopic ratio that is observed on several other Hawaiian volcanoes (Haleakala, East Molokai, Kauai) is also observed on Kohala. Chen and Frey (1983) explained the isotopic variability found on Haleakala as resulting from a partially molten, undepleted mantle diapir interacting with the MORB-related wall rock through which it is ascending by melting the wall rocks to a small degree. To fit the spectrum of compositions found on Kohala into this model would require the introduction of at least a third (and possibly more) mixing components. Because of the scatter in isotopic abundances for Pololu lavas (Lanphere and Frey, 1986; Hofmann, 1986), this mixing component must be isotopically heterogeneous. Feigenson (1984) proposed a slightly different mixing model to explain the observed isotopic heterogeneity of Hawaiian lavas. This model involves mixing melts formed by small degrees of melting of a MORB source with a mixture of ancient subducted crust, primitive mantle and depleted asthenosphere. This model can better accommodate the Kohala data because it involves more than two compositionally and isotopically distinct components, but is rather unconstrained in terms of absolute values for the various end member components.

Figure 35. Variation of $^{87}\text{Sr}/^{86}\text{Sr}$ and $^{143}\text{Nd}/^{144}\text{Nd}$ with stratigraphic position.



CONCLUSIONS

The major salient features of this study are summarized below:

A). The presence of soil horizons between flows of the Pololu and Hawi Formation are not conclusive proof of the existence of a long term hiatus in eruptive activity. Potassium-Argon dating of rocks on Kohala indicates that the hiatus in activity between sampled rocks was no more than .1 mA and was probably much less due the inaccessibility of the earliest erupted Hawi lavas which probably lie buried within the summit caldera complex. Additional dating of rocks termed transitional in this study would probably give ages intermediate between existing Hawi and Pololu data based on field relations and the intermediate chemical character of these lavas.

B). The relative proportion of rock types found on Kohala as a result of two years of field work are drastically different than initial estimates given in Stearns and Macdonald (1946) and Macdonald et al (1970). Hawaiiite is the most predominant rock type on Kohala followed in abundance by mugearite, benmorite and trachyte.

C). The concept of a "Kohala" type alkalic cap, where a clear cut long term cessation in eruptive activity occurred prior to the eruption of lavas of predominately mugearite and trachyte compositions, is thus dismissed. The other example of this type of alkalic cap, on West Maui, contains at least one interbedded hawaiiite in the upper section of the shield lavas and the transition to alkalic volcanism was also probably marked by a slowing rather than absolute cessation in activity.

D). The eruptive temperatures of Hawi magmas ranged from 1120°C (hawaiite)-1000°C (benmorite) based on apatite saturation considerations and feldspar compositions.

E). The chemical variation observed within the Hawi can be adequately modelled by fractional crystallization of plagioclase, olivine, apatite, magnetite and high pressure clinopyroxene. This fractionating assemblage is consistent with experimental studies performed on lavas of hawaiite composition at variable pressures. The agreement between calculated and observed values gets slightly worse for more evolved compositions, presumably due to the increased mobility of certain elements in these lavas having higher water contents and probable low ascent rates (due to increasingly large viscosities and yield strengths). The relatively systematic decrease in the number of flows as a function of differentiation also suggests that fractional crystallization was the main process responsible for the observed chemical variability.

F). The predominance of plagioclase fractionation in least squares modelling calculations despite its lower density than the associated magma suggests that fractionation did not occur within a static, differentiating magma chamber, but rather requires some sort of plating mechanism. Dynamic flow crystallization (Irvine, 1980) is a feasible fractionation mechanism for these lavas especially at shallower levels where the transition from turbulent to laminar flow occurs.

G). The importance of variable amounts of high pressure clinopyroxene fractionation in the petrogenesis of Hawi lavas is inferred from low initial and continuously decreasing Sc contents, the possible

crossing of the hypersthene/nepheline thermal divide in going from hawaiite to trachyte, and improvements in the least square modelling by addition of clinopyroxene as a fractionating component.

H). Apatite fractionation played a predominant role in controlling the abundances of rare earth elements throughout the suite.

I). The observed enrichment in certain highly incompatible elements (ie. Rb and Zr) over that predicted based on simple fractional crystallization calculations suggest that either an open system process played a role in the production of these lavas or that a systematic enrichment in these highly incompatible elements took place as differentiation proceeded.

J). The Pololu, Transitional and Hawi lavas can not be related in any simple manner to the same parental magma. Thus, at least three chemically distinct source regions are required to explain the diversity of compositions found on Kohala.

K). The amount of isotopic variability (larger than analytical uncertainty) observed for Sr and Nd in the Pololu and for Nd in the Hawi suggests that the sources for these lavas are isotopically heterogeneous.

L). The anomalously high concentrations of phosphorous and rare earth elements at a given degree of differentiation in Hawi lavas are the result of apatite assimilation. This assimilation may have occurred as these lavas ascended through the stalled initial products of melting from the Hawi source region.

REFERENCES

- Allegre, C.J., Treuil, M., Minster, J., Minster, B., and Albarede F, 1977, Systematic use of trace elements in igneous processes; Part 1: Fractional crystallization processes in volcanic suites. *Contrib. Mineral. Petrol.*, 60, pp 57-75.
- Beeson, M.H. and Jackson, E.D., 1970, Origin of the garnet pyroxenite xenoliths at Salt Lake Crater, Oahu. *Mineral Soc. Am. Spec. Paper*, 3, pp. 95-112.
- Bottinga, Y. and Weill, D.F., 1970, Densities of liquid silicate systems calculated from partial molar volumes of oxide components. *Am. Jour. Sci.* 269, pp. 169-182.
- Bottinga, Y. and Weill, D.F., 1972, The viscosity of magmatic silicate liquids: model for calculation. *Am. Jour. Sci.*, 272, pp. 438-475.
- Campbell, I.H., 1985, The difference between oceanic and continental tholeiites: a fluid dynamic explanation. *Contrib. Mineral. Petrol.*, 91, pp 37-43.
- Campbell, J.F. and Erlandson, D.L., 1981, Geology of the Kohala submarine terrace, Hawaii: *Mar. Geol.*, 41 No 1-2, pp 63-72.
- Chen, C-Y and Frey, F.A., 1983, Origin of Hawaiian tholeiite and alkalic

basalt. *Nature*, 302, pp 785-789.

Chen, C-Y and Frey, F.A., 1985, Trace element and isotopic geochemistry of lavas from Haleakala Volcano, East Maui, Hawaii. *J. Geophys. Res.*, 90, pp. 8743-8768.

Coombs, D.S. and Wilkinson, J.F.G., 1969, Lineages and fractionation trends in undersaturated volcanic rocks from the East Otago Volcanic Province (New Zealand) and related rocks. *J. Petrol.*, 10, pp 440-501.

Dalrymple, G.B., 1971, Potassium-argon ages from the Pololu Volcanic Series, Kohala volcano, Hawaii: *Geol. Soc. America Bull.*, 82, pp 1997-1999.

Diller, D.E., 1982, Contributions to the geology of West Maui volcano, Hawaii. Masters thesis, University of Hawaii, 237pp.

Doell, R.R. and Cox, A., 1965, Paleomagnetism of Hawaiian lava flows: *Jour. Geophys. Res.*, 70, pp 3377-3405.

Drake, M.J. and Weill, D.F., 1975, Partition of Sr, Ba, Ca, Y, Eu^{2+} , Eu^{3+} and other REE between plagioclase feldspar and magmatic liquid: an experimental study: *Geochimica et Cosmochimica Acta*, 39, pp 689-712.

Dudas, M.J., Schmitt, R.A. and Harward, M.E., 1971, Trace element partitioning between volcanic plagioclase and dacitic pyroclastic matrix. *Earth Planet. Sci. Lett.* 11, pp 440-446.

Feigenson, M.D., Hofmann, A.W. and Spera, F.J., 1983, Case studies on the origin of basalt II. The transition from tholeiitic to alkalic volcanism on Kohala Volcano, Hawaii. *Contrib. Mineral. Petrol.* 84, pp 390-405.

Feigenson, M.D., and Spera, F.J., 1981, Dynamical model for temporal variation in magma type and eruption interval at Kohala volcano, Hawaii. *Geology*, 9, pp 531-533.

Fiske, R.S. and Jackson, E.D., 1972, Orientation and growth of Hawaiian volcanic rifts; the effects of regional structure and gravitational stress. *Phil. Trans. Roy. Soc. Lond.*, 329A, pp 299-326.

Fodor, R.V., Keil, K. and Bunch T.E., 1975, Contributions to the mineral chemistry of Hawaiian rocks: IV. Pyroxenes in rocks from Haleakala and West Maui volcanoes, Maui, Hawaii. *Contrib. Mineral. Petrol.*, 50, pp. 173-195.

French, W.J. and Cameron, E.P., 1981, Calculation of the temperature of crystallization of silicates from basaltic melts. *Mineralogical Magazine*, 44, pp 19-26.

Furst, B.W., 1982, Petrology of the alkalic Hawi Volcanic Series of Kohala volcano, Hawaii. Masters thesis, California State Univ., Northridge, 147 pp.

- Gast, P.W., 1968, Trace element fractionation and the origin of tholeiitic and alkaline magma types. *Geochim. Cosmochim. Acta.*, 32, pp 1057-1086.
- Giza, J.G., 1979, Geology of northwest Kohala mountain, Island of Hawaii. Masters thesis, University of Hawaii, 105 pp.
- Goodman, R.J., 1972, The distribution of Ga and Rb in coexisting groundmass and phenocryst phases of some basic volcanic rocks. *Geochim. Cosmochim. Acta.*, 36, pp 303-318.
- Green, T.H. and Pearson, N.J., 1984, Rare earth element partitioning between clinopyroxene and silicate liquid at moderate to high pressure. *Contrib. Mineral. Petrol.* 91, pp 24-36.
- Grundy, H.D. and Brown, W.L., 1967, Preliminary single-crystal study of the lattice angle of triclinic feldspars at temperatures up to 1200°C. *Schweiz. Mineral. Petrog. Mitt.*, 47, pp 21-30.
- Harrison, M.T. and Watson, E.B., 1984, The behavior of apatite during crustal anatexis: Equilibrium and kinetic considerations: *Geochimica et Cosmochimica Acta*, 48, pp 1467-1477.
- Hart, S.R. and Brooks, C., 1974, Clinopyroxene matrix partitioning of K, Rb, Cs, Sr and Ba. *Geochim. Cosmochim. Acta.*, 38, pp 1799-1806.

Hawkesworth, C.J., O'Nions, R.K., and Arculus, R.J., 1979, Nd and Sr isotope geochemistry of island arc volcanics, Grenada, Lesser Antilles. Earth Planet. Sci. Lett., 45, pp 237-248.

Henderson, P., 1982, Inorganic Geochemistry, Pergamon Press, Oxford.

Higuchi, H. and Nagasawa, H., 1969, Partition of trace elements between rock-forming minerals and the host volcanic rocks. Earth Planet. Sci. Lett., 7, pp 281-287.

Hofmann, A.W. and Feigenson, M.D., 1983, Case studies on the origin of basalt I. Theory and reassessment of Grenada basalts. Contrib. Mineral. Petrol. 84, pp 382-389.

Hofmann, A.W., Feigenson, M.D. and Raczek, I., 1986, Kohala Revisited. Contrib. Mineral Petrol.

Hulme, G., 1973, Turbulent lava flow and the formation of lunar sinuous rilles. Modern Geol., 4, pp 107-117.

Huppert, H.E., Sparks, R.S.J, Turner, J.S. and Arndt, N.T., 1984, Emplacement and cooling of komatiitic lavas. Nature, 309, pp 19-22.

Irving, A.J., 1980, Petrology and geochemistry of composite ultramafic xenoliths in alkalic basalts and implications for magmatic processes within the mantle. Am. Jour. of Sci., 280A part 2, pp 389-426.

- Keil, K., Fodor, R.V. and Bunch, T.E., 1972, Contributions to the mineral chemistry of Hawaiian rocks: II. Feldspars and interstitial materials from rocks of Haleakala and West Maui volcanoes, Maui, Hawaii. *Contrib. Mineral. Petrol.* 37, pp 253-276.
- Klerkx, J., 1966, La cristallisation de l'apatite dans les laves de l'Etna. *Soc. Geol. Belg. Ann.*, 89, Bull. No. 5-10, pp 449-458.
- Knutson, J. and Green, T.H., 1975, Experimental duplication of a high pressure megacryst cumulate assemblage in a near saturated hawaiite. *Contrib. Mineral. Petrol.* 52, pp 121-132.
- Kushiro, I., Yoder, H.S. and Mysen, B.O., 1976, Viscosities of basalt and andesite melts at high pressure. *J. Geophys. Res.*, 81, pp 6351-6356.
- Kushiro, I. and Fujii, T., 1977, Flotation of plagioclase in magma at high pressures and its bearing on the origin of anorthosite. *Proc. Japan Acad.*, 53 Ser. B, pp 262-266.
- Lanphere, M.A. and Frey, F.A., 1986, Geochemical evolution of Kohala volcano, Hawaii. *Contrib. Mineral. Petrol.*
- Macdonald, G.A., 1949b, Hawaiian petrographic provinces. *Geol. Soc. Am. Bull.*, 60, pp 1541-1596.
- Macdonald, G.A., 1962, Relation of petrographic suites in Hawaii: The crust of the Pacific Basin. *Amer. Geophys. Union Mon.*, 6, pp 187-195.

- Macdonald, G.A. and Katsura, T., 1964, Chemical composition of Hawaiian lavas. *Jour. Petrol.*, 5, pp 82-103.
- Macdonald, G.A., 1968, Composition and origin of Hawaiian lavas. *Geol. Soc. Amer. Memoir*, 116, pp 447-522.
- Macdonald, G.A. and Abbot, A.T., 1970, Volcanoes in the Sea. Univ. of Hawaii Press, 441 pp.
- Malinowski, M.J., 1977, Geology of the Kawaihae Quadrangle, Kohala Mountain, Island of Hawaii. Masters thesis, University of Hawaii, 130 pp.
- McDougall, I and Swanson, D.A., 1972, Potassium-Argon ages of lavas from the Hawi and Pololu Volcanic Series, Kohala Volcano, Hawaii. *Geol. Soc. Amer. Bull.*, 83, pp. 3731-3738.
- Nagasawa, H. and Schnetzler, C.C., 1971, Partitioning of rare earth, alkali and alkalic earth elements between phenocrysts and acidic igneous magma. *Geochim. Cosmochim. Acta*, 35, pp 953-968.
- Nelson, S.A. and Carmichael, I.S.E., 1979, Partial molar volumes of oxide components in silicate liquids. *Contrib. Mineral. Petrol.*, 71, pp 117-124.

O'Hara, M.J., 1977, Geochemical evolution during fractional crystallization of a periodically refilled magma chamber. *Nature*, 266, pp 503-507.

O'Hara, M.J. and Mathews, R.E., 1981, Geochemical evolution in an advancing, periodically replenished, periodically tapped, continuously fractionated magma chamber. *Q. J. Geol. Soc. Lond.*, 138, pp 237-288.

Pearce, T.H., 1968, A contribution to the theory of variation diagrams. *Contrib. Mineral. Petrol.*, 19, pp 142-157.

Porter, S.C., 1979, Hawaiian Glacial Ages: *Quat. Res.*, 12, No 2, pp 161-186.

Presnall, D.C., Dixon, S.A., Dixon, J.R., O'Donnell, T.H., Brenner, N.L., Schrock, R.L. and Dycus, D.W., 1978, Liquidus phase relations on the join diopside-forsterite-anorthite from 1 Atm. to 20 Kbar; their bearing on the generation and crystallization of basaltic magma. *Contrib. Mineral. Petrol.* 66, pp. 203-220.

Presnall, D.C. Dixon, J.R., O'Donnell, T.H. and Dixon, S.A., 1979, generation of mid-ocean ridge tholeiites. *J. Petrol.*, 20, pp. 3-35.

Roeder, P.L. and Emslie, R.F., 1970, Olivine-liquid equilibrium. *Contrib. Mineral. Petrol.*, 29, pp 275-289.

Schilling, J.G. and Winchester, J.W., 1969, Rare earth contribution to the origin of Hawaiian lavas. *Contrib. Mineral. Petrol.*, 23, pp 27-37.

Schlichting, R., 1968, Boundary Layer Theory. McGraw-Hill, New York.

Schnetzler, C.C. and Philpotts, J.A., 1970, Partition coefficients of rare-earth elements and barium between igneous matrix material and rock forming mineral phenocrysts- II. *Geochim. Cosmochim. Acta*, 34, pp. 331-340.

Sibray, S., 1977, Mineralogy, petrology and geochemistry of some lavas from Kohala volcano, Hawaii. Masters thesis, Univ. of New Mexico, 113 pp.

Sparks, R.S.J., Pinkerton, H. and Macdonald, R., 1977, The transport of xenoliths in magmas. *Earth Planet. Sci. Lett.*, 35, pp. 234-238.

Stearns, H.T. and Macdonald, G.A., 1946, Geology and groundwater resources of the island of Hawaii. *Hawaii Division of Hydrography Bull.*, 9, 363 pp.

Thompson, R.N., 1974, Primary basalts and magma genesis I. Skye, North-West Scotland. *Contrib. Mineral. Petrol.*, 45, pp. 317-341.

Villemant, B., Jaffrezic, H, Joron, J.L. and Treuil, M., 1981, Distribution coefficients of major and trace elements: fractional crystallization in the alkali basalt series of Chaîne des Puys. *Geochimica et Cosmochimica Acta*, 45, pp 1997-2016.

Watson, E.B. and Green, T.H., 1981, Apatite/liquid partition coefficients for the rare earth elements and strontium. *Earth and Planet. Sci.*, 56, pp. 405-421.

West, H., In preparation.

Wilson, L and Head III, J.W., 1981, Ascent and eruption of basaltic magma on the Earth and Moon. *Jour. of Geophys. Res.*, 86, pp 2971-3001.

Wisham, C.M., 1975, The geology of the Honolua area of West Maui, Hawaii. Masters thesis, University of Hawaii, 46 pp.

Zielinski, R.A. and Frey, F.A., 1970, Gough Island: evaluation of a fractional crystallization model. *Contrib. Mineral. Petrol.*, 29, pp. 242-254.

DATE DUE

~~MAR 17 1998~~

~~MAY 09 2002~~

HIGH SMITH REORDER #45-230